Archaeological and Anthropological Sciences (2019) 11:2121–2150
https://doi.org/10.1007/s12520-018-0658-y

ORIGINAL PAPER

Geochemical characterisation of pozzolanic obsidian glasses used in the ancient mortars of Nora Roman theatre (Sardinia, Italy): provenance of raw materials and historical–archaeological implications

Stefano Columbu[1] · Anna Maria Garau[1] · Carlo Lugliè[2]

Received: 27 February 2018 / Accepted: 20 May 2018 / Published online: 13 June 2018

Abstract
The study focused on the volcanic glass used in the production of bedding mortars and concrete of the Roman theatre (I cent. AD) of the Nora site. The volcanic glasses were frequently used as aggregate and with pozzolanic function in all hydraulic mortars of the different sectors of the building (e.g., concretes of *tribunalia* vaults and external niches, jointing and foundation mortars of *cavea* tier ashlars, brick bedding), together with mainly quartz-feldspar sands, local Oligo-Miocenic andesitic-dacitic volcanics and Palaeozoic and Tyrrhenian sedimentary rocks. These volcanic glasses show characteristics closer to obsidian than to natural pozzolan normally used in the Roman period. They have definitely not sourced locally, unlike the other components that make up the aggregate. To identify their provenance, a petrochemical comparison between several samples taken from the theatre mortars and the volcanic outcrops of some probable Sardinian source areas is made. The use of the not local pozzolanic glass is a technical innovation in the mortars of the Nora archaeological site, and considering the wide use of obsidians in the prehistoric periods for the production of tools, significant considerations about its origin, procurement and use are made.

Keywords Pozzolan · Obsidian glass · Chemical analysis · Aggregate · Mt. Arci · Sardinian Neolithic

Introduction

The Roman theatre is one of the most important buildings of the Roman town of Nora, located in the Gulf of Cagliari (south-western Sardinia, Figs. 1 and 2). Nora was founded by the Phoenicians around the mid-eighth century BC, although there is evidence of earlier settlements (AA.VV. 2000; Lugliè 2009b; Wilson 1980). The theatre has a semi-circular isodomic front with a W–NW axis (Fig. 3) and was built during the Augustan or Giulio-Claudio period (first century AD; Bejor 1999; Ghiotto 2004). According to the use in Roman times (Adam 2006; Cagnana 2000; Giuliani Cairoli 2006), a variety of geomaterials (sandstones, conglomerates, volcanic rocks, marbles, bricks, etc.) and different kind of mortars (i.e., Roman concrete, bedding and jointing mortars of ashlars and bricks, plasters) were employed to construct the theatre. In the mortars, several different raw materials (i.e., quartz-feldspathic sands, fine and coarse volcanic aggregate) were used, according to the mortar function and the different sectors of the building: structure-wall, *tribunalia* vaults, wall of external niches, foundation of *cavea* tiers, and stage inner wall.

The volcanic glasses show characteristics similar to obsidian facies and not to natural pozzolan normally used in the Roman period for making the mortars. The use of these pozzolanic glasses, which at the outset does not show to share a local origin, is a novelty because, to date, they have never been found in the ancient mortars neither of the Nora archaeological site nor of other roman sites in the island. Given the wide use of obsidian supplied by the Sardinian Mt. Arci source for the production of tools and artefacts from the Neolithic to

✉ Stefano Columbu
columbus@unica.it

[1] Dipartimento di Scienze Chimiche e Geologiche, Università degli Studi di Cagliari, Via Trentino 51, 09127 Cagliari, Italy

[2] Dipartimento di Dipartimento di Storia, Beni culturali e Territorio, Cittadella dei Musei, Università degli Studi di Cagliari, Piazza Arsenale 1, 09124 Cagliari, Italy

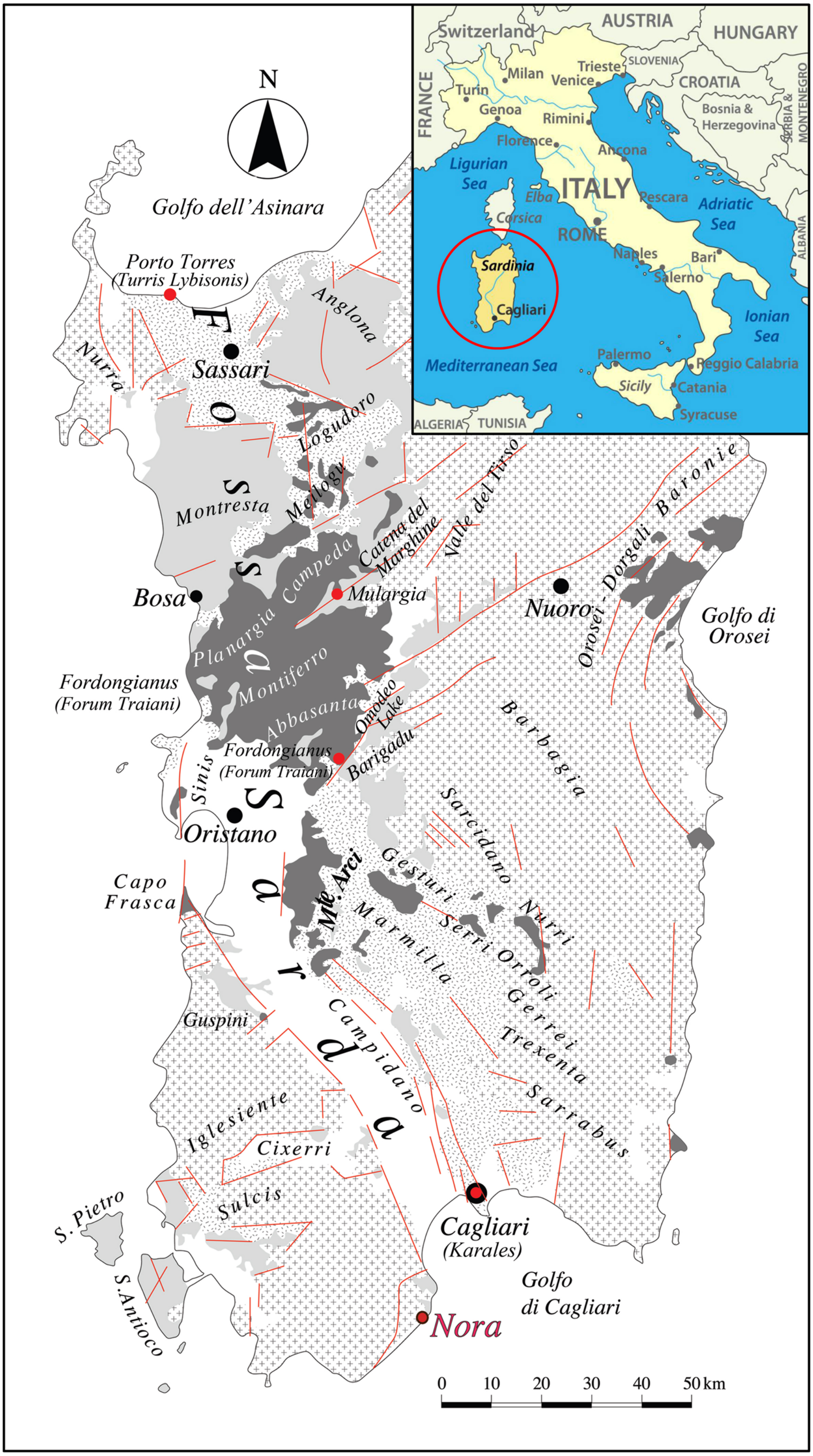
N
Golfo dell'Asinara
Porto Torres
(Turris Lybisonis)
Anglona
Nurra
Sassari
Fossa Sarda
Logudoro
Meilogu
Montresta
Catena del Marghine
Valle del Tirso
Baronie
Campeda
Bosa
Mulargia
Nuoro
Orosei - Dorgali
Golfo di Orosei
Planargia
Montiferro
Fordongianus
(Forum Traiani)
Abbasanta
Omodeo Lake
Barbagia
Fordongianus
(Forum Traiani)
Barigadu
Sinis
Oristano
Sarcidano
Capo Frasca
Gesturi
Mte. Arci
Marmilla
Serri
Nurri
Orroli
Gerrei
Trexenta
Guspini
Campidano
Sarrabus
Iglesiente
Cixerri
Sulcis
S. Pietro
S.Antioco
Cagliari
(Karales)
Golfo
di Cagliari
Nora
0 10 20 30 40 50 km
AUSTRIA
HUNGARY
Switzerland
SLOVENIA
CROATIA
Milan
Trieste
Venice
Turin
Genoa
Rimini
Bosnia &
Herzegovina
SERBIA &
MONTENEGRO
FRANCE
Florence
Ancona
Ligurian
Sea
Elba
ITALY
Pescara
Adriatic
Sea
Corsica
ROME
ALBANIA
Sardinia
Naples
Bari
Salerno
Cagliari
Ionian
Sea
Mediterranean Sea
Palermo
Reggio Calabria
Sicily
Catania
ALGERIA
TUNISIA
Syracuse

Fig. 1 Geological map of Sardinia with localization of the Roman Nora village and other important Punic-Roman city from the south to the north of the island, i.e., *Karales* (today Cagliari), *Forum Traiani* (Fordongianus), *Turris Lybisonis* (Porto Torres); from Columbu and Garau (2017). Legend of patterns and colours refers to lithologies: white, recent alluvial sediments; light gray, Oligo-Miocene volcanics; dark gray, Plio-Pleistocene volcanics; gray stippled, Miocene marine sediments; gray crosses, Palaeozoic crystalline basement and Mesozoic formations. Red continuous and dashed lines, faults

the late Bronze Age, significant considerations about its use, origin and exploitation can be made.

The archaeometric investigations on both the geochemical and petrographic features and origin of raw materials used in the ancient mortars are fundamental for understanding the ancient routes used by the Romans for the transport of stone materials and for obtaining information on the interconnection of Roman settlements and residential sites present in Sardinia. Moreover, these studies are useful to define the technologies and behaviours for the construction of ancient buildings in different historic times and to address the conservative and restorative works (Adriano et al. 2009; Alvarez et al. 2000; Antonelli et al. 2014b; Bertorino et al. 2002; Bianchini et al. 2004; Bultrini et al. 2006; Columbu 2017, 2018; Columbu et al. 2014a, b, 2015a; b, 2017a; b, 2018a; b; c; Columbu and Verdiani 2014; De Luca et al. 2013, 2015; Franzini et al. 2000; Gutiérrez et al. 2016; Lapuente 2014a, b; Lapuente et al. 2012; Lezzerini et al. 2016, 2018a; b ; Miriello et al. 2010, 2015; Maravelaki-Kalaitzaki et al. 2003; Moropoulou et al. 2000, 2004; Ramacciotti et al. 2018; Riccardi et al. 1998; Smith and Smith 2009; Stanislao et al. 2011; Verdiani and Columbu 2010, 2012; Vola et al. 2011).

To identify their geological provenance, the geochemical data of the glass samples were compared with those of new and literature data of acid volcanics (only the rhyolites and alkali-rhyolites were selected) for south and central Sardinia, where one may find similar lithologies: the island of St. Antioco and Mt. Arci, respectively. In the last of these areas, singled out as possible sources, despite more than 15 years of continuous and systematic surveys performed all around the massif (Lugliè 2003, 2013), there are no clues yet of quarrying nor of reduction activity during the Roman period, but striking

Fig. 2 Nora Roman theatre: (**a**) overview of Nora archaeological site with the theatre evidenced by red ellipse; (**b**) southwest view of the *hyposcenium* space under the stage (*palcoscenium*) and east-side *tribunalia* sector (see Fig. 3); (**c**) southeast view of *orchestra*, west-side of *cavea* tiers and (down) part of *hyposcenium*; (**d**) view of east-side *tribunalia* sector (with recent cement rebuilt-consolidation under the vault); (**e**) detail of east-side *cavea* sector with greyish sandstone ashlars, original purplish volcanic ashlars and concrete of the tier foundation; (**f**) original mosaic decoration of *orchestra* floor

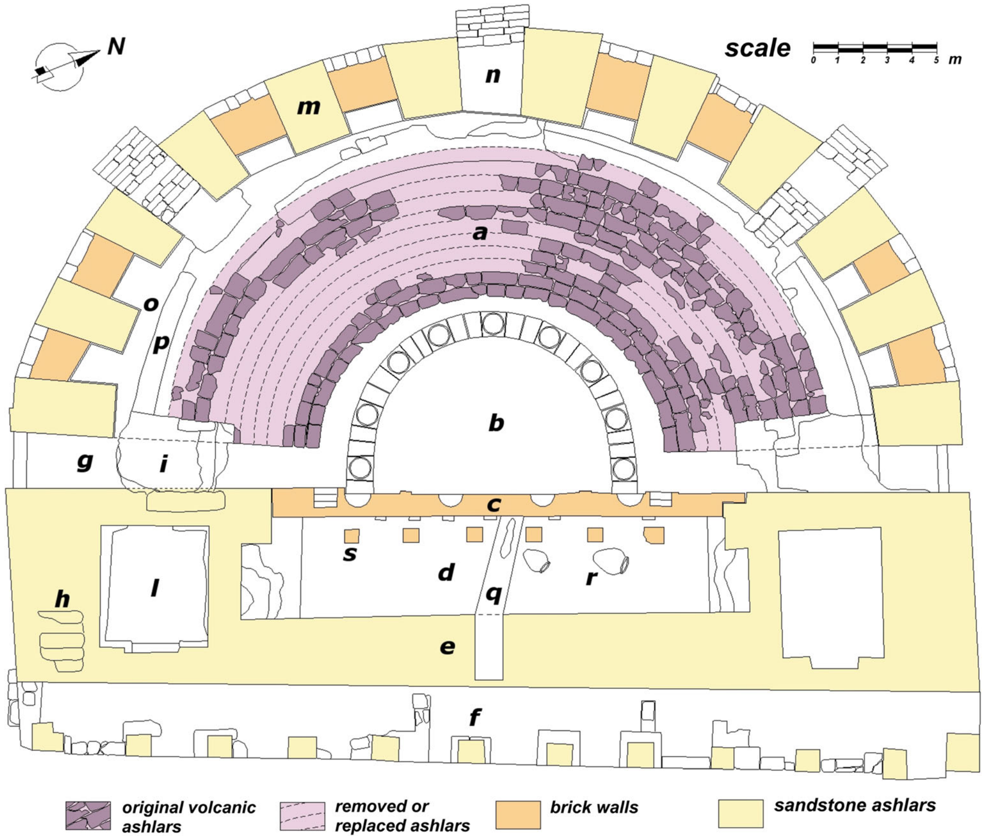

Fig. 3 Plan of the Nora Roman theatre. Legend of sectors: (**a**) *cavea* (auditorium); (**b**) *orchestra*; (**c**) wall of stage; (**d**) *hyposcenium* (space under the *palcoscenium*); (**e**) front scene; (**f**) portico behind the scene; (**g**) west archway entrance; (**h**) access ladder at the west *tribunalia*; (**i**) west *tribunalia*; (**l**) *parasceni*; (**m**) external niches; (**n**) enclosure; (**o**) via (corridor atop the *cavea*); (**p**) scalaria; (**q**) *euripus* (underground channel for water drainage); (**r**) *dolia*; (**s**) small pillars under the *palcoscenium* (from Columbu and Garau 2017, modified)

evidence from Neolithic to Bronze Age processing of obsidian.

More than 250 rock samples from both the outcrops (Mt. Arci and St. Antioco areas) and volcanic glasses of mortars from the main sectors of the theatre were analysed. The results of chemical analysis together with the petrographic characterisation were used in order to (a) geochemical classify the volcanic glasses from the mortars of Nora theatre, according to different diagrams; (b) define compositional inhomogeneity internal to the same glass samples; (c) identify framing of glasses in the magmatic series, analysing the geochemical trend of trace elements and the rare earth pattern; and (d) identify the geographical origin of these glasses employed in the mortars, to understand their supply in Sardinia in the Roman period.

Materials and analytical methods

Fifty pozzolanic volcanic glass fragments of aggregate among 48 selected and representative samples of mortars were analysed and studied. The mortar samples come from the following sectors of the theatre: *tribunalia* (9 samples, divided into 7 concretes of two vaults, 2 bedding mortars of ashlar structure); *cavea* (14 jointing/foundation mortars of volcanic and sandstone ashlars); external niches (16 samples, divided into 9 bedding mortars of outer brick-walls, 3 concrete mortars of inner structure-wall, 2 concrete of basement of via, corridor around the external side of the *cavea*, 1 concrete of only one vault overlying the niche); and *pulpitum* (7 bedding mortars and 4 samples of *arriccio* plasters of the *ribalta* wall and pillar of *hyposcenium*).

The mineralogical and petrographic analysis of volcanic rocks and mortars was performed on thin sections under the polarising microscope (Zeiss photomicroscope Pol II).

The major chemical elements of volcanic glass from the mortars were analysed in thin section under an electron microprobe with a Cambridge S360 scanning electron microscope, equipped with an energy-dispersive spectrometer Link QX2000, Pentafet detector and IBM 686 computer equipped with appropriate software for the acquisition of scanned images. Microanalyses were collected at 15 kV using a 3 μA beam current and a 25 μm spot size.

The analysis of the trace elements (including the full pattern of rare earth) of volcanic glasses included in the mortars was carried out with inductively coupled mass spectrometry combined with laser ablation as a sampling system. It has necessitated an ad hoc sample preparation: some volcanic glass fragments isolated from each mortar sample were embedded in two-component epoxy resin (RenLam M-1, viscosity 1300 mPa s at 25 °C) of cylindrical shape. The obtained test specimen was gradually treated with abrasives of silicon

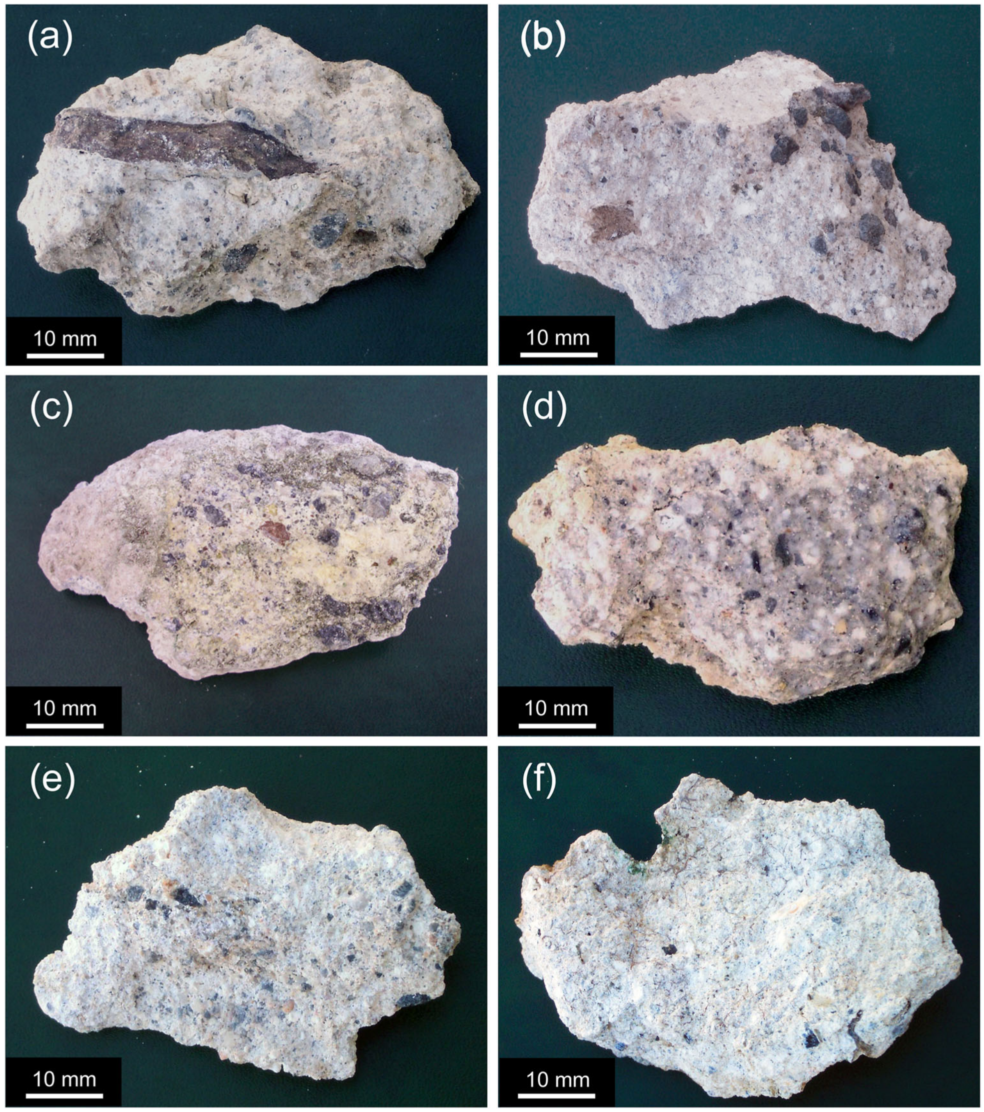

Fig. 4 Mortar samples from different sectors of Nora theatre. (**a**) Bedding mortar of Tirrenian sandstone ashlars of theatre structure with a flattened rock fragment of local Oligo-Miocenic volcanic stone; (**b**) bedding mortar of tier volcanic ashlars belonging to "Su Casteddu" outcrops (see Melis and Columbu 2000; Columbu and Garau 2017); (**c**) mortar sample from Roman concrete of *cavea* foundation; (**d**) entrapment mortar of *caementium* (Roman concrete) from east-side *tribunalia* vault; (**e**) entrapment mortar from Roman concrete of *cavea* foundation; (**f**) joint-mortar taken between the volcanic ashlars of *cavea* tiers

carbide and alumina powders to bring to the surface and polishing the embedded glass fragments. The diameter of the laser beam used is of 40 μm, with a frequency of 10 Hz and a fluence of about 15 J/cm^2. Data reduction was performed using software "Glitter" (Van Achterbergh et al. 1999). As external standards, synthetic glass NIST 610 and BCR-2 basalt have been used, while as a variable, internal standard ^{44}Ca was used. In this method, the intensity signals of the elements depend both on the concentration changes and the mass ablated in subsequent spot. To make independent analysis by mass variations, the internal standard technique with variable concentrations should be used: the concentration of the analyte is a linear function of the intensity ratio of the analyte in the unknown sample relative to that of the reference standard for the same element, with a correction linearly dependent on the ratio of concentration of the same element (internal standard) content in the unknown sample with respect to a fixed concentration of the same element in the reference sample. Consequently, the knowledge for each point analysis of the concentration of internal standard assumes great importance. The glasses, which have been preliminarily subjected to analysis by electron microprobe, were given an average concentration for Ca element of 01.34 ± 0.13 at 1σ. The content ^{29}Si% was used as a variation index (see the diagrams of Fig. 13a–c). Nevertheless, clearly the concentrations in ^{29}Si% (average 49.14%) obtained by this method have a high standard deviation (± 16:24 at 1σ) in relation to the variability of the concentration of calcium in each fragment and are consistently higher than those obtained in the electron microprobe.

The chemical composition of volcanic rock samples from St. Antioco and (a part) from Mt. Arci was determined with a spectrometer in X-ray fluorescence Philips PW1400 with a Rh tube to analyse the major elements and some trace elements (Rb, Sr, Pb, Zn, Y, Nb, Zr), and with a W tube to analyse Ni, Cr, Ba, V, La and Ce. Data reduction of major elements was performed by the method proposed by Franzini et al. (1975). Data reduction of trace elements was performed by the method of Criss (1977), modified. The measurement accuracy is ± 1% for SiO_2, TiO_2, Al_2O_3, Fe_2O_3, CaO, K_2O and MnO and ± 4% for MgO, Na_2O and P_2O_5. The detection limits are about 3 ppm to 3σ for most of the elements; the accuracy of trace elements is ± 2 ÷ 3% to 1000 ppm; ± 5 ÷ 10% at 100 ppm and ± 10 ÷ 20% to 10 ppm. The weight loss for calcination (L.o.I., Loss on Ignition) was determined by calculating the loss in wt.% at 1100 °C, while the FeO was determined by volumetric titration with $KMnO_4$ 10 N in acid solution.

The analysis of the major elements of obsidians and perlites from Mt. Arci was performed by electron probe microanalysis using Wavelength Dispersive Spectrometry with a device ARL-SEMQ, using standards such as silicates and natural oxides; the data reduction was performed with the ZAF method (Colby 1971). Detection limits of ~ 100–300 ppm are readily attained. During a typical multi-element analysis of a few minutes duration, 1σ precision of 0.3–1.5% relative is normally attained for major elements (i.e., those present at concentrations > 1% by weight). If desired, detection limits and precision may both be improved by increasing counting times, by increasing beam current and/or by assigning multiple spectrometers to a single element.

Characteristics of mortar aggregate

At the macroscopic observation, the mortars of the theatre (Fig. 4) show a reddish-grey-black and white/beige-grey aggregate (belonging to volcanic rock fragments and sialic mineral sands, respectively) with variable size and amounts, according to the different mortar functions in the sectors.

The main compositional characteristics of the aggregate determined by microscopic modal analysis are reported in Table 1, along with the binder/aggregate ratio (B/A) expressed in vol.% (by modal analysis) and in wt.% (after mechanical disintegration and acid attack of binder). The mortars show a greatest variability of vol.% B/A, due to the small size of the thin section that did not include the coarse fragments observed macroscopically, which probably do not reflect the real mixing proportions set by the manufacturer. B/A ratio calculated using the wt.% data is much closer to those recommended by ancient sources (0.3–0.5 vol.%; *Vitruvio* Pollione 1521).

The mortar aggregate consists mainly of quartz, orthoclase (Fig. 5e), microcline, plagioclase, black-grey volcanic glasses (Fig. 5a, b) and fragments of purplish volcanic rocks (Fig. 5c) with a local origin (according to Columbu and Garau 2017). Subordinately, crystalline rocks from the Palaeozoic basement (Fig. 5f), occasional mafic crystal-clasts (as pyroxene, Fig. 5d, biotite and opaque oxides), rare bioclasts and fragments of carbonate rocks (e.g., marble, limestone) were also used in the mortars. Not local volcanic glasses were used as aggregate

Table 1 Composition defined by polarized microscope analysis on thin sections of mortar samples taken from *tribunalia*, *cavea*, structure-walls and vault of niches, *hyposcenium* and *pulpitum* (stage) walls (from Columbu and Garau 2017, modified). The binder/aggregate ratio (B/A as wt.% after dissolution of binder and as vol.% by modal analysis) has also been reported

Theatre sector	Mortar function		B/A (wt.%)	B/A (vol.%)	B	± 2 s	A	± 2 s	Qz	± 2 s	Fds	± 2 s	Qz/ Fds	Mafic cryst.	± 2 s	Glass	± 2 s	Volc. rocks	± 2 s	Paleoz. basem.	± 2 s	Coccio-pesto	± 2 s	Bioclast	± 2 s
Tribunalia	Ashlar	Mean	0.97	1.58	59.61	3.98	40.39	3.98	4.88	1.6	4.11	1.31	1.97	0.41	0.37	23.79	3.2	2.77	1.18	2.05	1.05	1.37	0.94	1.01	0.66
	bedding, concrete	± σ	0.41	0.61	9.25	0.89	9.25	0.89	3.92	0.83	4.17	1.04	1.45	0.69	0.47	16.29	1.21	2.25	0.6	1.93	0.61	0.66	0.31	1.05	0.53
Cavea	Bedding of	Mean	0.74	1.54	59.13	3.04	40.87	3.04	13.92	2.12	6.17	1.49	2.34	1.14	0.48	13.42	1.95	1.91	0.73	3.21	0.92	0.63	0.42	0.47	0.38
	ashlars	± σ	0.21	0.49	8.49	0.22	8.49	0.22	5.66	0.37	1.61	0.22	0.85	2.27	0.53	10.17	0.7	1.83	0.46	3.55	0.58	0.72	0.32	0.4	0.21
Niche walls	Bedding of	Mean	0.90	1.48	59.22	3.36	40.78	3.36	10.98	2.01	5.79	1.5	2.09	0.55	0.41	16.06	2.09	2.13	0.82	3.08	1.08	0.96	0.59	1.22	0.62
	bricks	± σ	0.40	0.26	4.25	0.76	4.25	0.76	7.8	0.89	3.7	0.6	1.03	0.52	0.39	12.03	1.08	2.15	0.57	2.62	0.69	0.76	0.3	1.92	0.73
Niche vaults	Roman	Mean	0.80	1.36	57.16	3.21	42.84	3.21	9.24	1.84	4.32	1.25	2.87	0.45	0.4	21.24	2.41	4	1.21	2.2	0.83	0.71	0.48	0.68	0.43
	concrete	± σ	0.27	0.28	4.76	0.34	4.76	0.34	5.38	0.6	3.06	0.54	2.04	0.37	0.16	10.72	0.93	3.13	0.51	1.86	0.5	0.49	0.28	0.67	0.29
Hyposcenium	Bedding of	Mean	0.95	1.03	49.07	3.1	50.93	3.1	14.41	2.19	6.94	1.55	2.21	0.43	0.31	11.26	1.91	7.72	1.68	6.89	1.45	1.17	0.58	2.02	0.88
	brick/stone	± σ	0.60	0.42	10.55	0.68	10.55	0.68	4.54	0.63	2.45	0.18	0.89	0.38	0.21	4.42	0.22	0.31	0.37	4.74	0.45	1.73	0.66	1.3	0.43
Stage wall	Plasters	Mean	2.52	2.38	66.15	2.77	33.85	2.77	15	1.97	5.91	1.37	2.33	0.47	0.36	0.08	0.09	4.68	1.31	4.77	1.27	0.98	0.56	1.97	0.84
	(*arriccio*)	± σ	1.59	1.15	16.71	0.26	16.71	0.26	13.04	0.27	3.74	0.14	0.5	0.51	0.32	0.16	0.19	1.28	0.32	2.04	0.21	0.75	0.38	0.68	0.17

B, binder; A, aggregate; Qz, quartz; Fds, feldspar; Paleoz. Basem., Palaeozoic crystalline basement; σ, standard deviation; ±2 s, absolute error

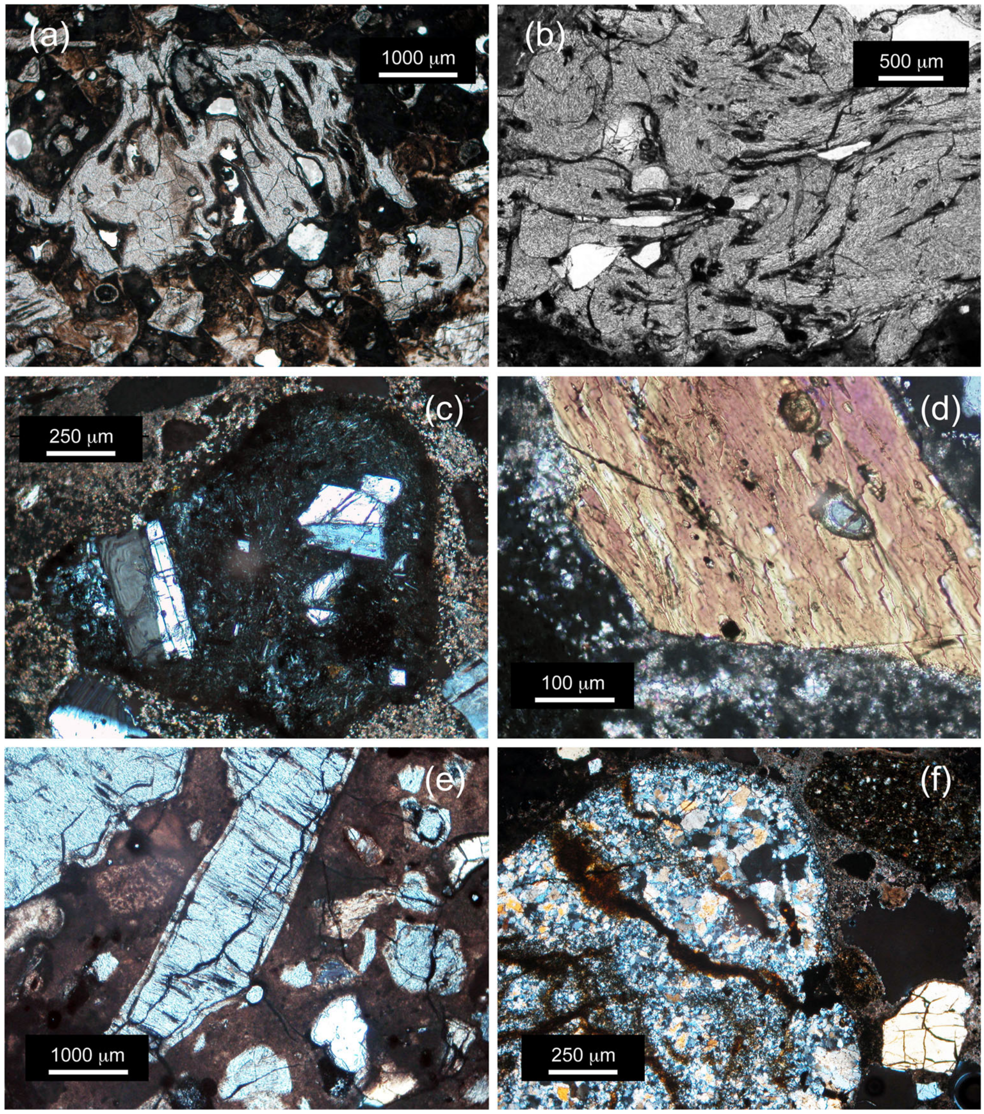

Fig. 5 Photograph details of mortar aggregate on polarized microscope. (**a**, **b**) Plain polars: fragment of volcanic glass with evident vacuolar (and fluidal) structure and borders of reaction with the binder; (**c**) cross Nicol: fragment of local Oligo-Miocenic dacitic volcanic rock with binder-reaction borders; (**d**) plain polars: orthopyroxene crystal; (**e**) cross Nicol: altered orthoclase crystals; (**f**) cross Nicol: rounded fragment of meta-sandstone from Palaeozoic crystalline basement

but also with pozzolanic function, as highlighted by the reaction edges with the binder (Figs. 5a and 6b). Then, *cocciopesto* has also been used as pozzolanic material but overall in very low percentages (Table 1). The binder consists mainly of calcite, often present as spherules (Fig. 6d), where occasionally there are immersed lumps of bad-carbonated lime (Fig. 6c).

The local volcanic rocks belong to the Sarroch-Pula volcanism, related to the Late Eocene–Miocene Sardinian magmatic activity that occurred between 38 and 15 Ma (Advokaat et al. 2014; Antonelli et al. 2014a; Beccaluva et al. 1985, 1989, 1994, 2005a, b, 2011; Cherchi et al. 2008; Columbu et al. 2011; Lustrino et al. 2004, 2009, 2011, 2013). Considering the medium-coarse size, it is probably that the purplish volcanic rocks were used mainly as (inert-) aggregate, although they also show pozzolanic characteristics (Figs. 5c and 6a) (see Türkmenoglu and Tankut 2002).

The different distribution of the main components in the aggregate has been showed in the ternary diagram of Fig. 7 where the modal percentages of quartz (Qz), feldspar (Fds) and volcanic glass (V) were reported. The volcanic glasses were used in almost all samples in varying proportions, according to the function of mortar in the theatre; they are less present in the plasters while they are more abundant in the structural concretes of *cavea* foundation and of the *tribunalia* vaults, where in some cases represent about 90% of the aggregate.

The sandy component is widely used in the bedding mortars of the wall bricks and in the plasters (Fig. 7), while it is found less frequently in the concretes of the *tribunalia* vaults and variously present in the *cavea* samples and external niches. It shows an almost constant ratio of quartz and feldspar (2:1, Fig. 7) in almost all mortar samples thus highlighting a unique sampling point of these sands (Columbu and Garau 2017).

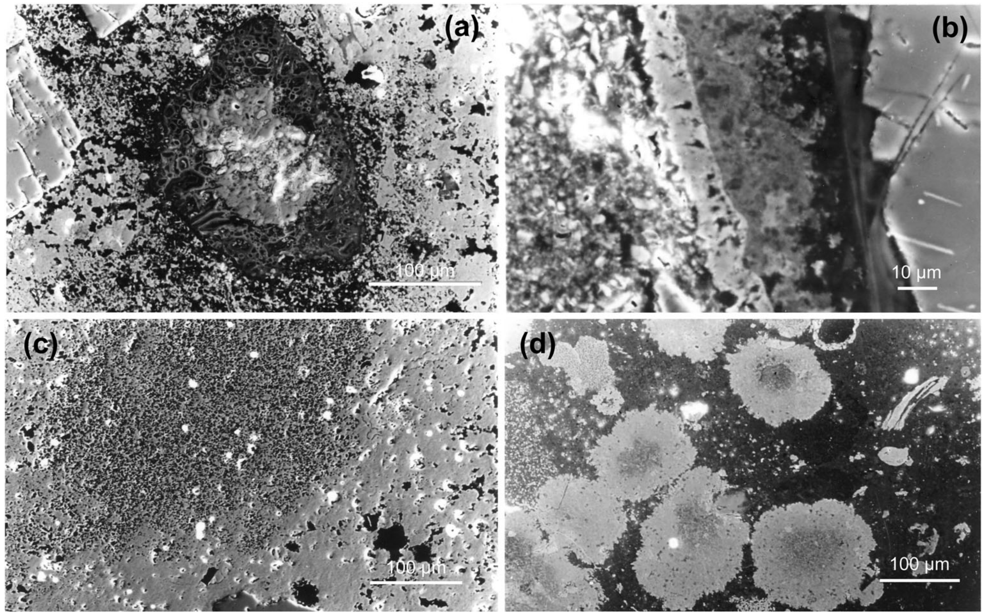

Fig. 6 Photograph details of mortars on electronic microscope (SEM). (**a**) Binder-reaction borders between volcanic aggregate and binder; (**b**) binder-reaction borders between a fragment of volcanic glass and the binder; (**c**) lump of bad-carbonated lime; (**d**) spherules of calcite

Regarding the particle size, according to the Folk (1968) classification, the aggregate is made from sand, slightly gravelled sands, gravelly sands and, in some cases, sandy gravel, while according to the Wentworth (1922)

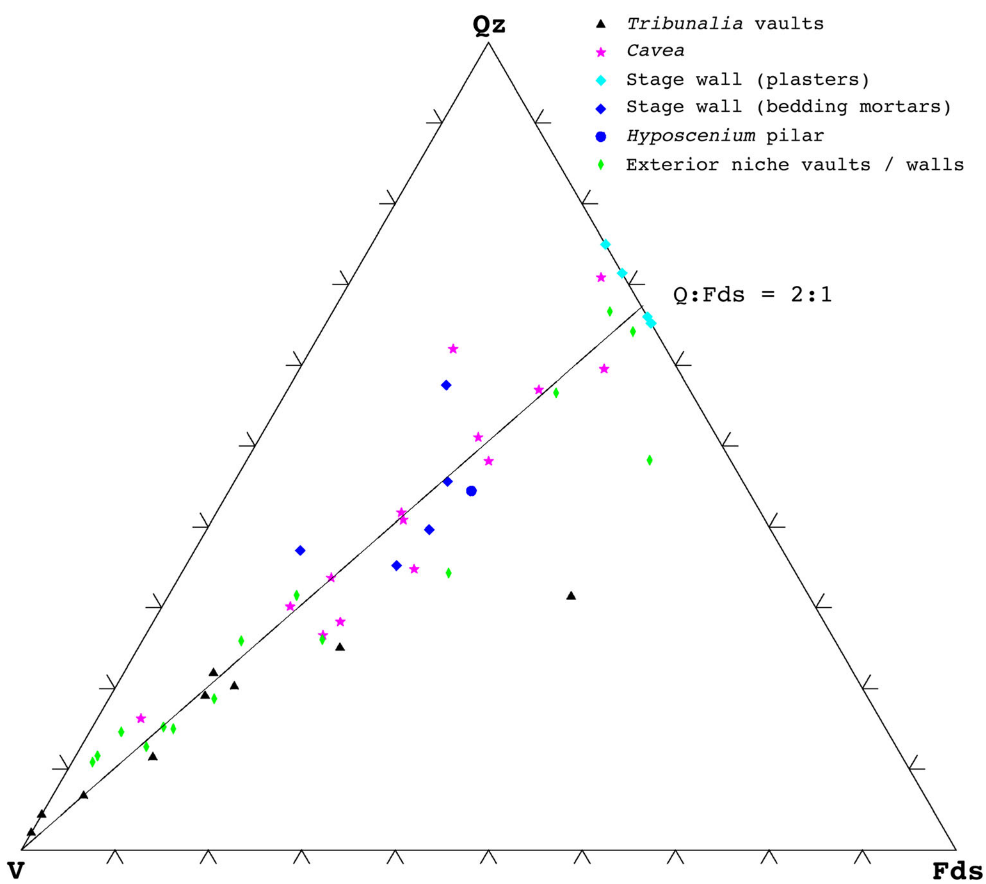

Fig. 7 Aggregate compositional distribution of quartz (Qz), feldspar (Fds) and volcanic glass (V) in the mortars from different sectors of the theatre (from Columbu and Garau 2017, modified)

Table 2 Chemical analysis of volcanic glasses from the theatre mortars, where reported the rock classification (according to De La Roche et al. 1980), wt.% of major elements and C.I.P.W. norm according to Cross et al. (1903)

	1	2	3	4	5	6	7	8	9	10	11	12	13	14	15	16	17	18	19	20	21	22	23	24	25
Sample	Sp142	Sp19	Sp4	Sp120	Sp7	Sp129	Sp2	Sp22	Sp18	Sp1	Sp32	Sp3	Sp23	Sp35	Sp34	Sp138	Sp8	Sp144	Sp128	Sp143	Sp177	Sp114	Sp70	Sp125	Sp154
Class.	Rhy	Rhy	Rhy	Rhy	Rhy	Rhy	Rhy	Rhy	Rhy	Rhy	Rhy	Rhy	Rhy	Rhy	Rhy	Rhy	Rhy	Rhy	Rhy	Rhy	Rhy	Rhy	Rhy	Rhy	Rhy
SiO_2	71.58	74.22	72.53	71.65	72.23	72.69	73.19	70.54	71.65	72.75	73.33	73.81	72.04	72.70	73.78	74.41	72.46	75.13	75.07	74.45	74.49	74.32	75.04	75.17	74.79
TiO_2	0.17	0.19	0.12	0.18	0.29	0.08	0.23	0.16	0.11	0.19	0.07	0.07	0.18	0.29	0.11	0.13	0.05	0.21	0.21	0.15	0.09	0.15	0.08	0.12	0.15
Al_2O_3	17.27	16.13	16.13	17.78	16.13	16.50	16.11	17.49	17.69	16.65	15.82	15.84	15.47	16.09	15.11	14.28	16.60	14.48	14.07	14.42	14.09	14.09	13.96	14.11	14.16
Fe_2O_3	1.31	1.07	1.61	1.15	1.43	1.55	1.28	1.19	0.88	0.92	1.28	1.15	1.75	1.06	1.20	1.23	0.96	1.12	1.47	1.39	1.18	1.37	1.35	1.10	1.33
FeO	n.d.	n.d.	n.d.	n.d.	n.d.	n.d.	n.d.	n.d.	n.d.	n.d.	n.d.	n.d.	n.d.	n.d.	n.d.	n.d.	n.d.	n.d.	n.d.	n.d.	n.d.	n.d.	n.d.	n.d.	n.d.
MnO	0.05	0.14	0.02	0.05	0.07	0.04	0.02	0.11	n.d.	0.08	0.07	0.10	0.03	0.12	0.15	n.d.	n.d.	n.d.	n.d.	0.16	0.18	0.13	0.09	0.12	n.d.
MgO	0.07	0.15	0.16	0.05	0.17	0.12	0.09	0.06	0.07	0.06	n.d.	0.01	0.25	0.08	0.10	n.d.	0.04	0.13	0.07	n.d.	0.11	0.06	0.03	0.05	0.21
CaO	1.39	1.21	1.56	1.11	1.57	1.27	1.42	1.44	1.56	1.33	1.49	1.29	1.38	1.22	1.35	1.83	1.36	1.30	1.36	1.37	1.37	1.37	1.34	1.43	1.33
Na_2O	2.13	1.82	2.68	1.98	2.82	2.43	2.33	2.83	3.39	2.58	2.73	2.40	2.74	2.83	2.88	3.55	2.79	2.71	2.68	3.06	3.04	3.13	3.00	2.77	3.25
K_2O	5.18	4.40	4.37	5.11	4.54	4.65	4.48	5.39	3.97	4.59	4.65	4.59	5.49	4.75	4.87	3.99	4.93	4.66	4.67	4.74	4.80	4.69	4.80	4.73	4.63
P_2O_5	0.43	0.44	0.66	0.61	0.50	0.47	0.62	0.51	0.67	0.54	0.35	0.47	0.40	0.54	0.23	0.31	0.67	0.12	0.28	0.17	0.20	0.27	0.02	0.28	0.08
L.o.I.	--	--	--	--	--	--	--	--	--	--	--	--	--	--	--	--	--	--	--	--	--	--	--	--	--
Total	99.58	99.77	99.84	99.67	99.75	99.80	99.77	99.72	99.99	99.69	99.79	99.73	99.73	99.68	99.78	99.73	99.86	99.86	99.88	99.91	99.55	99.58	99.71	99.88	99.93
S.I.	0.82	2.04	1.84	0.61	1.92	1.39	1.12	0.64	0.85	0.74	0.00	0.12	2.48	0.93	1.12	0.00	0.46	1.53	0.80	0.00	1.22	0.66	0.33	0.58	2.26
A.I.	0.53	0.48	0.57	0.49	0.59	0.55	0.54	0.60	0.56	0.55	0.60	0.56	0.68	0.61	0.66	0.71	0.60	0.66	0.67	0.70	0.72	0.73	0.73	0.69	0.73
Q	36.78	44.59	37.58	39.23	35.52	38.26	40.43	31.01	34.72	38.27	36.65	40.09	31.92	36.32	35.21	34.79	35.73	38.36	38.63	35.18	35.09	35.06	35.51	37.92	34.52
C	6.66	7.23	5.74	8.43	4.92	6.29	6.33	5.60	6.58	6.31	4.43	5.70	3.47	5.37	3.20	1.54	5.81	2.90	2.80	2.17	1.88	2.02	1.44	2.50	1.58
Or	30.61	26.00	25.82	30.20	26.83	27.48	26.47	31.85	23.46	27.12	27.48	27.12	32.44	28.07	28.78	23.58	29.13	27.54	27.60	28.01	28.36	27.71	28.36	27.95	27.36
Ab	18.02	15.40	22.68	16.75	23.86	20.56	19.71	23.94	28.68	21.83	23.10	20.31	23.18	23.94	24.37	30.04	23.61	22.93	22.68	25.89	25.72	26.48	25.38	23.44	27.50
An	4.09	3.13	3.43	1.52	4.52	3.23	2.99	3.81	3.36	3.07	5.10	3.33	4.23	2.52	5.19	7.05	2.37	5.67	4.92	5.69	5.49	5.03	6.52	5.26	6.08
Ac	0	0	0	0	0	0	0	0	0	0	0	0	0	0	0	0	0	0	0	0	0	0	0	0	0
Ns	0	0	0	0	0	0	0	0	0	0	0	0	0	0	0	0	0	0	0	0	0	0	0	0	0
Di	0	0	0	0	0	0	0	0	0	0	0	0	0	0	0	0	0	0	0	0	0	0	0	0	0
Ed	0	0	0	0	0	0	0	0	0	0	0	0	0	0	0	0	0	0	0	0	0	0	0	0	0
Sl	0	0	0	0	0	0	0	0	0	0	0	0	0	0	0	0	0	0	0	0	0	0	0	0	0
En	0.17	0.37	0.40	0.12	0.42	0.30	0.22	0.15	0.17	0.15	0.00	0.02	0.62	0.20	0.25	0.00	0.10	0.32	0.17	0.00	0.27	0.15	0.07	0.12	0.52
Fs	1.59	1.40	2.02	1.36	1.59	2.05	1.39	1.56	1.01	1.08	1.75	1.63	2.13	1.18	1.73	1.46	1.22	1.17	1.65	1.94	1.79	1.85	1.87	1.52	1.56
Hy	1.76	1.77	2.42	1.48	2.02	2.35	1.62	1.71	1.19	1.23	1.75	1.66	2.76	1.38	1.98	1.46	1.32	1.50	1.82	1.94	2.06	2.00	1.94	1.64	2.08
Mt	0.23	0.18	0.28	0.20	0.25	0.27	0.22	0.21	0.15	0.16	0.22	0.20	0.30	0.18	0.21	0.21	0.17	0.19	0.25	0.24	0.20	0.24	0.23	0.19	0.23
Il	0.32	0.36	0.23	0.34	0.55	0.15	0.44	0.30	0.21	0.36	0.13	0.13	0.34	0.55	0.21	0.25	0.09	0.40	0.40	0.28	0.17	0.28	0.15	0.23	0.28
Ap	1.00	1.02	1.53	1.41	1.16	1.09	1.44	1.18	1.55	1.25	0.81	1.09	0.93	1.25	0.53	0.72	1.55	0.28	0.65	0.39	0.46	0.63	0.05	0.65	0.19
D.I.	85.4	86.0	86.1	86.2	86.2	86.3	86.6	86.8	86.9	87.2	87.2	87.5	87.6	88.3	88.4	88.4	88.5	88.8	88.9	89.1	89.2	89.3	89.3	89.3	89.4
SAL	96.2	96.3	95.2	96.1	95.7	95.8	95.9	96.2	96.8	96.6	96.8	96.6	95.3	96.2	96.8	97.0	96.6	97.4	96.6	96.9	96.6	96.3	97.2	97.1	97.0
FEM	3.3	3.3	4.5	3.4	4.0	3.9	3.7	3.4	3.1	3.0	2.9	3.1	4.3	3.4	2.9	2.6	3.1	2.4	3.1	2.9	2.9	3.2	2.4	2.7	2.8

	26	27	28	29	30	31	32	33	34	35	36	37	38	39	40	41	42	43	44	45	46	47	48	49	50
Sample	Sp140	Sp50	Sp51	Sp130	Sp83	Sp145	Sp126	Sp141	Sp152	Sp94	Sp134	Sp25	Sp169	Sp165	Sp121	Sp166	Sp155	Sp71	Sp77	Sp82	Sp91	Sp10	Sp81	Sp156	Sp101
Class.	Rhy	Rhy	Rhy	Rhy	Rhy	Rhy	Rhy	Rhy	Rhy	Rhy	Rhy	Rhy	Rhy	Rhy	Rhy	Rhy	Rhy	Rhy	Rhy	Rhy	Rhy	Rhy	Rhy	Rhy	Rhy
SiO_2	75.34	74.84	74.06	74.66	74.85	75.31	75.46	74.74	75.35	75.31	75.22	72.52	75.24	74.98	74.9	75.25	75.18	75.05	74.87	75.16	75.25	74.69	75.02	74.89	74.7
TiO_2	0.26	0.24	0.33	0.07	0.24	0.07	0.28	0.11	0.14	0.14	0.13	0.24	0.18	0.06	0.19	0.2	0.07	0.2	0.17	n.d.	0.14	0.17	0.16	0.31	0.09
Al_2O_3	14.09	14.12	13.88	14.24	14.22	14	14.1	14.31	13.88	14.06	13.93	15.63	13.92	13.85	13.7	13.89	13.82	13.92	14.02	13.86	13.91	14.64	13.84	13.75	14.22
Fe_2O_3	1.13	1.2	1.36	1.4	1.15	1.28	0.98	1.26	1.15	1.02	1.12	1.08	1.1	1.17	1.22	1.07	1.22	0.85	1.14	1.15	0.98	0.78	0.86	1.04	0.88
FeO	n.d.	n.d.	n.d.	n.d.	n.d.	n.d.	n.d.	n.d.	n.d.	n.d.	n.d.	n.d.	n.d.	n.d.	n.d.	n.d.	n.d.	n.d.	n.d.	n.d.	n.d.	n.d.	n.d.	n.d.	n.d.
MnO	0.06	0.02	0.26	n.d.	0.22	n.d.	0.07	n.d.	0.21	0.05	n.d.	0.14	n.d.	0.03	n.d.	0.01	0.07	0.1	0.04	0.11	0.14	n.d.	0.05	n.d.	n.d.
MgO	0.03	0.11	0.06	0.03	0.01	0.03	n.d.	0.09	0.05	0.02	0.07	0.13	n.d.	0.07	0.04	0.05	n.d.	0.05	0.02	0.1	0.07	n.d.	n.d.	n.d.	0.04
CaO	1.37	1.26	1.47	1.37	1.29	1.34	1.33	1.27	1.23	1.32	1.4	1.05	1.46	1.4	1.33	1.29	1.4	1.33	1.28	1.27	1.18	1.25	1.31	1.18	1.06
Na_2O	2.46	2.8	3.56	3	3.03	2.87	2.54	2.77	2.86	2.37	2.97	3.01	2.92	3.15	2.65	3.11	3.25	3.02	3.26	3.3	3.14	3.07	2.9	2.75	3.02
K_2O	4.91	4.98	4.63	4.98	4.64	4.57	4.73	4.98	4.81	5.36	4.7	5.57	4.64	4.84	5.25	4.75	4.67	4.96	4.78	4.67	4.81	4.86	5.35	5.76	5.42
P_2O_5	0.3	0.08	0.14	0.12	0.2	0.31	0.33	0.28	0.11	0.16	0.22	0.32	0.36	0.28	0.42	0.2	0.3	0.23	0.24	0.3	0.18	0.4	0.31	0.12	0.3
L.o.I.	--	--	--	--	--	--	--	--	--	--	--	--	--	--	--	--	--	--	--	--	--	--	--	--	--
Totale	99.95	99.65	99.75	99.87	99.85	99.78	99.82	99.81	99.79	99.81	99.76	99.69	99.82	99.83	99.70	99.82	99.98	99.71	99.82	99.92	99.80	99.86	99.80	99.80	99.73
S.I.	0.36	1.22	0.63	0.32	0.11	0.35	0.00	1.00	0.57	0.23	0.80	1.34	0.00	0.77	0.44	0.56	0.00	0.57	0.22	1.10	0.79	0.00	0.00	0.00	0.43
A.I.	0.66	0.71	0.78	0.73	0.70	0.69	0.66	0.70	0.71	0.69	0.72	0.70	0.71	0.75	0.73	0.74	0.75	0.74	0.75	0.76	0.75	0.70	0.76	0.78	0.76
Q	39.56	36.28	31.98	34.70	36.54	38.35	40.21	36.81	37.13	38.04	36.88	31.55	37.84	35.12	37.06	36.19	35.49	35.77	34.91	35.27	35.84	36.33	35.29	34.25	34.43
C	2.96	2.02	0.67	1.71	2.35	2.64	3.17	2.72	2.00	2.34	1.94	3.51	2.30	1.55	2.25	1.77	1.59	1.72	1.73	1.79	1.82	3.01	1.64	1.13	2.18
Or	29.01	29.43	27.36	29.43	27.42	27.00	27.95	29.43	28.42	31.67	27.77	32.91	27.42	28.60	31.02	28.07	27.60	29.31	28.25	27.60	28.42	28.72	31.61	34.04	32.03
Ab	20.81	23.69	30.12	25.38	25.64	24.28	21.49	23.44	24.20	20.05	25.13	25.47	24.71	26.65	22.42	26.31	27.50	25.55	27.58	27.92	26.57	25.98	24.54	23.27	25.55
An	4.84	5.73	6.38	6.01	5.09	4.62	4.44	4.47	5.38	5.50	5.51	3.12	4.89	5.12	3.85	5.09	4.99	5.10	4.78	4.34	4.68	3.59	4.47	5.07	3.30
Ac	0	0	0	0	0	0	0	0	0	0	0	0	0	0	0	0	0	0	0	0	0	0	0	0	0
Ns	0	0	0	0	0	0	0	0	0	0	0	0	0	0	0	0	0	0	0	0	0	0	0	0	0
Di	0	0	0	0	0	0	0	0	0	0	0	0	0	0	0	0	0	0	0	0	0	0	0	0	0
Ed	0	0	0	0	0	0	0	0	0	0	0	0	0	0	0	0	0	0	0	0	0	0	0	0	0
Sl	0	0	0	0	0	0	0	0	0	0	0	0	0	0	0	0	0	0	0	0	0	0	0	0	0
En	0.07	0.27	0.15	0.07	0.02	0.07	0.00	0.22	0.12	0.05	0.17	0.32	0.00	0.17	0.10	0.12	0.00	0.12	0.05	0.25	0.17	0.00	0.00	0.00	0.10
Fs	1.22	1.27	1.78	1.78	1.57	1.62	1.00	1.53	1.72	1.25	1.31	1.33	1.20	1.54	1.34	1.14	1.67	1.01	1.34	1.77	1.36	0.78	1.00	0.90	1.05
Hy	1.29	1.54	1.93	1.86	1.60	1.70	1.00	1.75	1.84	1.30	1.48	1.65	1.20	1.72	1.44	1.27	1.67	1.13	1.39	2.01	1.53	0.78	1.00	0.90	1.15
Mt	0.19	0.21	0.23	0.24	0.20	0.22	0.17	0.22	0.20	0.18	0.19	0.19	0.19	0.20	0.21	0.18	0.21	0.15	0.20	0.20	0.17	0.13	0.15	0.18	0.15
Il	0.49	0.46	0.63	0.13	0.46	0.13	0.53	0.21	0.27	0.27	0.25	0.46	0.34	0.11	0.36	0.38	0.13	0.38	0.32	0.00	0.27	0.32	0.30	0.59	0.17
Ap	0.70	0.19	0.32	0.28	0.46	0.72	0.76	0.65	0.25	0.37	0.51	0.74	0.83	0.65	0.97	0.46	0.70	0.53	0.56	0.70	0.42	0.93	0.72	0.28	0.70
D.I.	89.4	89.4	89.5	89.5	89.6	89.6	89.7	89.7	89.8	89.8	89.8	89.9	90.0	90.4	90.5	90.6	90.6	90.6	90.7	90.8	90.8	91.0	91.5	91.6	92.0
SAL	97.2	97.2	96.5	97.2	97.0	96.9	97.3	96.9	97.1	97.6	97.2	96.6	97.2	97.0	96.6	97.4	97.2	97.4	97.3	96.9	97.3	97.6	97.6	97.8	97.5
FEM	2.7	2.4	3.1	2.5	2.7	2.8	2.5	2.8	2.6	2.1	2.4	3.0	2.6	2.7	3.0	2.3	2.7	2.2	2.5	2.9	2.4	2.2	2.2	2.0	2.2

S.I. (wt.% solidification index of Kuno 1968) = (MgO · 100) / (MgO + FeO_{tot} + Na_2O + K_2O); A.I. (Agpaitic Index of Shand 1951) = (Na_2O + K_2O) / Al_2O_3; D.I. (Differentiation Index of Thornton and Tuttle 1960) = normative Q + Ab + Or + Ne + Kp + Lc; SAL, sum of sialic minerals; FEM, sum of mafic minerals; n.d., not detected; Rhy, rhyolite; alRhy, alkali-rhyolite

Table 3 Chemical analysis of selected volcanic rocks from Monte Arci (central-western Sardinia), where reported the rock classification (according to De La Roche et al. 1980), wt% of major elements and C.I.P.W. norm according to Cross et al. (1903)

	1	2	3	4	5	6	7	8	9	10	11	12	13	14	15	16	17	18	19	20	21	22	23	24	25
Class.	Rhy	Alrhy	AlRhy	AlRhy	AlRhy	AlRhy	AlRhy	AlRhy	AlRhy	AlRhy	AlRhy	AlRhy	AlRhy	AlRhy	AlRhy	AlRhy	AlRhy	AlRhy	AlRhy	AlRhy	Rhy	Rhy	Rhy	Rhy	Rhy
SiO_2	74.99	72.49	75.53	75.58	74.07	74.93	75.47	75.54	75.65	75.02	75.12	75.53	74.88	75.45	74.93	74.80	73.04	73.00	74.34	74.12	71.99	73.28	73.76	73.91	75.47
TiO_2	0.10	0.10	0.09	0.08	0.16	0.12	0.14	0.14	0.10	0.13	0.13	0.07	0.09	0.11	0.10	0.10	0.12	0.08	0.12	0.10	0.13	0.18	0.14	0.09	0.16
Al_2O_3	13.64	12.08	12.32	12.44	12.21	12.34	12.46	12.41	12.39	12.36	12.43	12.21	12.58	12.43	12.38	12.18	13.26	13.24	13.56	13.28	13.38	13.03	13.37	13.32	13.47
Fe_2O_3	1.24	1.25	1.27	1.32	1.27	1.29	1.39	1.25	1.30	1.28	1.27	1.24	1.36	1.29	1.29	1.33	1.24	1.22	1.18	1.17	1.12	1.02	1.14	1.04	0.94
FeO	n.d.	n.d.	n.d.	n.d.	n.d.	n.d.	n.d.	n.d.	n.d.	n.d.	n.d.	n.d.	n.d.	n.d.	n.d.	n.d.	n.d.	n.d.	n.d.	n.d.	n.d.	n.d.	n.d.	n.d.	n.d.
MnO	0.10	0.02	0.09	0.06	0.06	0.08	0.07	0.06	0.07	0.03	0.08	0.09	0.07	0.08	0.08	0.07	0.03	0.05	0.08	0.08	0.07	0.08	0.03	0.03	0.04
MgO	0.08	0.06	0.05	0.05	0.02	0.02	0.02	0.05	0.01	0.06	0.05	n.d.	0.05	0.02	0.06	0.07	0.09	0.04	0.08	0.06	0.06	0.12	0.14	0.09	0.07
CaO	0.60	0.44	0.47	0.49	0.45	0.47	0.45	0.45	0.47	0.48	0.46	0.47	0.45	0.45	0.46	0.46	0.60	0.61	0.60	0.58	0.59	0.62	0.62	0.64	0.65
Na_2O	2.54	4.33	4.32	4.31	4.29	4.27	4.26	4.16	4.14	4.11	3.63	3.36	3.33	3.27	3.02	2.97	3.48	3.28	3.21	2.67	2.06	2.14	2.49	2.51	2.77
K_2O	5.51	5.04	5.05	5.05	5.02	5.08	5.16	5.11	5.07	5.16	5.11	5.10	5.15	5.12	5.02	5.07	5.41	5.45	5.45	5.44	5.15	5.71	5.95	5.90	6.09
P_2O_5	n.d.	n.d.	n.d.	n.d.	n.d.	n.d.	n.d.	n.d.	n.d.	n.d.	n.d.	n.d.	n.d.	n.d.	n.d.	n.d.	n.d.	n.d.	n.d.	n.d.	n.d.	n.d.	n.d.	n.d.	0.02
L.o.I.	–	–	–	–	–	–	–	–	–	–	–	–	–	–	–	–	–	–	–	–	–	–	–	–	–
Total	98.80	95.81	99.19	99.38	97.55	98.60	99.42	99.17	99.20	98.63	98.28	98.07	97.96	98.22	97.34	97.05	97.27	96.97	98.62	97.50	94.55	96.18	97.64	97.53	99.68
S.I.	0.86	0.57	0.47	0.47	0.19	0.19	0.19	0.48	0.10	0.57	0.50	0.00	0.51	0.21	0.65	0.75	0.89	0.40	0.82	0.65	0.72	1.35	1.46	0.95	0.72
A.I.	0.74	1.04	1.02	1.01	1.02	1.01	1.01	1.00	0.99	1.00	0.93	0.90	0.88	0.88	0.84	0.85	0.87	0.85	0.82	0.77	0.67	0.74	0.79	0.79	0.83
Q	36.95	27.99	30.22	29.89	29.28	29.65	29.77	30.49	30.81	30.04	32.64	34.67	33.93	35.06	36.29	36.23	29.98	30.96	32.70	35.73	38.29	36.91	34.35	34.63	34.12
C	2.41	0.00	0.00	0.00	0.00	0.00	0.00	0	0	0	0.09	0.31	0.71	0.69	1.14	0.97	0.59	0.84	1.29	1.95	3.34	2.20	1.71	1.64	1.19
Or	32.56	29.78	29.84	29.84	29.66	30.02	30.49	30.20	29.96	30.49	30.20	30.14	30.43	30.25	29.66	29.96	31.97	32.20	32.20	32.15	30.43	33.74	35.16	34.86	35.99
Ab	21.49	34.07	35.25	35.87	34.85	35.19	35.36	35.20	35.03	34.78	30.71	28.43	28.18	27.67	25.55	25.13	29.44	27.75	27.16	22.59	17.43	18.11	21.07	21.24	23.44
An	2.98	0.00	0.00	0.00	0.00	0.00	0.00	0.10	0.25	0.04	2.28	2.33	2.23	2.23	2.28	2.28	2.98	3.03	2.98	2.88	2.93	3.08	3.08	3.17	3.09
Ac	0	0.43	0.44	0.45	0.44	0.44	0.48	0	0	0	0	0	0	0	0	0	0	0	0	0	0	0	0	0	0
Ns	0	0.48	0.19	0.02	0.22	0.10	0.03	0	0	0	0	0	0	0	0	0	0	0	0	0	0	0	0	0	0
Di	0	0.18	0.15	0.15	0.06	0.06	0.06	0.16	0.03	0.20	0	0	0	0	0	0	0	0	0	0	0	0	0	0	0
Ed	0	1.74	1.91	2.00	1.92	2.01	1.93	1.73	1.82	1.86	0	0	0	0	0	0	0	0	0	0	0	0	0	0	0
Sl	0	1.92	2.06	2.15	1.98	2.07	1.98	1.88	1.85	2.06	0	0	0	0	0	0	0	0	0	0	0	0	0	0	0
En	0.20	0.07	0.06	0.05	0.02	0.02	0.02	0.05	0.01	0.06	0.12	0.00	0.12	0.05	0.15	0.17	0.22	0.10	0.20	0.15	0.15	0.30	0.35	0.22	0.17
Fs	1.70	0.76	0.85	0.84	0.68	0.76	0.90	0.66	0.76	0.59	1.66	1.74	1.83	1.72	1.73	1.77	1.54	1.62	1.55	1.57	1.44	1.24	1.37	1.32	1.09
Hy	1.90	0.83	0.91	0.89	0.70	0.78	0.92	0.71	0.77	0.65	1.78	1.74	1.95	1.77	1.88	1.94	1.77	1.72	1.75	1.72	1.59	1.54	1.72	1.54	1.26
Mt	0.21	0.00	0.00	0.00	0.00	0.00	0.00	0.22	0.22	0.22	0.22	0.21	0.23	0.22	0.22	0.23	0.21	0.21	0.20	0.20	0.19	0.18	0.20	0.18	0.16
Il	0.19	0.19	0.17	0.15	0.30	0.23	0.27	0.27	0.19	0.25	0.25	0.13	0.17	0.21	0.19	0.19	0.23	0.15	0.23	0.19	0.25	0.34	0.27	0.17	0.30
Ap	0.00	0.00	0.00	0.00	0.00	0.00	0.00	0.00	0.00	0.00	0.00	0.00	0.00	0.00	0.00	0.00	0.00	0.00	0.00	0.00	0.00	0.00	0.00	0.00	0.05
D.I.	91.0	91.8	95.3	95.6	93.8	94.9	95.6	95.9	95.8	95.3	93.6	93.2	92.5	93.0	91.5	91.3	91.4	90.9	92.1	90.5	86.2	88.8	90.6	90.7	93.5
SAL	96.4	91.8	95.3	95.6	93.8	94.9	95.6	96.0	96.1	95.3	95.9	95.9	95.5	95.9	94.9	94.6	95.0	94.8	96.3	95.3	92.4	94.0	95.4	95.6	97.8
FEM	2.3	3.9	3.8	3.7	3.6	3.6	3.7	3.1	3.0	3.2	2.3	2.1	2.4	2.2	2.3	2.4	2.2	2.1	2.2	2.1	2.0	2.1	2.2	1.9	1.8
	1	2	3	4	5	6	7	8	9	10	11	12	13	14	15	16	17	18	19	20	21	22	23	24	25
Class.	AlRhy	AlRhy	AlRhy	AlRhy	AlRhy	AlRhy	AlRhy	AlRhy	AlRhy	AlRhy	AlRhy	AlRhy	AlRhy	AlRhy	AlRhy	AlRhy	AlRhy	AlRhy	AlRhy	AlRhy	AlRhy	AlRhy	AlRhy	AlRhy	AlRhy
SiO_2	75.70	75.72	75.39	75.69	75.52	75.49	75.67	75.43	75.57	75.43	75.18	75.57	75.25	75.59	75.61	75.42	75.84	75.57	75.29	75.68	75.48	75.34	75.54	75.50	75.40
TiO_2	0.11	0.11	0.11	0.11	0.11	0.11	0.08	0.11	0.11	0.12	0.11	0.11	0.11	0.11	0.11	0.11	0.11	0.11	0.11	0.11	0.11	0.12	0.11	0.11	0.11
Al_2O_3	13.07	13.07	13.11	12.98	13.04	13.19	13.07	13.05	13.07	13.01	13.11	12.91	13.03	12.94	13.12	12.99	12.85	13.06	13.07	13.04	12.98	13.09	13.05	13.00	12.97
Fe_2O_3	0.31	0.17	0.32	0.31	0.32	0.29	0.32	0.39	0.33	0.30	0.37	0.34	0.44	0.22	0.27	0.48	0.39	0.32	0.42	0.30	0.24	0.58	0.23	0.30	0.24
FeO	1.18	1.30	1.20	1.21	1.18	1.22	1.16	1.14	1.16	1.23	1.13	1.14	1.11	1.27	1.25	1.05	1.11	1.17	1.16	1.19	1.23	0.99	1.28	1.20	1.25
MnO	0.07	0.07	0.07	0.07	0.07	0.08	0.07	0.07	0.07	0.07	0.07	0.07	0.07	0.07	0.07	0.07	0.07	0.07	0.07	0.07	0.07	0.07	0.07	0.07	0.07
MgO	0.07	0.11	0.09	0.08	0.10	0.08	0.07	0.11	0.09	0.08	0.10	0.17	0.08	0.07	n.d.	0.05	0.07	0.08	0.07	0.07	0.06	0.09	n.d.	0.07	0.08
CaO	0.60	0.60	0.61	0.62	0.64	0.60	0.61	0.61	0.60	0.61	0.60	0.59	0.62	0.59	0.60	0.61	0.60	0.59	0.62	0.59	0.60	0.60	0.60	0.60	0.59
Na_2O	3.35	3.37	3.50	3.36	3.54	3.48	3.47	3.53	3.50	3.54	3.64	3.63	3.65	3.60	3.50	3.63	3.52	3.62	3.62	3.58	3.72	3.72	3.58	3.66	3.76
K_2O	5.05	5.06	5.10	5.14	5.01	5.07	5.02	5.08	5.03	5.10	5.09	4.98	5.13	4.99	5.08	5.06	5.00	5.01	5.20	5.04	4.97	5.08	5.08	5.05	5.00
P_2O_5	0.07	0.07	0.06	0.06	0.07	0.06	0.06	0.07	0.06	0.06	0.06	0.06	0.06	0.06	0.06	0.06	0.06	0.06	0.07	0.06	0.06	0.06	0.07	0.07	0.06
L.o.I.	0.42	0.33	0.43	0.36	0.39	0.34	0.40	0.41	0.41	0.46	0.55	0.41	0.45	0.49	0.33	0.46	0.38	0.36	0.31	0.28	0.48	0.26	0.39	0.36	0.47
Total	100.00	99.98	99.99	99.99	99.99	100.01	100.00	100.00	100.00	100.01	100.01	99.98	100.00	100.00	100.00	99.99	100.00	100.02	100.01	100.01	100.00	100.00	100.00	99.99	100.00
S.I.	0.7	1.10	0.88	0.79	0.99	0.79	0.70	1.08	0.89	0.78	0.97	1.66	0.77	0.69	0.00	0.49	0.70	0.79	0.67	0.69	0.59	0.86	0.00	0.68	0.77
A.I.	0.84	0.84	0.86	0.85	0.86	0.85	0.85	0.87	0.86	0.87	0.88	0.88	0.89	0.88	0.86	0.88	0.87	0.87	0.89	0.87	0.89	0.89	0.87	0.88	0.89
Q	34.72	34.53	33.25	34.20	33.45	33.61	34.04	33.19	33.74	33.07	32.28	33.08	32.10	33.37	33.70	32.74	34.03	33.15	32.07	33.39	32.65	32.01	33.19	32.71	32.20
C	1.17	1.13	0.87	0.91	0.80	1.03	0.96	0.80	0.92	0.70	0.67	0.62	0.49	0.69	0.92	0.58	0.70	0.75	0.53	0.77	0.53	0.52	0.74	0.59	0.44
Or	29.84	29.90	30.14	30.37	29.60	29.96	29.66	30.02	29.72	30.14	30.08	29.43	30.31	29.49	30.02	29.90	29.55	29.60	30.73	29.78	29.37	30.02	30.02	29.84	29.55
Ab	28.34	28.51	29.61	28.43	29.95	29.44	29.36	29.87	29.61	29.95	30.80	30.71	30.88	30.46	29.61	30.71	29.78	30.63	30.63	30.29	31.48	31.48	30.29	30.97	31.81
An	2.52	2.52	2.63	2.68	2.72	2.58	2.63	2.57	2.58	2.63	2.58	2.53	2.68	2.53	2.58	2.63	2.58	2.53	2.62	2.53	2.58	2.58	2.52	2.52	2.53
Ac	0	0	0	0	0	0	0	0	0	0	0	0	0	0	0	0	0	0	0	0	0	0	0	0	0
Ns	0	0	0	0	0	0	0	0	0	0	0	0	0	0	0	0	0	0	0	0	0	0	0	0	0

Table 3 (continued)

	1	2	3	4	5	6	7	8	9	10	11	12	13	14	15	16	17	18	19	20	21	22	23	24	25
Di	0	0	0	0	0	0	0	0	0	0	0	0	0	0	0	0	0	0	0	0	0	0	0	0	0
Ed	0	0	0	0	0	0	0	0	0	0	0	0	0	0	0	0	0	0	0	0	0	0	0	0	0
Sl	0	0	0	0	0	0	0	0	0	0	0	0	0	0	0	0	0	0	0	0	0	0	0	0	0
En	0.17	0.27	0.22	0.20	0.25	0.20	0.17	0.27	0.22	0.20	0.25	0.42	0.20	0.17	0	0.12	0.17	0.20	0.17	0.17	0.15	0.22	0	0.17	0.20
Fs	2.15	2.14	2.19	2.19	2.16	2.20	2.18	2.20	2.15	2.19	2.16	2.13	2.22	2.16	2.20	2.18	2.15	2.15	2.27	2.15	2.13	2.21	2.19	2.17	2.16
Hy	2.32	2.41	2.42	2.39	2.41	2.40	2.36	2.47	2.37	2.39	2.40	2.55	2.42	2.34	2.20	2.31	2.33	2.35	2.44	2.33	2.28	2.44	2.19	2.34	2.36
Mt	0.28	0.28	0.29	0.29	0.28	0.28	0.28	0.29	0.28	0.29	0.28	0.28	0.29	0.28	0.29	0.28	0.28	0.28	0.29	0.28	0.28	0.29	0.28	0.28	0.28
Il	0.21	0.21	0.21	0.21	0.21	0.21	0.15	0.21	0.21	0.23	0.21	0.21	0.21	0.21	0.21	0.21	0.21	0.21	0.21	0.21	0.21	0.23	0.21	0.21	0.21
Ap	0.16	0.16	0.14	0.14	0.16	0.14	0.14	0.16	0.14	0.14	0.14	0.14	0.14	0.14	0.14	0.14	0.14	0.14	0.16	0.14	0.14	0.14	0.16	0.16	0.14
D.I.	92.91	92.9	93.0	93.0	93.0	93.0	93.1	93.1	93.1	93.2	93.2	93.2	93.3	93.3	93.3	93.4	93.4	93.4	93.4	93.5	93.5	93.5	93.5	93.5	93.6
SAL	96.59	96.6	96.5	96.6	96.5	96.6	96.7	96.4	96.6	96.5	96.4	96.4	96.5	96.5	96.8	96.6	96.7	96.7	96.6	96.8	96.6	96.6	96.8	96.6	96.5
FEM	2.97	3.1	3.1	3.0	3.1	3.0	2.9	3.1	3.0	3.1	3.0	3.2	3.1	3.0	2.8	2.9	3.0	3.0	3.1	3.0	2.9	3.1	2.9	3.0	3.0

Abbreviations as caption in Table 2a

classification, it is mostly composed of large and medium sands. The aggregate shows a moderately selected sorting (according to Folk 1954).

By analysis under a reflection microscope, the volcanic glass makes up the majority of the aggregate fraction below 2000 μm, along with the more rare andesitic-dacitic rocks aggregate from local volcanic outcrops. The sand fraction is mostly represented by quartz, feldspar, Palaeozoic rock fragments, Oligo-Miocenic volcanic rocks, volcanic glass and rare *cocciopesto*.

Results

Petrographic features of volcanic rocks

In the mortars and concretes of the theatre, two different kind of volcanic stones were employed: (1) medium-welded rocks, mainly used as medium-coarse aggregate and (2) grey-black obsidian glasses with no local origin, used as aggregate and also as pozzolanic material.

(1) Medium-welded rocks By macroscopic observation, the first rocks, characterised by chromatisms varying from grey-reddish to purplish-brown, show an evident self-clastic structure typical of a volcanic autobreccia, with sub-centimetric lava-clasts. By microscopic analysis, these volcanic rocks show a hypo-crystalline porphyritic structure (with variable porphyritic index between 5 and 8) for phenocrysts of early opaque, dominant plagioclase, pyroxene and hornblende. Due to the squat form, the opaque minerals are formed, presumably, by titan-magnetite or magnetite.

On the base of volcanological and petrographical features, these rocks show a similarity with the dacitic rocks of territory around the Nora village (e.g., "Perdu Pranu" outcrop, NE to the site) and especially with the volcanic stones used for the tiers of the theatre (*cavea*, see Fig. 3) belonging to the ancient quarry of "Su Casteddu" (Melis and Columbu 2000; Previato 2016; Columbu and Garau 2017; Columbu 2018). The latter is a volcanic structure (of which today essentially remains just at the neck) located about 1.5 km north-west from the Nora site. In fact, the outcrop rock shows the same characteristics already observed in the volcanic-coarse aggregates, characterised by the chaotic presence of large lava-clasts (usually sharp-edged) and smaller lava-clasts with rounded contour, with maximum dimensions of 1 cm immersed in a glassy matrix with a lower degree of welding, compared to the clasts.

(2) Grey-black obsidian glasses The grey-black obsidian glasses show a hyaline structure with rare phenocrysts of

Table 4 Chemical analysis of selected volcanic rocks from St. Antioco area (Sulcis, south-western Sardinia), where reported the rock classification (according to De La Roche et al. 1980), wt.% of major elements and C.I.P.W. norm according to Cross et al. (1903)

	1	2	3	4	5	6	7	8	9	10	11	12	13	14	15	16	17	18	19	20	21	22	23	24	25
Class.	Rhy	Rhy	Rhy	Rhy	Rhy	Rhy	AlRhy	AlRhy	AlRhy	AlRhy	AlRhy	AlRhy	AlRhy	AlRhy	AlRhy	AlRhy	AlRhy	AlRhy	AlRhy	AlRhy	AlRhy	AlRhy	AlRhy	AlRhy	AlRhy
SiO_2	70.45	67.67	73.69	67.68	70.05	71.09	76.58	68.90	73.98	77.01	70.39	70.14	71.42	70.76	71.02	71.39	70.94	70.75	71.16	72.10	71.05	73.39	73.83	71.38	76.70
TiO_2	0.14	0.49	0.10	0.47	0.45	0.43	0.26	0.50	0.21	0.22	0.17	0.47	0.28	0.36	0.37	0.17	0.37	0.37	0.44	0.16	0.38	0.18	0.16	0.41	0.18
Al_2O_3	13.74	15.18	13.48	15.07	14.07	14.13	9.43	15.22	11.14	9.45	13.76	15.34	14.05	14.48	14.53	15.41	14.45	14.25	13.91	14.51	14.31	13.61	13.55	13.89	11.06
Fe_2O_3	2.12	2.65	0.70	2.59	2.33	2.33	4.38	2.49	4.09	4.05	2.06	2.53	2.38	2.41	2.10	1.82	2.09	1.09	1.27	2.00	2.31	2.15	2.00	0.83	2.97
FeO	n.d.	n.d.	1.36	n.d.	n.d.	n.d.	0.04	0.22	n.d.	n.d.	n.d.	n.d.	0.09	n.d.	0.30	n.d.	0.36	1.28	1.03	n.d.	0.21	n.d.	n.d.	1.46	n.d.
MnO	0.07	0.06	0.05	0.06	0.07	0.06	0.10	0.06	0.09	0.09	0.06	0.05	0.06	0.07	0.03	0.05	0.04	0.07	0.06	0.03	0.03	0.05	0.03	0.08	0.04
MgO	0.16	0.25	0.37	0.27	0.44	1.02	0.22	0.24	0.09	0.12	0.12	0.16	0.16	0.53	0.17	0.04	0.12	0.22	0.23	0.10	0.30	0.09	0.10	0.23	0.20
CaO	1.32	1.21	1.90	1.28	1.83	0.70	0.27	0.78	0.16	0.17	0.79	0.86	0.82	0.84	0.65	0.48	0.57	0.83	0.70	0.53	0.61	0.78	0.55	0.81	0.09
Na_2O	2.94	3.82	3.92	3.64	4.47	4.23	4.05	3.94	4.90	3.94	3.81	4.46	3.92	4.78	4.66	3.82	4.61	4.62	4.35	3.98	4.68	3.94	3.57	4.29	4.10
K_2O	4.53	5.26	3.13	5.70	4.58	5.71	3.97	6.13	4.55	3.88	5.70	5.45	5.73	5.36	5.38	6.03	5.48	5.67	5.79	5.79	5.59	5.53	5.58	6.01	4.30
P_2O_5	0.03	0.09	0.05	0.03	0.04	0.06	0.02	0.05	0.03	0.02	0.01	0.02	0.08	0.05	0.06	0.02	0.05	0.05	0.06	0.02	0.05	0.02	0.02	0.05	0.03
L.o.I.	4.51	3.32	1.26	3.20	1.69	0.24	0.66	1.48	0.76	1.06	3.13	0.52	1.01	0.36	0.73	0.79	0.91	0.79	0.99	0.77	0.48	0.25	0.61	0.56	0.34
Total	100.01	100.00	100.01	99.99	100.02	100.00	99.98	100.01	100.00	100.01	100.00	100.00	100.00	100.00	100.00	100.02	99.99	99.99	99.99	99.99	100.00	99.99	100.00	100.00	100.01
S.I.	1.67	2.13	3.92	2.26	3.79	7.80	1.79	1.87	0.68	1.03	1.04	1.29	1.33	4.12	1.37	0.35	0.96	1.72	1.83	0.86	2.33	0.78	0.90	1.80	1.77
A.I.	0.71	0.79	0.73	0.81	0.87	0.93	1.16	0.86	1.17	1.13	0.90	0.86	0.90	0.94	0.93	0.83	0.94	0.96	0.96	0.88	0.96	0.92	0.88	0.98	1.03
Q	31.77	21.29	33.10	20.34	21.77	20.70	38.33	19.27	30.07	39.40	23.43	20.07	23.55	19.07	20.60	24.03	20.60	19.40	21.20	24.43	19.77	26.46	29.30	20.82	34.78
C	1.67	1.22	0.31	0.66	0.00	0.00	0.00	0.81	0.00	0.00	0.00	0.59	0.10	0.00	0.00	1.77	0.02	0.00	0.00	0.78	0.00	0.00	0.69	0.00	0.00
Or	26.77	31.08	18.50	33.68	27.06	33.74	23.46	36.22	26.89	22.93	33.68	32.20	33.86	31.67	31.79	35.63	32.38	33.50	34.21	34.21	33.03	32.68	32.97	35.51	25.41
Ab	24.88	32.32	33.17	30.80	37.82	35.79	26.40	33.34	31.97	27.00	32.24	37.74	33.17	40.44	39.43	32.32	39.01	39.09	36.81	33.68	39.60	33.34	30.21	36.30	32.95
An	6.35	5.41	9.10	6.15	4.80	2.70	0.00	3.54	0.00	0.00	3.61	4.14	3.55	2.22	2.83	2.25	2.50	1.40	1.33	2.50	1.53	3.12	2.60	0.89	0.00
Ac	0	0	0	0	0	0	1.52	0	1.41	1.39	0	0	0	0	0	0	0	0	0	0	0	0	0	0	1.02
Ns	0	0	0	0	0	0	1.43	0	1.84	1.11	0	0	0	0	0	0	0	0	0	0	0	0	0	0	0.14
Di	0	0	0	0	1.13	0.17	0.10	0	0.02	0.04	0.02	0	0	0.48	0	0	0	0.37	0.30	0	0.23	0.05	0	0.46	0.03
Ed	0	0	0	0	2.29	0.15	0.97	0	0.51	0.59	0.19	0	0	0.89	0	0	0	1.71	1.22	0	0.78	0.50	0	1.97	0.19
Sl	0	0	0	0	3.42	0.31	1.06	0	0.53	0.63	0.21	0	0	1.37	0	0	0	2.08	1.52	0	1.01	0.55	0	2.43	0.22
En	0.40	0.62	0.92	0.67	0.57	2.46	0.50	0.60	0.21	0.28	0.29	0.40	0.40	1.10	0.42	0.1	0.30	0.38	0.43	0.25	0.64	0.20	0.25	0.36	0.49
Fs	2.78	2.90	2.93	2.85	1.33	2.49	5.68	3.00	5.50	5.38	2.53	2.75	3.02	2.33	2.75	2.28	2.84	2.02	2.02	2.51	2.47	2.45	2.51	1.76	4.00
Hy	3.18	3.52	3.85	3.52	1.91	4.95	6.19	3.60	5.72	5.67	2.81	3.15	3.41	3.43	3.17	2.38	3.14	2.40	2.45	2.76	3.11	2.65	2.76	2.11	4.48
Mt	0.37	0.46	0.38	0.45	0.40	0.40	0.00	0.47	0.00	0.00	0.36	0.44	0.43	0.42	0.42	0.31	0.43	0.43	0.42	0.34	0.44	0.37	0.34	0.42	0.00
Il	0.27	0.93	0.19	0.89	0.85	0.82	0.49	0.95	0.40	0.42	0.32	0.89	0.53	0.68	0.70	0.32	0.70	0.70	0.84	0.30	0.72	0.34	0.30	0.78	0.34
Ap	0.07	0.21	0.12	0.07	0.09	0.14	0.05	0.12	0.07	0.05	0.02	0.05	0.19	0.12	0.14	0.05	0.12	0.12	0.14	0.05	0.12	0.05	0.05	0.12	0.07
D.I.	83.4	84.7	84.8	84.8	86.7	90.2	88.2	88.8	88.9	89.3	89.4	90.0	90.6	91.2	91.8	92.0	92.0	92.0	92.2	92.3	92.4	92.5	92.5	92.6	93.1
SAL	91.4	91.3	94.2	91.6	91.5	92.9	88.2	93.2	88.9	89.3	93.0	94.7	94.2	93.4	94.7	96.0	94.5	93.4	93.5	95.6	93.9	95.6	95.8	93.5	93.1
FEM	3.9	5.1	4.5	4.9	6.7	6.6	10.7	5.1	10.0	9.3	3.7	4.5	4.6	6.0	4.4	3.1	4.4	5.7	5.4	3.5	5.4	4.0	3.5	5.9	6.3

Abbreviations as caption in Table 2a

Table 5 Distribution of analysed volcanic samples within sodium (Na), potassium (K) and high in potassium (HK) series, according to Middlemost (1975) and De La Roche et al. (1980) rock classification

Origin of rock samples	Geochemical characteristics			
	Classification	Volcanic series affinity		
		Na	K	HK
Volcanic glass aggregates from the mortars of Nora theater	Rhy	–	25	25
Volcanic rocks (perlites and obsidians) from Monte Arci outcrops (central-west Sardinia)	Rhy	–	1	5
	AlRhy	–	17	94
	Subtotal	–	*18*	*99*
	AlRhy	–	35	2
Volcanic rocks from Sant'Antioco outcrops (south-west Sardinia)	Rhy	–	6	–
	AlRhy	–	20	–
	Subtotal	–	*26*	–
	Total samples	**–**	**104**	**126**

Abbreviations as caption in Table 2a

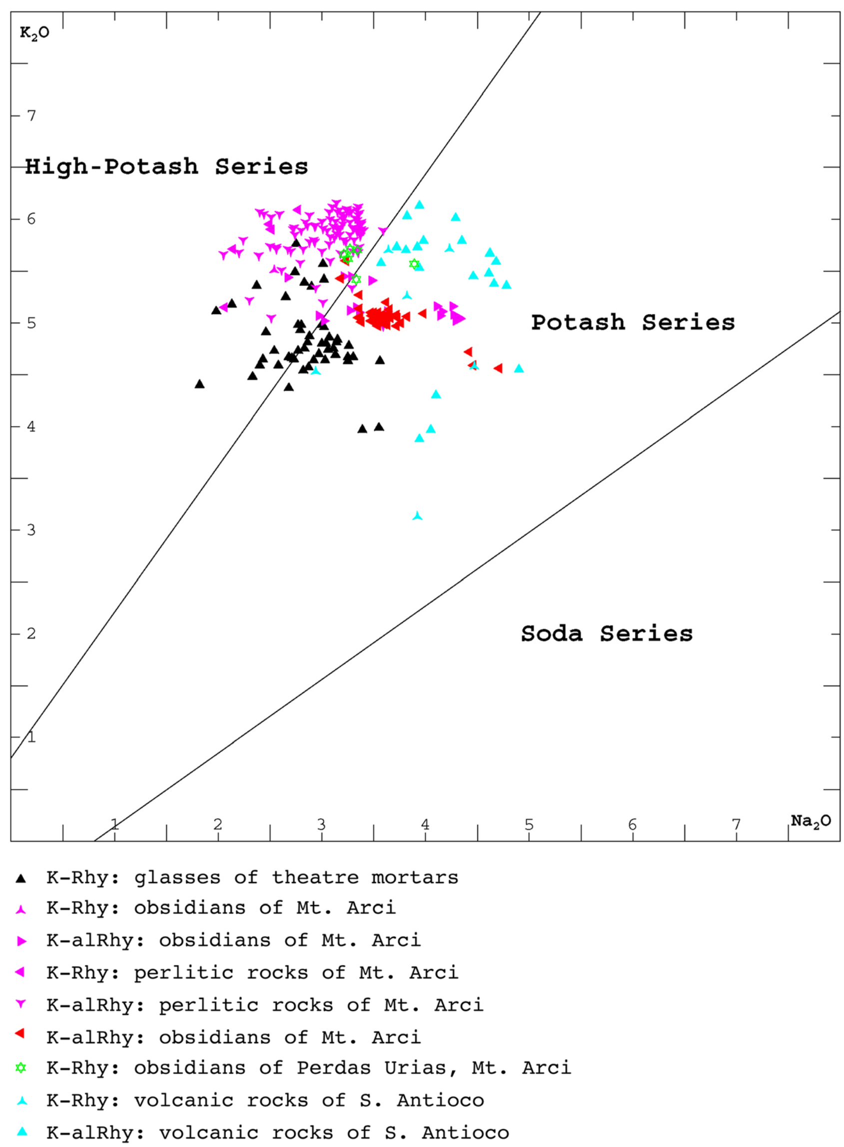

Fig. 8 Na_2O vs. K_2O wt.% classification diagram of Middlemost (1975) between the high-potash, potash and soda volcanic series, where plotted the volcanic samples from the outcrops and aggregate glasses from the mortars of the Nora theatre. Abbreviations of the legend: K-Rhy, potash rhyolite; K-alRhy, potash alkali-rhyolite

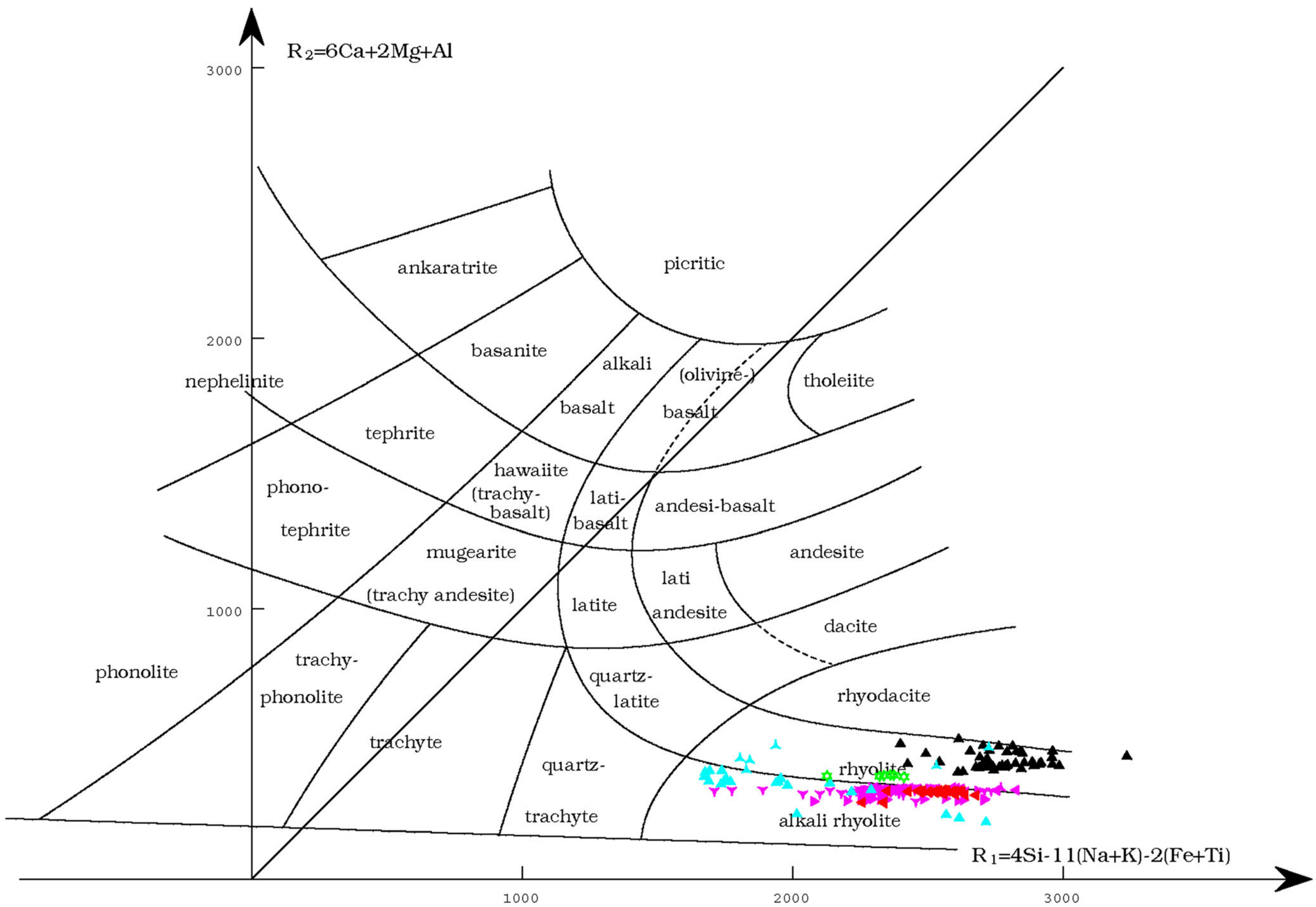

Fig. 9 R_1 vs. R_2 classification diagram of De La Roche et al. (1980), where plotted the volcanic samples from the outcrops and aggregate glasses from the mortars of the Nora theatre. Symbols as legend in Fig. 8

plagioclase and biotite. These glasses are characterised by pearlitic fractures or from a vacuolar and/or fluidal texture. In some cases, there are typical devitrification structures as spherulites (in agreement with Lofgren

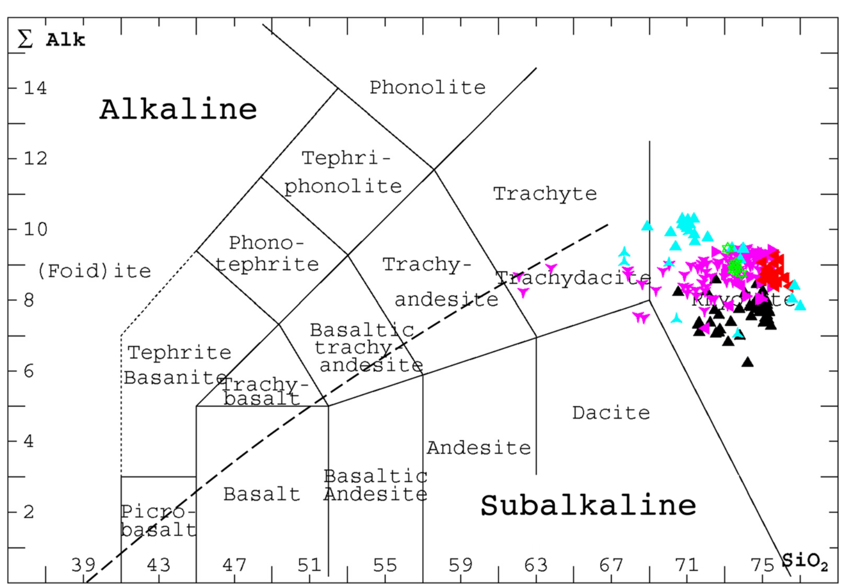

Fig. 10 Total alkali-silica diagram [$(Na_2O + K_2O)$ vs. SiO_2 wt.%] of Le Maitre et al. (2002), where plotted the volcanic samples from the outcrops and aggregate glasses from the mortars of the Nora theatre. Symbols as legend in Fig. 8

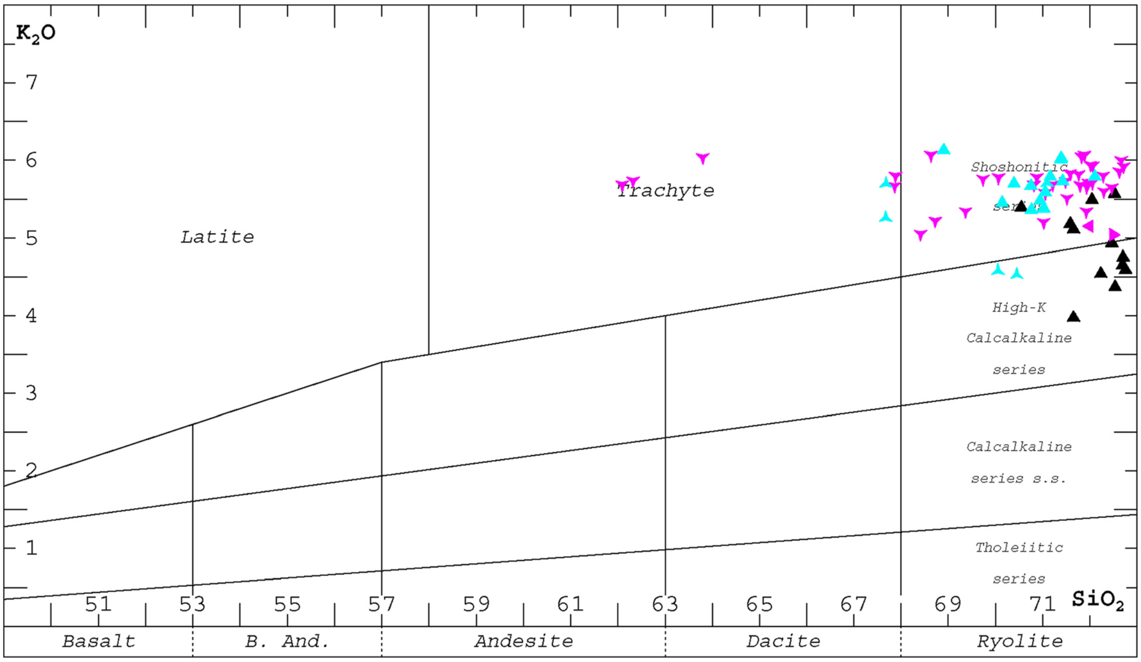

Fig. 11 K_2O vs. SiO_2 wt.% classification diagram of Peccerillo and Taylor (1976) where plotted the volcanic samples from the outcrops and aggregate glasses from the mortars of the Nora theatre. Note: it was not possible to plot all analyses, because some samples have higher values of SiO_2 to 73%. Symbols as legend in Fig. 8

1971). These volcanic fragments are always characterised by the presence of reaction rims between the glass and the binder of mortar (Fig. 6b).

Geochemical characteristics of obsidian glasses

Analysis of major elements and rock classification

Table 2a, b shows the results of the chemical analysis of the glasses used in the mortars of Roman theatre, where the analytical values of major elements and the C.I.P.W. norm are reported (according to Cross et al. 1903). Table 3a, b shows the results of chemical analysis on the volcanics (perlites and obsidians) of Mt. Arci (Fig. 1). Table 4 shows the analytical values of the volcanics from St. Antioco area (Fig. 1).

Table 5 shows a summary of the rock classification of the glasses from the theatre mortars and volcanic samples from Mt. Arci and St. Antioco, according to the diagrams of Middlemost (1975) (Fig. 8) and De La Roche et al. (1980) (Fig. 9). According to the latter diagram, the glasses of the mortars are classified as rhyolites. The samples of perlite and obsidian from Mt. Arci are classified as alkali-rhyolites and (as transition products) to the rhyolites. The acidic volcanics of St. Antioco constitute a separate group with respect to both the mortar glasses and the samples from the Mt. Arci outcrops.

According to the TAS (Total Alkali Silica) diagram of Le Maitre et al. (2002); Fig. 10), most of the samples fall within the field of the rhyolites, while only some perlites from Mt. Arci and some volcanics from St. Antioco fall within the trachy-dacite and dacite fields.

All samples fall under the dashed discriminant line of Irvine and Baragar (1971) between the alkaline and subalkaline series, which have been overlapped to the TAS diagram in Fig. 10.

Also, the diagram of De La Roche et al. (Fig. 9) shows the subalkaline character of the volcanics which, falling between the line of the critical plane of unsaturation (and away from it) and the abscissa axis, are strongly supersaturated.

In the classification diagram of Peccerillo and Taylor (1976); Fig. 11), most of the samples fall within the field of shoshonitic series and subordinately of K-high series. Almost all samples are classified as rhyolites, except some perlites of Mt. Arci and Sant'Antioco, which are classified as trachytes of shoshonitic series.

Figure 12 reports the variation diagrams of major elements versus the differentiation index (D.I.) of Thornton and Tuttle (1960). Regarding the volcanic glasses of the mortars, the typical trend of common magmatic series, with a decidedly positive correlation between SiO_2 and D.I. is observed. Even the K_2O and Na_2O are positively correlated with D.I., although weakly. A negative correlation exists, however, between

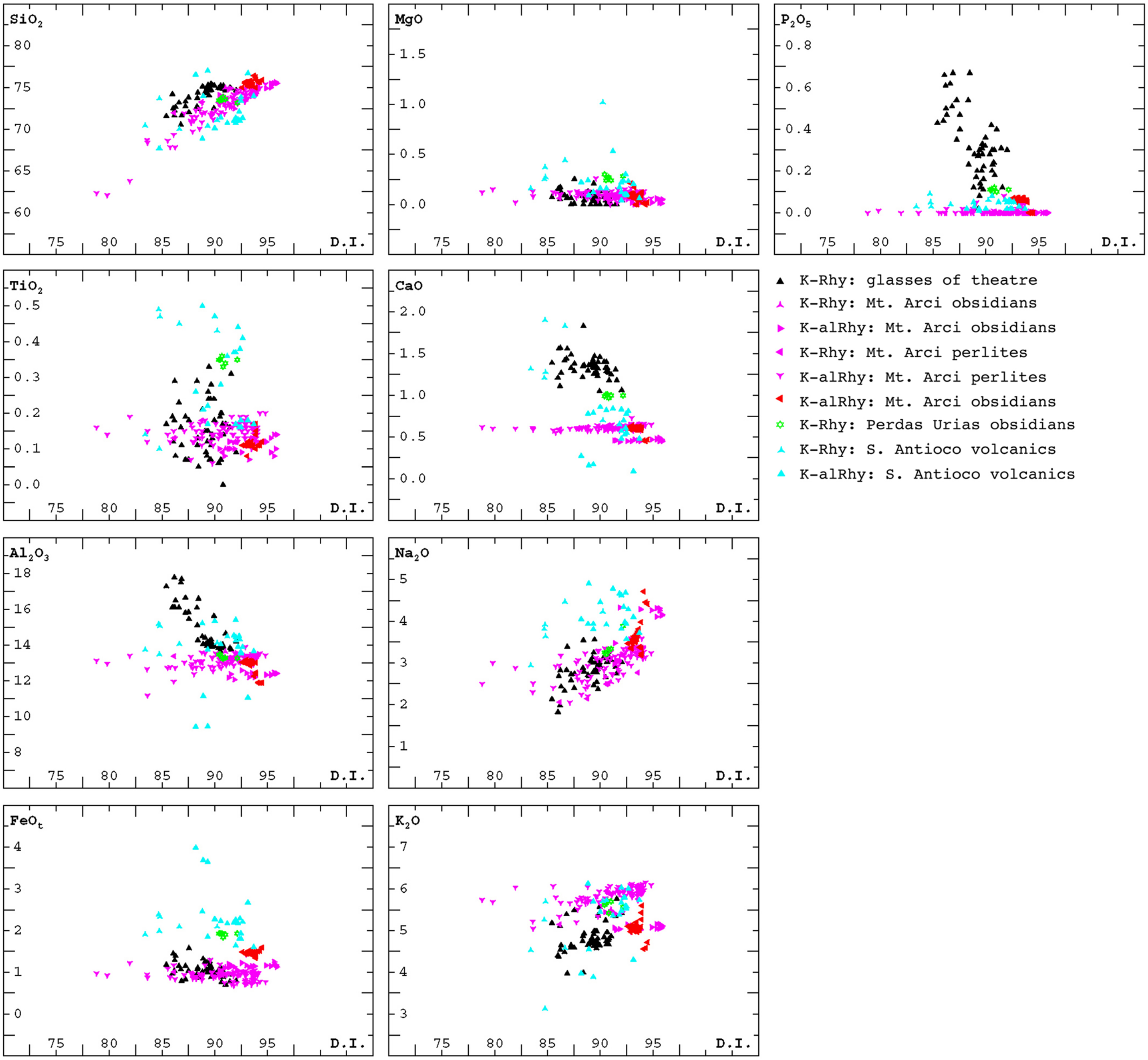

Fig. 12 Variation diagrams: major elements (wt.%) vs. differentiation index (D.I.) of Thornton and Tuttle (1960) (where D.I. = normative Q + Ab + Or + Ne + Kp + Lc) for the volcanic samples from the outcrops and aggregate glasses from the mortars of the Nora theatre

Al_2O_3 and P_2O_5, typical of the evolved rocks which splits the apatite. Other oxides, such as MgO and TiO_2, are quite dispersed.

Almost always, similar trends are even noted for the elements of obsidian and perlite samples from Mt. Arci, except for Al_2O_3 and CaO that remain almost constant. All diagrams of Fig. 12 show a different behaviour of the mortar glasses (that form a distinct group) compared to the samples from St. Antioco and Mt. Arci. Even among samples from Mt. Arci, it is possible to distinguish two different groups: the perlites and the obsidians. In particular, the perlite samples are characterised by higher values of Al_2O_3, CaO and K_2O and from lower values of P_2O_5 and Na_2O.

The behaviour of K_2O and Na_2O has already been highlighted by Cioni et al. (2001), according to which the interaction between the anhydrous volcanic glasses (obsidian) and the meteoric waters lead to the formation of hydrate glass (perlite) with leaching of Na_2O and relative enrichment in K_2O.

Instead, the samples of the Perdas Urias outcrops (eastern side of Mt. Arci) form a group almost always superimposed on the mortar glass samples, as already

Table 6 Chemical analysis of three plagioclase phenocrystals from the aggregate of theatre mortars

Sample	36_ob15-5	39_ob15-8	13_ob40-1
^{7}Li	82.2	61.13	67.21
^{11}B	1.15	1.31	1.33
^{23}Na	96,621.82	92,136.09	89,979.59
^{25}Mg	152.49	273.24	106.18
^{29}Si	614,887.75	572,032.5	556,738.69
^{45}Sc	1.87	1.78	2.47
^{49}Ti	73.48	94.56	72.99
^{51}V	0.61	0.3	< 0.1410
^{53}Cr	< 1.20	10.94	< 1.9300
^{59}Co	0.44	0.08	0.14
^{60}Ni	0.44	0.75	< 0.0000
^{66}Zn	30.08	43.14	18.69
^{85}Rb	1.82	2.58	1.48
^{88}Sr	1372.23	1311.37	1512.18
^{89}Y	0.22	0.29	0.28
^{90}Zr	< 0.0360	0.81	0.06
^{93}Nb	< 0.0206	0.2	< 0.031
^{133}Cs	< 0.0107	0.03	0.01
^{137}Ba	545.66	560.16	580
^{139}La	19.86	19	20.86
^{140}Ce	31.11	28.86	29.18
^{141}Pr	1.93	1.86	1.89
^{146}Nd	5.3	4.26	4.66
^{149}Sm	0.13	0.27	0.19
^{151}Eu	4.03	3.82	4.37
^{157}Gd	0.1	0.33	< 0.00
^{159}Tb	0.03	< 0.0073	< 0.0180
^{163}Dy	0.14	< 0.0500	0.19
^{165}Ho	< 0.0068	0.01	< 0.0107
^{167}Er	< 0.00	0.07	< 0.0540
^{169}Tm	< 0.00	0.01	< 0.0099
^{173}Yb	< 0.0410	< 0.0440	0.09
^{175}Lu	< 0.0116	< 0.0073	< 0.0075
^{177}Hf	< 0.048	0.08	< 0.055
^{181}Ta	< 0.0072	0.06	< 0.0142
^{208}Pb	17.41	14.43	15.55
^{232}Th	< 0.0072	0.01	< 0.0165
^{238}U	0.02	< 0.0060	9.6

noted in the above-mentioned diagrams, showing a certain similarity geochemistry with them.

Analysis of trace elements

Tables 6 and 7a–e show the results of the chemical analysis of trace elements of the obsidian glasses from the mortars, where also some major elements are reported. The analytical values are plotted in the diagrams of Fig. 13a–c versus ^{29}Si (expressed in % for graphic reasons). The patterns are comparable with those of common magmatic series, highlighting the validity of the ^{29}Si% as variation index.

There was a positive correlation between ^{29}Si% and ^{23}Na, ^{66}Zn, ^{49}Ti, ^{85}Rb, ^{133}Cs, ^{137}Ba, ^{93}Nb, ^{139}La, ^{208}Pb and ^{238}U, while there is a negative correlation with the ^{88}Sr; the values of the other elements are dispersed.

The analytical values of some elements (Table 7a–e) are far higher than the average of the same element in the other analysed points; these values, which may depend on the presence of phases within the micro volume of vaporised sample by the laser, or by a lack of homogeneity at the microscopic level in the distribution of the elements, were regarded as outsiders and therefore excluded from the variation diagrams.

The trends of some rare earth elements normalized to chondrites (factors taken from Anders and Grevesse 1989) are shown in Fig. 14a. They are characterised by a moderate variability (minimum 157.47 ± 9:49 ppm/chondrite for Ce; maximum: 13.66 ± 3.2 ppm/chondrite for Eu), indicating that they belong to a single magmatic series. Furthermore, while the light rare earths have parallel trends that do not intersect between them, the trends of the heavy rare earths are less correlated and tend to interbreed. Table 8 shows the correlation matrix for the rare earths showed in Fig. 14a; the maximum correlation for light rare earths coarsely tends to decrease for heavy rare earths, as highlighted by the variation diagrams vs. ^{29}Si% in Fig. 13a–c.

In general, the patterns are characterised by a negative peak in correspondence with europium, which indicates in all probability the fractionation of plagioclase, in good agreement with the petrographic observations and chemical analysis of some plagioclase phenocrystals of mortar glasses; in fact, in the plagioclases, there is a greater europium content with respect to the content of the same element in the glasses (Table 6). The Eu negative peak also indicates the apatite fractionation (Cox et al. 1979), according to the trend of P_2O_5 vs. D.I. (Fig. 12).

The pattern of the rare earths is characteristic of the final stages of the magmatic series and it is comparable with the pattern already observed in Sardinia for the dacitic and comenditic rocks from Sulcis area (Morra et al. 1994) and for dacites and rhyolites of Mt. Arci (Beccaluva et al. 1984).

Similarly, the pattern of trace elements normalized to primitive mantle according to Wood 1979 (Fig. 14b) shows that the whole sequence analysis has a regular distribution, with a not very wide range of variation (minimum 5.69 ± 0.31 ppm/primitive mantle for Sr; maximum 13.22 ± 2.48 ppm/primitive mantle for Hf); only some samples deviate on the performance more generally in correspondence of the tantalum and niobium, hafnium and zirconium. The pattern is characterised by an

Table 7 Chemical analysis of trace (and some major) elements of volcanic glasses from the theatre mortars. The values are reported in ppm

	1	2	3	4	5	6	7	8	9	10	11	12	13	14	15	16	17	18	19	20	21	22	23
^{7}Li	31.88	45.17	23.03	54.95	39.09	41.16	33.74	40.77	49.18	41.12	45.96	53.93	46.77	47.48	47.39	40.67	37.31	26.96	40.65	53.80	47.21	47.65	41.73
^{11}B	40.83	41.31	45.29	46.94	45.15	43.81	46.35	43.70	48.47	49.72	50.24	51.22	44.95	42.80	36.87	43.59	46.11	40.47	46.91	46.02	44.40	42.34	43.62
^{23}Na	31230	30511	29406	34897	30191	31725	30168	29524	34315	31528	32595	35654	34375	34979	23927	33908	34349	31520	32275	35156	36508	34222	32610
^{25}Mg	892	977	789	1174	924	976	956	904	1078	1070	1010	1022	1000	1140	2337	1002	866	911	841	1061	1132	912	973
^{29}Si	418274	413153	442866	507975	442950	426193	435235	416267	450405	431837	448281	449651	455746	462573	488815	451910	469982	500246	469368	444181	482501	439085	453683
^{45}Sc	4.72	4.52	4.72	5.82	4.81	4.50	4.72	4.65	5.13	4.57	4.36	4.83	4.90	5.03	6.01	4.77	4.63	5.05	4.50	3.48	4.27	3.97	5.17
^{49}Ti	899.78	866.32	965.88	1102.21	997.52	902.24	942.47	899.10	1006.13	952.63	938.47	947.30	876.03	1038.17	1337.02	947.98	958.46	989.39	985.65	927.68	990.51	909.72	947.54
^{51}V	1.01	1.11	1.24	0.83	2.90	1.14	1.12	1.02	1.40	0.93	1.05	0.83	1.35	1.26	1.65	0.88	0.99	5.30	1.09	1.43	1.65	1.31	1.05
^{53}Cr	<1.66	<1.37	<1.46	0.92	<1.28	<1.04	<1.40	<1.09	<0.98	<1.37	<1.23	<1.71	<0.95	<2.02	<1.24	<2.04	3.02	2.84	<1.77	2.61	2.03	<1.42	<1.67
^{59}Co	0.69	1.02	0.67	0.64	0.82	0.86	0.81	1.10	0.86	0.79	0.74	0.89	0.84	0.80	0.75	0.89	0.75	0.87	0.84	0.89	0.92	0.89	0.71
^{60}Ni	0.22	0.36	0.37	1.30	11.97	0.09	<0.124	0.25	0.56	0.74	0.26	0.41	0.11	<0.36	0.21	0.66	0.93	416.04	0.66	0.15	0.86	0.47	<0.24
^{66}Zn	63.69	60.44	60.27	118.45	72.70	64.90	63.50	61.44	68.36	71.67	65.43	68.95	70.00	67.44	68.61	67.33	64.45	52.89	65.01	67.81	70.30	78.64	66.13
^{85}Rb	189.74	180.90	194.30	202.84	209.53	193.68	196.53	189.33	201.87	196.62	206.41	200.45	209.38	198.02	157.58	227.75	226.74	185.90	209.93	200.20	212.24	192.92	206.25
^{88}Sr	128.98	130.47	134.21	127.31	129.22	127.43	131.16	132.26	129.25	131.15	131.96	130.75	122.79	137.82	115.68	129.06	121.24	135.96	127.40	130.49	126.86	125.02	134.47
^{89}Y	17.02	16.70	17.39	16.54	16.26	16.38	17.46	17.34	16.76	17.48	18.75	17.82	17.59	18.28	15.33	17.76	16.82	20.74	15.76	17.35	16.89	16.80	18.77
^{90}Zr	159.94	155.51	190.06	183.31	164.91	153.68	164.02	165.64	162.18	170.93	174.58	165.64	158.10	193.21	291.34	174.68	171.90	232.88	162.01	166.60	173.37	162.99	181.31
^{93}Nb	17.63	17.29	19.04	23.24	19.87	18.66	19.24	19.20	19.16	19.59	20.23	19.63	20.61	20.77	23.57	19.53	19.46	21.22	19.05	19.73	20.48	19.22	19.41
^{133}Cs	5.11	4.84	5.29	6.47	5.23	5.19	5.30	4.94	5.14	5.14	5.28	5.27	5.31	5.27	6.68	5.02	5.37	5.08	5.27	5.28	5.55	5.24	5.20
^{137}Ba	790.60	763.31	839.92	771.69	847.88	781.86	816.42	815.92	802.34	830.84	832.41	828.87	807.24	852.51	663.46	849.39	839.96	797.72	817.87	809.48	821.15	807.95	842.30
^{139}La	47.76	46.26	50.18	46.16	49.88	45.49	49.06	47.70	44.79	49.51	49.79	47.65	46.61	52.65	41.76	49.31	49.09	54.28	46.80	47.43	48.37	47.62	51.52
^{140}Ce	92.04	91.91	94.94	93.99	100.32	94.81	95.33	93.28	96.80	95.96	99.53	98.15	95.16	100.42	75.54	98.19	98.69	93.14	96.53	97.36	96.07	93.68	100.35
^{141}Pr	8.26	8.22	8.40	7.77	8.79	8.06	8.81	8.47	8.74	8.91	8.85	8.26	8.14	9.22	7.17	9.15	8.75	9.04	8.37	8.50	8.80	8.46	9.09
^{146}Nd	27.55	26.21	28.35	30.27	29.14	25.90	27.40	27.46	26.63	29.99	30.12	29.48	26.31	31.81	26.23	28.81	29.74	31.45	27.62	27.46	29.25	26.86	29.17
^{149}Sm	4.19	4.96	5.21	4.47	3.85	3.92	4.30	4.96	4.93	5.09	4.67	4.49	5.60	5.42	4.16	4.96	4.81	5.30	4.49	3.95	4.30	4.77	4.36
^{151}Eu	0.71	0.88	0.61	0.76	0.75	0.75	0.71	0.75	0.86	0.80	0.90	0.75	0.64	0.92	0.30	0.75	0.83	0.79	0.77	0.85	0.65	0.83	0.85
^{157}Gd	2.86	3.35	3.26	3.29	3.75	3.15	3.40	3.26	3.53	2.98	3.57	3.23	2.89	2.95	2.65	3.02	2.98	3.82	2.63	2.86	2.85	2.88	3.46
^{159}Tb	0.46	0.47	0.53	0.59	0.58	0.44	0.51	0.51	0.53	0.46	0.63	0.55	0.53	0.53	0.41	0.44	0.49	0.62	0.43	0.44	0.48	0.53	0.55
^{163}Dy	2.71	3.00	3.01	2.51	2.49	2.67	3.13	3.15	3.00	2.85	2.73	2.88	3.52	3.15	2.61	3.25	2.75	3.77	2.94	2.55	3.05	2.96	3.49
^{165}Ho	0.62	0.60	0.58	0.62	0.63	0.56	0.62	0.70	0.59	0.50	0.64	0.60	0.60	0.76	0.55	0.68	0.51	0.58	0.52	0.65	0.67	0.64	0.64
^{167}Er	1.43	1.48	2.02	1.25	1.30	1.55	1.61	1.77	1.78	1.79	1.76	1.99	1.55	1.94	1.39	2.01	1.45	1.95	1.53	1.60	1.68	1.65	1.63
^{169}Tm	0.23	0.26	0.31	0.20	0.24	0.25	0.26	0.28	0.24	0.24	0.26	0.28	0.27	0.30	0.23	0.29	0.24	0.32	0.21	0.28	0.25	0.27	0.23
^{173}Yb	1.97	1.83	1.86	2.52	1.94	1.98	2.41	1.69	1.92	2.30	2.12	1.80	1.45	2.10	1.75	2.01	1.77	2.21	1.80	2.08	1.97	1.52	1.70
^{175}Lu	0.29	0.29	0.33	0.24	0.27	0.27	0.28	0.33	0.27	0.30	0.34	0.34	0.35	0.36	0.31	0.25	0.29	0.36	0.26	0.29	0.26	0.28	0.26
^{177}Hf	4.59	4.27	5.33	4.38	4.38	3.78	4.32	4.74	4.68	4.83	4.93	4.19	4.41	5.31	7.51	4.09	4.63	6.59	4.62	4.80	4.90	4.95	4.63
^{181}Ta	1.23	1.18	1.35	1.33	1.29	1.13	1.37	1.39	1.29	1.39	1.56	1.52	1.51	1.61	2.14	1.29	1.47	1.78	1.22	1.25	1.55	1.34	1.26
^{208}Pb	24.09	22.38	23.26	30.22	27.29	24.38	23.97	26.56	26.45	25.88	25.50	24.85	28.21	25.57	22.90	25.87	26.92	28.07	26.46	25.26	33.76	29.06	27.73
^{232}Th	17.06	17.15	18.65	17.50	18.05	16.61	18.54	17.94	17.74	18.95	19.42	18.10	18.25	20.11	16.61	18.84	18.31	20.41	16.60	16.92	18.45	17.46	19.32
^{238}U	4.81	4.68	4.99	4.30	5.04	4.90	4.98	4.88	5.30	5.05	4.84	5.08	5.35	5.00	3.73	5.26	5.36	4.81	5.41	4.76	5.15	4.74	5.33

	24	25	26	27	28	29	30	31	32	33	34	35	36	37	38	39	40	41	42	43	44	45	46
^{7}Li	33.29	29.17	31.90	43.08	35.25	33.26	39.75	25.47	21.23	26.46	39.17	39.40	65.37	44.56	39.12	39.19	33.00	39.45	35.19	53.30	40.90	56.55	38.49
^{11}B	28.66	38.89	40.87	37.84	37.59	35.96	36.45	37.61	46.85	43.79	37.70	44.32	47.34	46.15	41.74	38.33	52.36	44.24	42.94	44.10	43.69	44.15	36.85
^{23}Na	28517	31811	31661	31869	32473	31556	31537	31741	30538	32138	36776	35556	34408	33091	37001	35013	33661	36102	34351	32829	40506	35604	31776
^{25}Mg	867	784	832	936	866	909	909	832	690	837	1005	903	1146	1032	873	993	882	1007	918	1000	869	973	815
^{29}Si	351543	450465	426647	431538	451171	419737	410243	429918	447503	404081	453428	450741	458061	443823	474845	437064	501317	451888	451195	444741	498190	455833	381816
^{45}Sc	3.55	4.26	4.38	3.85	4.29	3.98	3.65	4.00	3.96	3.75	4.20	4.00	4.03	3.28	4.12	3.60	3.50	3.84	3.78	3.68	3.87	4.26	3.26
^{49}Ti	725.47	923.99	889.74	894.00	922.49	820.94	861.24	866.36	897.40	814.90	972.53	907.27	879.11	896.18	962.50	874.46	923.25	869.91	886.81	876.39	1026.43	874.74	727.86
^{51}V	0.88	1.01	0.87	1.12	1.03	1.02	0.94	0.95	1.14	1.19	1.19	1.02	1.26	1.57	0.95	1.15	1.48	1.22	1.13	1.13	1.48	1.44	0.86
^{53}Cr	<1.54	<2.00	<1.77	<1.65	<1.55	<1.73	<1.42	1.97	<2.77	2.65	<2.04	<1.96	<0.86	<1.43	<1.73	40.88	<2.05	<1.72	1.88	<1.60	<2.06	<1.50	<2.83
^{59}Co	0.89	0.71	0.69	1.05	0.78	0.64	0.76	0.67	0.59	0.55	0.87	0.56	1.07	0.89	0.81	0.87	0.74	0.91	0.78	0.78	0.64	0.65	0.53
^{60}Ni	0.29	0.43	0.28	0.54	0.28	0.38	0.28	<0.30	0.28	<0.41	<0.39	0.32	0.58	0.51	0.32	0.41	<0.35	0.75	0.42	<0.31	0.47	<0.31	16.58
^{66}Zn	60.71	65.41	60.86	64.83	70.24	56.39	60.94	60.33	65.60	57.84	65.33	70.94	81.17	62.87	70.93	62.63	127.90	62.13	66.54	64.07	65.60	92.33	54.17
^{85}Rb	138.26	200.78	198.73	190.46	199.14	184.01	185.03	190.88	201.17	174.19	198.92	200.15	206.10	184.74	208.84	185.66	202.71	192.59	193.89	189.39	215.72	189.68	159.41
^{88}Sr	153.27	137.65	134.53	130.88	132.66	132.87	129.13	149.03	133.68	134.87	138.51	133.64	127.11	130.40	139.21	128.79	125.10	127.89	131.97	129.04	137.67	127.02	149.30
^{89}Y	15.05	18.52	17.48	17.98	17.19	18.32	17.24	17.88	17.02	15.90	17.93	17.77	16.35	16.41	17.45	17.07	14.89	17.03	15.89	16.90	17.78	17.06	13.19
^{90}Zr	147.70	177.94	174.26	170.63	175.95	179.35	166.91	171.49	175.07	161.05	174.72	164.96	150.50	164.40	175.40	165.55	175.46	159.19	163.76	167.95	184.45	164.59	131.31
^{93}Nb	15.18	19.33	18.29	18.17	19.81	18.34	18.20	19.95	20.68	17.56	20.19	19.95	20.10	18.30	19.68	18.87	21.24	19.78	18.63	18.74	21.60	18.75	16.05
^{133}Cs	4.01	5.21	4.91	5.10	5.71	4.74	4.95	5.06	5.42	4.61	5.33	5.71	5.48	4.85	5.46	4.99	5.70	5.07	5.29	4.98	5.40	4.79	4.11
^{137}Ba	584.06	841.11	810.20	799.36	822.03	812.24	792.28	838.50	855.53	854.40	859.27	839.82	800.07	792.79	855.21	796.37	802.97	825.83	785.69	821.43	895.81	789.84	716.37
^{139}La	40.38	51.34	49.58	50.29	48.74	51.55	48.87	49.79	50.57	45.21	51.05	49.88	48.78	47.72	50.58	46.85	46.37	47.49	46.70	48.04	52.59	46.43	39.44
^{140}Ce	79.75	98.73	93.85	96.72	95.60	93.86	94.61	95.20	97.65	89.49	100.41	97.68	100.48	96.16	100.21	93.35	90.07	94.18	93.68	96.91	104.48	93.97	78.93
^{141}Pr	7.18	8.42	8.70	8.43	8.60	8.60	8.66	8.67	8.96	7.71	9.31	9.01	8.02	8.39	8.66	8.59	7.88	8.61	8.55	8.64	9.52	8.67	6.81
^{146}Nd	24.19	29.16	29.07	28.21	28.70	30.12	28.03	29.12	28.24	24.96	27.55	29.93	27.99	28.66	28.94	26.87	28.69	26.92	27.50	29.98	30.00	28.37	23.20
^{149}Sm	4.16	4.62	4.45	4.91	4.72	5.02	5.14	5.45	4.35	3.91	4.57	5.25	4.68	4.85	5.17	4.69	4.28	5.61	4.23	4.96	4.98	4.90	3.52
^{151}Eu	0.67	0.76	0.74	0.74	0.67	0.76	0.73	0.87	0.78	0.80	0.80	0.77	0.69	1.03	0.82	0.85	0.86	0.85	0.72	0.68	0.94	0.79	0.87
^{157}Gd	2.31	2.94	3.13	3.33	3.14	3.00	2.66	3.08	3.03	2.75	2.86	3.14	2.75	2.50	2.95	2.71	3.32	3.52	2.89	2.95	3.06	3.31	2.38
^{159}Tb	0.42	0.48	0.49	0.47	0.52	0.58	0.53	0.51	0.48	0.47	0.51	0.50	0.42	0.42	0.55	0.48	0.50	0.56	0.43	0.47	0.54	0.40	0.44
^{163}Dy	2.51	2.90	3.22	3.01	3.09	3.34	2.65	2.76	3.21	2.89	2.98	2.94	2.74	3.07	2.93	3.11	3.14	2.87	2.59	3.06	2.86	2.99	1.97
^{165}Ho	0.52	0.56	0.58	0.58	0.61	0.65	0.65	0.63	0.63	0.52	0.64	0.60	0.56	0.55	0.61	0.66	0.54	0.63	0.57	0.58	0.55	0.61	0.53
^{167}Er	1.49	1.94	1.70	1.64	1.62	2.01	1.68	1.68	1.74	1.43	2.04	1.66	1.71	1.66	1.89	1.56	1.75	2.02	1.79	1.76	1.60	1.77	1.38
^{169}Tm	0.22	0.27	0.27	0.26	0.26	0.26	0.27	0.25	0.25	0.23	0.24	0.25	0.23	0.24	0.28	0.26	0.22	0.25	0.28	0.26	0.24	0.29	0.22
^{173}Yb	1.44	2.09	1.92	2.11	1.68	2.07	1.79	2.00	1.79	1.51	2.24	2.09	1.95	2.17	1.95	1.89	1.81	1.31	1.93	1.67	1.95	2.02	1.59
^{175}Lu	0.24	0.33	0.30	0.27	0.27	0.30	0.32	0.27	0.26	0.23	0.28	0.29	0.33	0.25	0.32	0.27	0.27	0.21	0.30	0.26	0.29	0.29	0.24
^{177}Hf	4.43	5.06	4.78	4.88	4.79	4.91	4.13	4.63	4.97	4.40	4.86	4.51	3.96	4.84	4.77	4.18	4.64	5.13	3.80	4.81	5.27	4.24	3.74
^{181}Ta	1.10	1.33	1.35	1.26	1.37	1.39	1.24	1.30	1.27	1.21	1.35	1.19	1.14	1.30	1.35	1.20	1.29	1.40	1.37	1.19	1.44	1.25	1.11
^{208}Pb	16.94	24.84	24.90	24.16	26.60	23.77	24.68	26.28	26.27	23.88	25.23	26.53	29.51	24.27	27.50	25.34	31.94	25.74	24.86	25.58	27.19	26.60	21.61
^{232}Th	14.74	18.60	17.96	18.18	17.98	19.32	17.07	18.06	18.16	17.48	17.91	17.67	16.89	17.13	18.10	16.71	16.87	17.57	16.88	17.44	19.15	17.55	14.34
^{238}U	4.00	4.92	4.88	4.85	5.17	4.48	4.84	4.80	4.98	4.71	5.05	5.09	5.39	4.80	5.26	4.88	5.33	5.13	4.89	4.89	5.29	5.13	4.28

enrichment of the lithophile elements with wide ionic radius (LILE). Some elements, such as Sr and Ba, show the negative peaks, surely due to the fractionation of plagioclase and K-feldspar. In fact, as can be seen from Tables 6 and 7, the value

	47	48	49	50	51	52	53	54	55	56	57	58	59	60	61	62	63	64	65	66	67	68	69
^{7}Li	44.02	55.10	54.57	43.35	60.07	30.83	41.92	29.06	51.73	52.95	30.86	28.53	39.91	21.59	43.05	33.92	57.23	21.58	27.12	20.64	45.55	31.99	43.18
^{11}B	45.28	45.72	42.80	48.19	60.58	48.54	48.13	41.54	41.38	47.68	44.54	45.65	46.14	49.45	44.27	45.81	48.50	48.43	44.60	39.12	37.31	40.64	40.58
^{23}Na	35214	37491	38501	36149	36460	30568	34978	29949	33239	33988	33804	33511	37220	33701	32593	30807	37980	35372	34886	34052	32806	34070	34568
^{25}Mg	1104	1219	977	926	911	901	1020	943	908	1050	909	1103	908	877	862	884	1035	727	781	732	1025	866	1001
^{29}Si	456129	471532	434988	465321	485840	478494	556002	485609	463397	452543	470865	476245	452636	486411	428616	476826	467360	492075	499628	442972	433669	470357	443228
^{45}Sc	3.63	3.65	4.41	4.09	4.10	3.28	4.43	4.85	4.02	3.65	3.76	3.17	3.52	4.08	3.53	3.91	4.13	3.75	4.21	2.98	3.28	3.49	3.52
^{49}Ti	900.82	948.85	876.34	872.10	922.27	983.47	1036.20	1036.02	926.49	904.61	950.27	1148.89	926.96	970.84	876.18	935.92	963.39	1123.02	1070.28	878.60	955.79	990.65	946.76
^{51}V	0.81	1.92	0.76	1.02	1.37	1.11	1.48	1.04	0.87	1.37	0.87	1.49	1.22	1.04	1.13	1.02	1.31	1.02	1.23	0.49	1.38	0.72	1.43
^{53}Cr	<1.57	<1.82	<2.10	<1.68	<1.14	2.14	<1.54	1.71	<1.92	2.15	<1.91	<1.58	<1.70	<1.60	<1.48	<1.38	<1.96	<1.72	<2.37	<1.91	<1.80	<1.90	<1.67
^{59}Co	0.86	1.14	0.84	0.67	0.97	0.85	0.87	0.73	0.81	1.06	1.02	0.87	0.83	0.82	0.84	1.13	0.72	0.55	0.63	0.76	1.13	0.89	0.76
^{60}Ni	0.55	0.85	<0.23	0.86	0.46	<0.26	1.11	<0.29	0.35	0.13	<0.163	0.99	<0.187	<0.181	0.99	12.05	<0.146	0.12	<0.50	<1.56	0.33	0.19	0.83
^{66}Zn	66.47	77.53	62.78	71.41	84.95	69.14	74.98	69.74	72.53	70.51	69.33	77.81	67.72	68.32	72.80	70.74	70.54	82.25	76.33	68.99	64.54	71.95	65.01
^{85}Rb	197.66	206.71	190.20	205.51	224.10	190.89	218.69	192.90	199.50	201.39	213.96	214.16	210.75	226.01	195.38	205.35	217.84	229.48	230.05	194.93	199.47	227.44	208.14
^{88}Sr	129.36	126.10	126.29	126.54	129.36	129.72	143.54	134.02	127.90	133.56	133.96	128.81	133.33	137.35	119.91	116.57	126.69	135.46	136.55	127.51	129.84	139.33	137.02
^{89}Y	15.15	17.29	16.56	15.57	15.71	16.94	16.16	18.22	15.67	16.89	17.21	16.75	16.57	21.91	15.94	14.60	16.04	16.40	16.32	15.62	16.95	16.24	16.84
^{90}Zr	155.72	160.47	162.47	158.91	159.14	180.64	181.98	279.43	159.36	166.21	168.44	162.19	163.31	168.38	154.16	154.62	155.19	170.65	166.50	164.06	167.19	171.63	161.01
^{93}Nb	18.85	18.81	18.46	19.33	19.30	22.46	21.30	23.37	20.02	18.78	19.48	24.48	19.03	21.24	18.63	20.18	19.28	20.37	20.36	18.04	18.48	19.02	18.43
^{133}Cs	4.86	5.08	5.04	5.20	5.84	5.04	5.27	5.17	5.21	5.55	5.80	5.27	5.66	5.53	5.19	5.12	5.53	5.64	5.86	5.04	4.78	5.57	5.72
^{137}Ba	782.07	795.02	783.51	789.44	800.44	758.93	1029.00	797.02	782.09	819.20	835.54	866.38	826.85	896.40	788.74	734.64	838.92	855.45	852.77	797.47	790.49	825.78	815.67
^{139}La	44.99	47.63	47.40	46.48	46.95	48.86	48.06	52.64	47.00	48.74	48.41	48.41	48.94	49.51	46.00	42.53	47.24	47.78	47.66	46.89	47.78	48.34	47.98
^{140}Ce	93.32	95.69	94.00	94.72	99.01	89.80	92.09	92.07	96.17	95.34	100.08	98.54	98.74	102.69	92.91	89.41	99.18	98.56	99.02	90.36	93.49	96.93	98.59
^{141}Pr	8.34	8.60	8.47	8.70	8.08	8.09	7.73	8.62	8.53	8.29	8.68	8.73	8.57	8.68	8.04	7.52	8.42	8.25	8.20	8.05	8.37	8.60	8.30
^{146}Nd	26.77	30.10	27.31	27.64	28.06	27.33	27.22	30.01	26.35	29.10	27.59	26.84	27.98	27.82	28.41	23.42	28.13	26.45	25.32	25.02	28.67	26.10	26.83
^{149}Sm	4.26	4.61	4.33	3.84	4.14	4.39	5.57	4.77	3.78	4.41	4.80	4.21	5.03	4.67	3.68	3.63	4.64	4.56	5.14	4.63	4.89	4.72	4.17
^{151}Eu	0.66	0.80	0.79	0.74	0.90	0.85	0.93	0.84	0.62	0.90	0.79	0.70	0.57	0.86	0.78	0.75	0.86	0.86	0.74	0.60	0.79	0.77	0.78
^{157}Gd	2.64	2.67	2.93	2.44	2.68	2.97	3.32	3.39	2.67	2.67	2.79	3.21	2.67	3.05	3.19	2.57	3.07	2.61	2.42	2.69	2.80	2.38	2.87
^{159}Tb	0.50	0.53	0.48	0.50	0.52	0.50	0.43	0.55	0.51	0.42	0.49	0.42	0.54	0.50	0.49	0.38	0.44	0.45	0.55	0.45	0.49	0.48	0.41
^{163}Dy	3.26	2.87	3.13	2.94	2.91	2.91	2.64	3.42	2.64	2.97	2.98	2.97	2.41	2.61	2.92	2.78	2.66	2.49	2.53	2.36	3.16	2.88	2.84
^{165}Ho	0.55	0.48	0.53	0.49	0.57	0.57	0.55	0.69	0.51	0.64	0.52	0.63	0.60	0.72	0.53	0.52	0.57	0.52	0.65	0.50	0.66	0.60	0.67
^{167}Er	1.55	1.75	1.90	1.71	1.28	2.01	1.57	1.61	1.76	1.66	1.73	1.50	1.51	1.98	1.73	1.32	2.06	1.32	1.57	1.55	1.67	1.58	1.53
^{169}Tm	0.25	0.27	0.24	0.24	0.31	0.25	0.24	0.29	0.17	0.31	0.25	0.26	0.28	0.33	0.22	0.21	0.30	0.22	0.27	0.27	0.29	0.26	0.24
^{173}Yb	1.97	1.95	1.90	1.62	1.32	2.06	2.78	2.22	1.88	2.02	1.80	1.82	1.51	2.29	1.76	1.79	1.92	1.75	1.88	1.91	2.53	1.73	1.86
^{175}Lu	0.29	0.30	0.34	0.21	0.25	0.31	0.20	0.28	0.21	0.28	0.28	0.29	0.32	0.35	0.31	0.29	0.28	0.19	0.25	0.24	0.36	0.28	0.26
^{177}Hf	4.30	5.54	4.30	4.11	3.95	5.03	5.33	9.26	4.06	4.44	4.45	4.73	4.57	3.92	3.66	4.29	3.71	4.20	4.67	4.80	4.35	4.24	4.16
^{181}Ta	1.31	1.07	1.48	1.47	1.35	1.42	1.62	1.70	1.25	1.35	1.37	1.54	1.34	1.42	1.31	1.40	1.26	1.37	1.39	1.33	1.33	1.33	1.19
^{208}Pb	25.11	29.61	24.86	26.56	31.85	27.58	31.57	28.29	27.34	29.45	26.08	26.94	25.82	27.90	25.27	28.60	27.41	26.79	27.98	24.48	24.56	26.49	24.73
^{232}Th	16.23	17.33	17.18	17.19	18.04	17.70	18.84	22.12	15.83	16.66	17.19	17.03	17.28	17.74	16.29	14.53	15.96	16.90	16.55	16.15	16.69	16.69	15.36
^{238}U	4.77	5.41	5.08	5.39	6.04	4.71	5.46	4.81	5.16	5.24	5.15	5.37	5.31	5.50	5.06	5.12	5.41	5.45	5.34	4.66	4.42	4.97	4.80

	70	71	72	73	74	75	76	77	78	79	80	81	82	83	84	85	86	87	88	89	90	91	92
^{7}Li	48.13	40.20	38.32	33.35	31.13	33.49	65.86	38.21	62.70	43.19	66.05	68.02	68.50	74.86	56.87	44.73	55.30	56.95	43.61	27.02	22.86	38.51	35.25
^{11}B	39.92	44.89	38.67	45.51	42.72	35.94	52.41	42.54	40.82	41.70	46.06	42.55	74.42	58.44	45.53	44.97	51.70	45.95	43.19	37.22	43.69	41.42	38.38
^{23}Na	36579	35974	38370	36074	32078	30246	35906	31426	34883	34080	38414	38173	45942	38537	38635	34093	36252	35833	34613	32166	31498	32757	36656
^{25}Mg	949	908	930	878	936	1032	990	891	1041	966	1151	1218	1878	1336	1051	1012	988	999	979	830	703	1034	1023
^{29}Si	465937	457216	467500	460550	474759	440701	462465	434913	463107	460494	503052	514313	767413	519921	491875	449494	497317	476861	449848	464144	424494	420946	461175
^{45}Sc	4.18	3.70	3.92	3.44	4.06	2.76	3.62	3.38	3.81	3.64	3.74	3.46	8.21	4.00	3.17	3.02	4.44	4.21	3.99	3.73	4.11	4.33	4.36
^{49}Ti	988.21	945.16	980.63	948.25	963.39	862.99	898.34	886.01	960.74	907.49	948.23	990.85	1385.32	985.01	945.60	877.58	1021.61	1002.54	915.95	969.79	950.12	903.98	1090.24
^{51}V	1.10	0.99	0.84	1.20	1.04	0.94	0.98	1.18	0.98	1.14	1.06	1.32	3.03	2.04	1.30	1.13	1.26	1.35	1.33	0.93	0.93	1.37	1.46
^{53}Cr	<1.94	2.58	<3.49	<2.13	<1.58	2.38	<1.46	4.22	2.23	<1.31	<1.36	4.41	<1.70	31.56	1.70	<1.07	<1.62	<1.49	<1.71	<1.91	<1.67	1.85	<2.38
^{59}Co	0.91	1.01	0.77	0.82	0.85	0.82	0.99	0.69	1.16	0.93	1.21	1.11	1.09	1.61	0.84	0.86	0.92	0.97	0.87	0.63	0.62	0.81	0.93
^{60}Ni	0.19	<0.37	<0.27	<0.29	0.45	0.45	0.42	0.95	0.17	0.23	0.14	1.67	2.48	7.05	0.39	0.56	<0.130	0.57	0.43	0.54	<0.00	<0.152	0.76
^{66}Zn	71.87	79.26	68.01	71.23	62.61	57.13	70.85	73.60	73.43	76.40	86.35	86.02	272.06	321.18	78.23	77.63	71.84	72.73	60.59	99.88	50.29	56.65	89.83
^{85}Rb	216.02	210.49	218.88	214.40	202.90	191.66	210.90	200.94	220.46	208.91	242.52	257.00	282.54	245.96	231.10	206.26	221.31	207.99	199.05	207.42	185.66	187.50	209.87
^{88}Sr	142.89	132.26	142.28	139.53	128.27	127.05	127.83	127.94	126.22	128.54	121.51	112.40	120.05	121.10	114.13	124.27	132.89	125.34	138.83	124.56	140.62	119.19	126.89
^{89}Y	17.04	16.34	17.68	17.21	15.96	21.07	15.94	15.52	16.47	15.96	15.15	15.60	16.81	14.90	16.37	15.65	16.72	15.87	16.19	15.81	14.78	15.19	18.33
^{90}Zr	179.31	167.36	174.07	171.53	159.43	206.38	155.43	148.24	155.09	158.99	148.63	154.04	149.24	140.09	155.91	155.45	162.47	153.16	158.49	165.62	148.07	152.66	190.76
^{93}Nb	18.84	17.22	19.75	19.18	18.08	17.40	18.38	17.51	18.00	19.15	19.72	19.75	36.02	22.65	19.54	18.37	20.73	19.41	19.41	19.58	18.08	17.26	21.52
^{133}Cs	5.76	5.32	5.73	5.18	5.16	5.14	5.28	5.00	5.95	5.53	7.16	6.66	7.51	6.11	5.47	5.28	5.80	5.59	5.51	5.25	4.81	4.78	5.39
^{137}Ba	844.69	806.53	876.05	841.19	771.13	750.64	795.69	762.34	801.39	809.69	821.03	883.84	857.60	782.36	844.88	796.67	838.42	811.49	773.24	822.06	797.73	743.04	855.33
^{139}La	50.84	46.79	51.72	49.99	46.05	49.11	46.91	44.38	45.73	47.25	45.80	46.43	45.09	43.32	47.14	46.32	47.28	45.51	45.14	47.13	44.66	44.10	49.61
^{140}Ce	99.56	95.83	101.68	98.28	91.57	86.77	93.63	88.98	94.88	92.43	98.10	101.68	106.11	99.78	104.38	97.48	104.41	100.20	98.04	98.95	87.76	90.58	100.45
^{141}Pr	8.95	7.94	8.54	8.51	8.27	8.51	7.94	7.54	8.15	8.28	8.00	8.41	8.40	8.14	8.53	8.43	8.52	8.61	7.94	8.44	7.76	7.90	8.41
^{146}Nd	26.87	27.61	29.76	27.03	25.78	27.67	25.61	24.78	28.09	26.10	25.04	25.80	27.98	26.31	27.16	26.88	27.48	25.14	27.34	27.48	24.51	25.92	27.71
^{149}Sm	4.64	4.13	5.48	4.71	4.55	4.23	4.28	4.26	4.52	4.76	4.13	5.36	4.01	3.77	4.56	4.23	4.36	3.48	3.78	4.34	4.49	4.71	4.13
^{151}Eu	0.75	0.84	0.96	0.79	0.70	0.39	0.68	0.82	0.83	0.79	0.75	0.86	0.97	0.61	0.81	0.79	0.84	0.70	0.84	0.78	0.93	0.66	0.94
^{157}Gd	2.96	3.52	2.32	2.73	2.88	3.49	2.99	3.07	3.08	2.84	3.30	2.30	2.76	2.46	3.11	2.77	3.20	3.19	2.70	2.91	2.10	3.29	2.60
^{159}Tb	0.48	0.48	0.46	0.39	0.40	0.46	0.50	0.38	0.56	0.56	0.50	0.54	0.33	0.43	0.42	0.45	0.41	0.41	0.48	0.39	0.46	0.37	0.35
^{163}Dy	3.11	2.61	3.23	2.87	2.74	3.65	2.63	2.46	3.26	2.75	2.76	3.37	2.89	2.53	3.24	2.27	2.81	2.84	2.74	2.57	2.85	2.46	2.80
^{165}Ho	0.53	0.53	0.64	0.57	0.61	0.69	0.62	0.47	0.68	0.63	0.55	0.71	0.70	0.56	0.54	0.50	0.56	0.58	0.47	0.57	0.67	0.66	0.67
^{167}Er	1.58	1.58	1.59	2.05	1.56	2.00	1.36	1.41	1.20	1.73	1.50	1.68	1.74	1.62	1.89	1.46	1.68	1.90	1.59	1.72	1.67	1.28	1.55
^{169}Tm	0.16	0.27	0.22	0.26	0.29	0.35	0.29	0.23	0.21	0.25	0.23	0.30	0.24	0.22	0.23	0.26	0.27	0.24	0.22	0.23	0.29	0.26	0.20
^{173}Yb	1.77	2.13	2.36	1.61	1.89	1.96	1.90	1.59	1.51	2.08	1.58	2.08	1.90	1.71	1.99	1.70	1.84	2.08	1.59	1.98	1.56	2.09	1.51
^{175}Lu	0.27	0.27	0.36	0.26	0.24	0.38	0.25	0.27	0.28	0.31	0.28	0.33	0.26	0.27	0.31	0.34	0.31	0.23	0.25	0.29	0.25	0.26	0.27
^{177}Hf	4.79	4.44	4.64	4.22	4.70	5.95	4.15	4.00	3.81	4.47	3.71	3.90	3.61	3.73	4.19	3.73	3.94	4.16	4.27	4.39	3.16	4.02	5.07
^{181}Ta	1.29	1.40	1.37	1.30	1.05	1.32	1.13	1.04	1.07	1.20	1.15	1.07	1.51	1.09	1.21	1.20	1.37	1.47	1.27	1.33	1.21	1.14	1.49
^{208}Pb	26.62	41.13	27.50	26.25	27.51	24.44	26.99	24.04	24.77	26.72	29.33	33.73	57.32	32.15	31.68	25.75	29.02	26.76	24.14	26.28	21.87	22.34	27.79
^{232}Th	16.15	16.23	17.44	17.13	15.68	18.00	15.65	14.61	14.57	16.15	15.09	14.58	14.83	14.62	15.95	16.01	16.65	16.28	15.78	17.35	15.77	15.97	17.92
^{238}U	4.89	4.94	5.28	4.92	4.94	4.41	4.94	4.66	4.50	5.12	5.33	5.44	6.32	6.34	5.78	4.88	5.55	5.37	4.85	5.21	4.77	4.66	5.16

of Sr (in ppm) in plagioclase is much higher than the value of Sr present in the glass. It also shows an impoverishment compared to the primordial mantle, due probably to the fractionation of iron and titanium oxides.

Provenance of pozzolanic glasses

Considering that in the areas adjacent to Nora's site there are no rock outcrops with similar geochemical-petrographic

	93	94	95	96	97	98	99	100	101	102	103	104	105	106	107	108	109	110	111	112
^{7}Li	45.73	58.30	35.47	57.06	40.81	68.11	44.10	70.68	23.84	29.51	38.46	53.24	36.54	62.16	33.70	38.67	25.30	57.85	44.59	37.92
^{11}B	44.20	41.52	44.71	40.80	38.10	53.42	40.95	44.02	48.13	37.36	42.23	38.03	40.77	44.71	45.21	38.42	52.30	37.11	43.16	47.90
^{23}Na	37060	33683	32720	34941	28614	38825	36903	39680	38064	32457	38060	31993	35274	35942	35986	35308	34556	38462	35261	37641
^{25}Mg	995	883	895	969	686	1002	733	927	684	945	1377	908	910	1080	900	1107	936	1059	910	1012
^{29}Si	431630	437493	466787	454435	362093	488190	444460	491218	445426	492724	694862	423837	415526	471776	474512	452758	613992	423275	467731	472478
^{45}Sc	3.86	4.11	3.94	3.77	3.24	4.50	4.58	3.61	3.62	3.27	4.94	3.57	2.92	4.45	3.26	3.41	4.36	3.45	3.55	3.35
^{49}Ti	906.44	885.77	949.18	925.55	694.49	930.48	1038.90	1112.19	1017.01	1188.28	1240.13	952.73	948.40	1039.80	987.92	956.58	1364.70	893.07	1022.21	956.40
^{51}V	1.18	1.39	0.88	<0.22	0.76	1.27	1.12	1.51	1.00	0.95	1.49	0.99	0.87	1.42	1.14	1.34	1.81	0.97	1.15	0.92
^{53}Cr	<2.69	<1.45	<1.72	<1.83	<1.45	<1.94	<3.54	<3.58	<3.74	1.97	<2.42	<1.64	<2.02	<1.38	<1.92	<2.21	3.59	<2.43	3.75	<2.05
^{59}Co	0.72	0.65	0.92	0.78	0.64	0.90	0.73	<0.32	0.86	0.55	1.38	0.82	0.65	1.01	0.41	0.91	0.68	0.73	0.73	<0.24
^{60}Ni	<0.33	0.76	<9.19	<0.31	0.75	0.95	<0.37	<0.00	<0.47	0.64	1.27	<0.21	0.71	0.79	<0.31	1.59	3.79	<0.00	0.71	<0.192
^{66}Zn	93.25	62.58	66.40	75.85	44.47	67.15	55.80	59.26	55.31	52.79	85.55	55.95	57.15	73.83	76.33	154.56	185.32	70.33	65.27	65.42
^{85}Rb	191.13	195.39	206.51	198.13	157.98	230.46	226.40	273.64	211.38	175.53	197.98	192.77	185.55	216.72	199.12	189.05	215.41	197.48	197.93	203.31
^{88}Sr	121.34	128.39	130.62	135.18	118.14	120.14	143.21	127.26	145.79	130.42	143.40	129.09	136.11	129.34	140.50	129.41	129.32	129.50	134.42	134.51
^{89}Y	17.04	16.39	16.54	17.28	12.51	15.77	18.79	20.48	18.24	15.57	20.07	16.65	19.42	19.36	17.58	16.73	19.93	18.82	16.90	18.17
^{90}Zr	168.85	155.46	170.95	177.74	117.29	158.79	190.21	209.42	191.21	211.33	199.05	166.64	189.27	175.41	185.95	169.05	309.66	184.11	173.50	179.21
^{93}Nb	18.60	18.11	19.07	19.90	14.32	19.47	23.10	26.16	24.44	28.68	35.80	21.78	22.85	23.93	20.88	21.07	30.88	21.31	22.37	22.34
^{133}Cs	4.94	5.04	5.33	5.32	3.85	5.46	5.45	6.01	5.38	4.60	5.33	5.23	4.99	5.98	5.15	5.21	6.05	4.93	4.83	5.53
^{137}Ba	777.50	775.91	826.05	828.12	585.73	784.36	916.54	969.69	896.51	762.62	793.07	797.21	817.10	848.63	833.65	774.09	800.43	802.00	819.68	829.90
^{139}La	48.61	45.34	48.57	49.63	34.19	44.20	48.27	51.29	48.36	40.05	44.55	42.58	47.22	44.78	47.61	41.83	44.34	46.67	43.05	45.54
^{140}Ce	92.60	92.90	98.02	97.98	69.03	95.35	98.44	106.02	93.95	82.53	85.73	89.18	91.39	97.16	95.94	88.63	88.61	88.42	89.20	93.27
^{141}Pr	8.25	7.94	8.40	8.48	6.03	8.04	9.66	9.86	10.06	7.86	8.70	8.63	8.93	8.56	9.24	8.37	8.18	8.69	8.62	9.36
^{146}Nd	27.27	24.73	28.03	28.40	19.19	26.43	28.86	30.97	29.65	25.81	29.52	27.21	29.41	27.92	30.83	27.26	24.89	28.65	28.40	29.07
^{149}Sm	4.31	4.50	4.53	5.24	3.52	5.05	5.21	5.00	4.60	3.88	4.77	5.25	4.95	4.85	4.11	4.24	4.66	5.43	4.29	4.98
^{151}Eu	0.60	0.80	0.70	0.78	0.61	0.53	0.69	0.74	0.85	0.72	0.80	0.64	0.74	0.70	0.66	0.44	0.70	0.81	0.70	0.74
^{157}Gd	2.60	2.44	3.84	3.27	2.57	2.97	2.55	3.57	2.95	2.37	3.42	2.79	4.03	2.42	2.74	3.44	2.67	3.17	2.99	2.77
^{159}Tb	0.45	0.50	0.52	0.55	0.36	0.45	0.49	0.45	0.42	0.44	0.45	0.50	0.58	0.50	0.51	0.44	0.39	0.60	0.40	0.48
^{163}Dy	2.91	2.74	3.02	2.87	2.21	2.72	3.36	3.43	2.77	2.73	3.72	3.13	2.45	2.88	3.05	2.93	2.92	3.13	2.98	3.29
^{165}Ho	0.58	0.51	0.61	0.60	0.41	0.54	0.73	0.68	0.71	0.51	0.76	0.51	0.63	0.62	0.69	0.49	0.59	0.69	0.63	0.61
^{167}Er	1.45	1.56	1.60	2.03	1.19	1.80	2.07	1.91	2.16	1.70	2.26	1.77	1.70	1.84	2.23	1.71	2.25	1.92	1.73	2.22
^{169}Tm	0.21	0.25	0.27	0.23	0.20	0.27	0.31	0.31	0.29	0.23	0.32	0.25	0.23	0.22	0.30	0.27	0.27	0.32	0.22	0.26
^{173}Yb	1.99	1.35	2.24	2.06	1.32	1.92	1.75	2.20	1.86	1.29	1.96	2.02	1.86	1.90	2.03	1.49	1.83	2.13	1.94	2.08
^{175}Lu	0.19	0.25	0.27	0.34	0.22	0.23	0.23	0.22	0.26	0.21	0.35	0.17	0.32	0.31	0.27	0.29	0.26	0.31	0.30	0.30
^{177}Hf	4.77	4.60	4.54	5.10	3.05	4.33	5.24	4.96	5.26	5.79	6.43	3.85	5.13	4.37	4.71	4.57	8.77	4.87	4.68	3.85
^{181}Ta	1.51	1.26	1.41	1.39	1.05	1.25	1.66	1.85	1.75	2.01	2.40	1.85	1.36	1.67	1.34	1.49	2.17	1.57	1.69	1.52
^{208}Pb	27.93	25.91	26.17	25.40	19.46	26.67	22.93	24.76	22.74	20.75	32.99	21.11	24.34	28.28	26.29	27.65	37.65	24.95	24.24	25.61
^{232}Th	17.70	16.31	18.28	18.47	12.72	16.43	18.42	19.63	18.71	15.18	17.28	16.35	17.63	17.99	19.35	16.17	16.99	18.08	17.76	17.62
^{238}U	5.03	5.35	5.30	4.99	3.92	5.51	5.31	5.59	5.14	4.39	4.74	4.93	4.88	5.74	5.65	5.24	5.31	5.03	5.31	5.87

characteristics, in order to identify the sources of supply, the composition geochemistry of these glasses with new and literature analytical data of similar volcanic rocks (rhyolites/alkali-rhyolites) from Mt. Arci and St. Antioco areas was compared, using the linear discriminant analysis.

Discriminant analysis using major elements

The discriminant analysis (performed using the Statistical Mac program) was applied to subdivide the groups defined a priori that are represented by the glasses used as aggregate and pozzolan in the theatre mortars, the volcanic samples (obsidians and perlites) from Mt. Arci and the volcanics coming from the St. Antioco.

In detail, 232 analyses (divided as in Table 9) were considered. The variables chosen for the discrimination of the groups are represented by the following major elements: SiO_2, TiO_2, Al_2O_3, FeO_T, MnO, MgO, CaO, Na_2O, K_2O and P_2O_5. Among them, those that are found to be significant (based on the discriminant analysis) are the following: CaO, FeO, Al_2O_3 and P_2O_5.

The samples will be classified as belonging to the group that has the higher score (Table 10a).

The classification score of a sample for a group, for example from the Nora theatre (TN), is calculated as follows:

$$\text{Score(TN)} = -295,945 + \text{CaO} + \text{FeO}_\text{T}{*}16,546{*}63,419 + \text{P}_2\text{O}_5{*}(191,734){*}37784 + \text{Al}_2\text{O}_3.$$

Table 10b shows the summary diagram of the classification results, according to the classification score groups. All analyses of the mortar glasses are properly classified as belonging to the "Theatre" group. Also, all analyses of samples from "Mt. Arci" are properly classified. For "St. Antioco" samples, 92.86% of the total analysis was correctly classified, and single analysis was attributed to the theatre group and a second one to the Mt. Arci group.

Table 11a shows the canonical functions, which are equal to the number of groups minus one. For each sample, each variable must be multiplied by the coefficient shown in the table according to the following scheme:

$$\text{Root 1} = 3.9207 + \text{CaO} + \text{FeO}_\text{T}{*}4.52979{*}(-0.79973) + \text{Al}_2\text{O}_3 + \text{P}_2\text{O}_5{*}10.70594-0.54622.$$

In the diagram in Fig. 15 are projected the points of the canonical score R1 and R2, calculated according to the functions given in Table 11a.

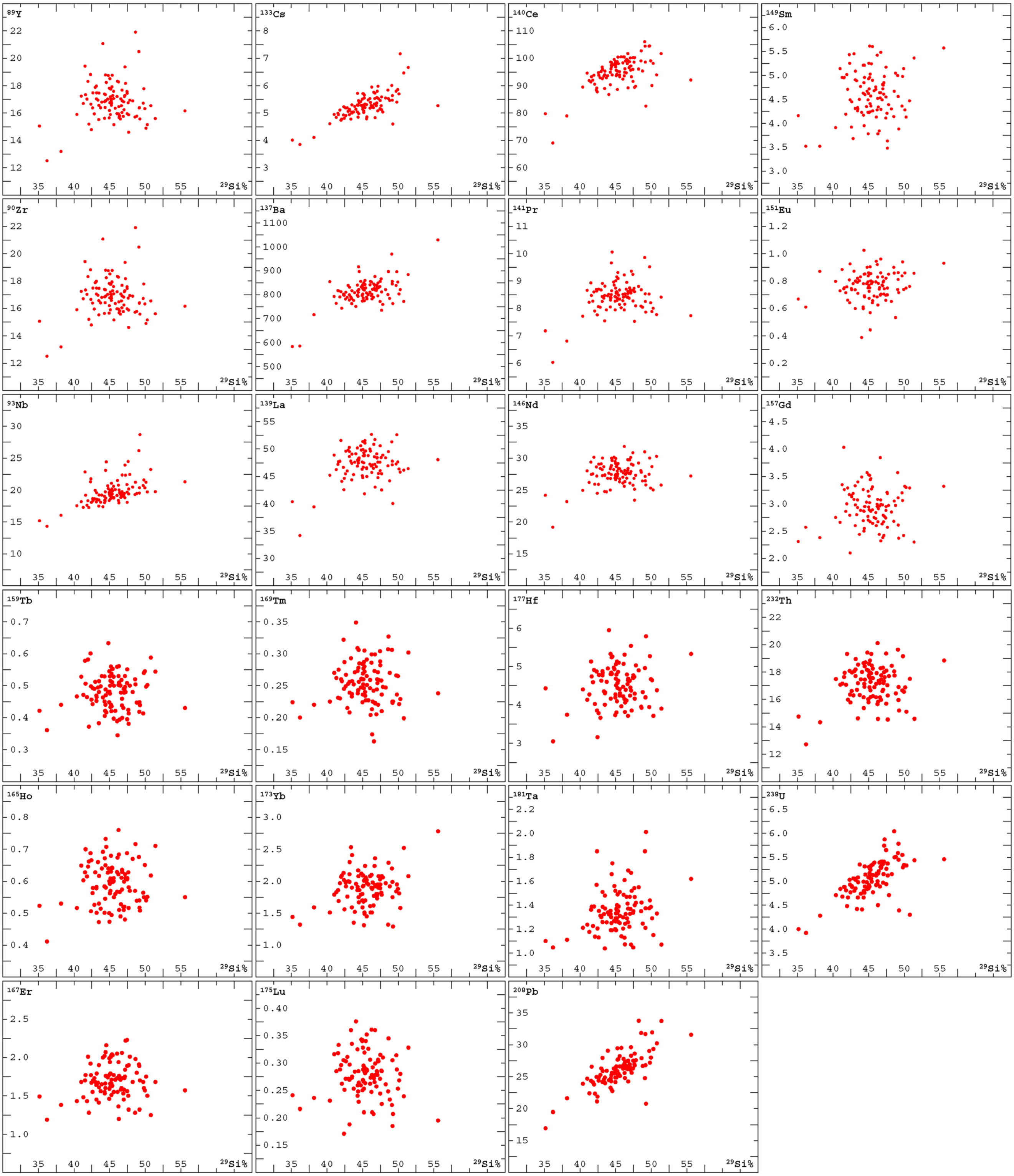

Fig. 13 (**a**–**c**) Variation diagrams: selected major and trace elements (ppm) vs. ^{29}Si% for the volcanic samples from the outcrops and aggregate glasses from the mortars of the Nora theatre

In Table 11b, the three equations (with $y = ax + b$) of straight lines dividing between the three groups are reported.

Observing the discriminating diagram of Fig. 15, the volcanic glasses used in the mortars constitute a distinct group compared with those of other samples from Mt. Arci and St. Antioco. The analysed samples from Perdas Urias outcrops (belonging to the Mt. Arci area), though falling within the field of St. Antioco group

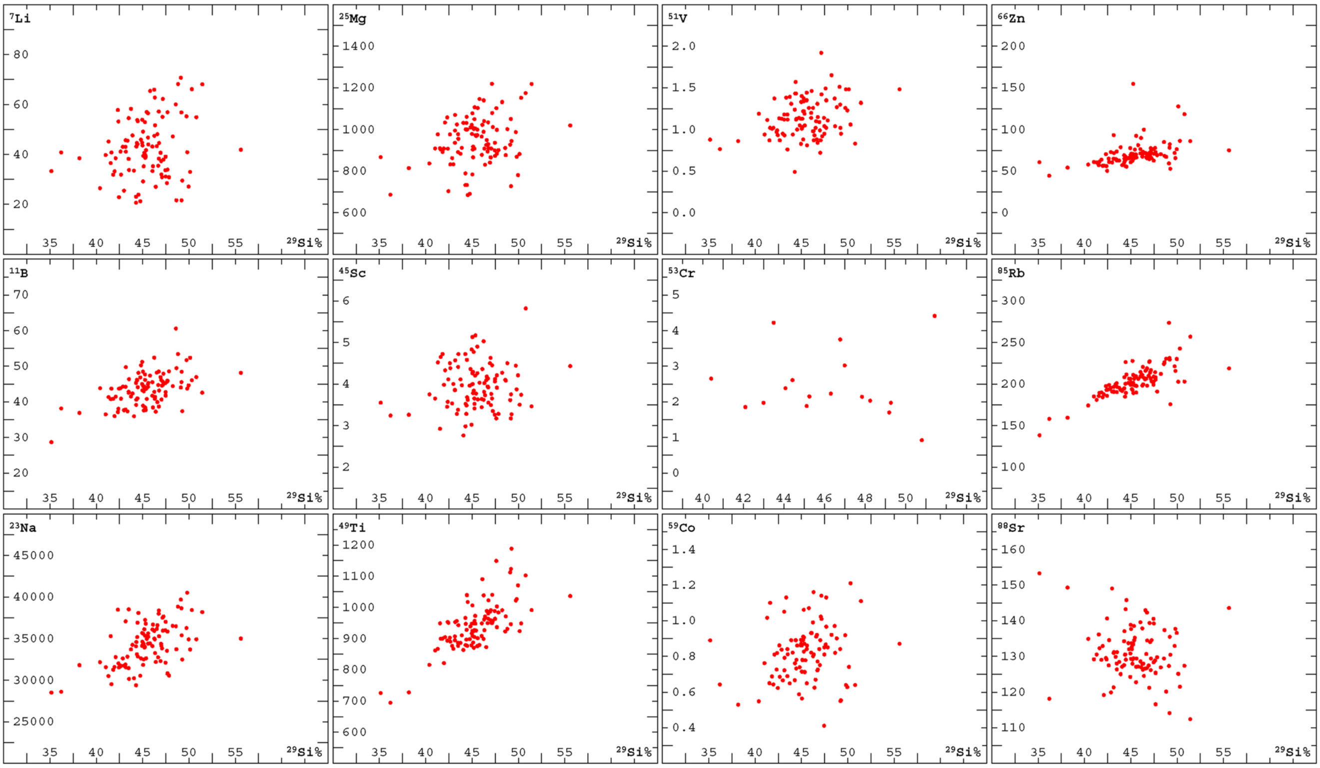

Fig. 13 (Continued)

(Fig. 15), are very close to the analysis of mortar glasses.

Discriminant analysis using trace elements

The discriminant analysis was applied using the trace elements of the mortar glasses, obsidians of Mt. Arci and volcanics of St. Antioco.

One hundred and sixty-three analyses were considered, among which 112 were related to mortar glasses, 37 obsidians to Mt. Arci and 12 to St. Antioco. The variables chosen for the discrimination of the groups are represented by the following elements: Ti, V, Cr, Zn, Rb, Sr, Y, Zr, Nb, Cs, Ba, La, Ce and Pb. Among them (based on discriminant analysis), those that perform most significant results are as follows: Sr, Ce, V, Ba, Rb and Y. Similarly to the case of major elements, each sample is classified as belonging to the group that shows the higher score, calculated using the coefficients in Table 12a.

Table 12b shows a summary diagram of the classification results, according to the classification score groups. In the case of the mortar glasses, obsidians of Mt. Arci and volcanics of St. Antioco, the classification is correct in 100% of cases.

Table 13a shows the canonical functions, which, also in this case, are equal to two (number of groups minus one). For each sample, each variable must be multiplied by the coefficient shown, according to the scheme of previous paragraph.

In Fig. 16 are projected the points of the canonical score R1 and R2. In Table 13b, the three equations (with $y = ax + b$) of straight lines dividing between the three groups are reported.

The analysis of samples from the mortars of the theatre, from Mt. Arci and St. Antioco, constitutes separate fields, while the analysis of samples from Perdas Urias falls under the volcanic glasses from the mortars of the theatre with a good overlap.

Discussion of results

Inside the Nora Roman theatre, a great amount of obsidian glasses together with quartz/feldspar sands is mainly used as aggregate in the hydraulic mortars. These glasses have been also used as pozzolan materials, although their characteristics are different with respect to the natural pozzolans normally used in the Roman period. Thus, the volcanic glass gives good hydraulic characteristics to the mortars, as shown by the constant presence of reaction edges with the binder (Fig. 6b) with consequent chemical exchanges: a decrease of Si, Al and K and a simultaneous increase of Ca and volatiles compared with glass (Columbu and Garau 2017). Given the good pozzolanic characteristics of the volcanic glass, it is conceivable that the Romans voluntarily used this type of material in place

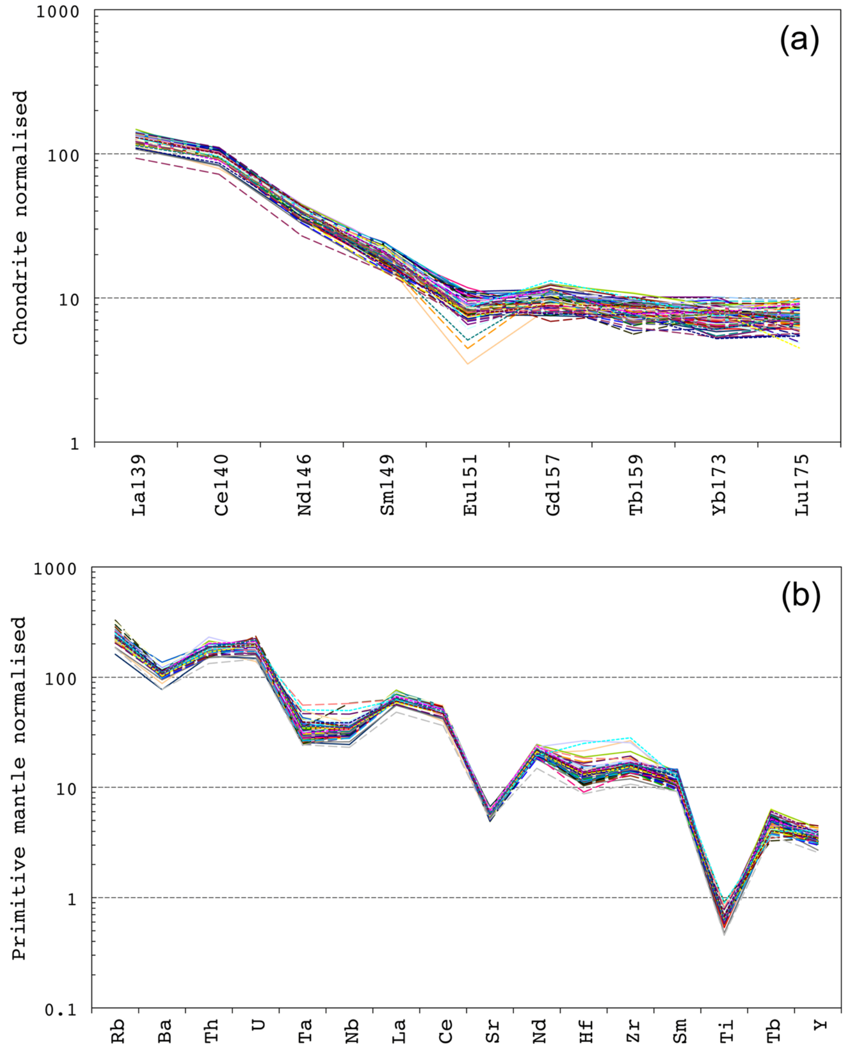

Fig. 14 (**a**, **b**) Geochemical characteristics of the mortar glasses: (**a**) pattern of selected rare earths normalized to chondrite (factors from Anders and Grevesse 1989); (**b**) spider diagram of selected elements normalized to primitive mantle, according to Wood (1979)

of *cocciopesto* (scarcely present in the mortars or absent in some samples) to make as much resistant mortar from the structure of the theatre, an open work subject to weathering processes.

The use of these volcanic glasses in the archaeological site of Nora, as well as in other Sardinian Roman monuments, at the moment was not known. Differently from the other components of the aggregate, these obsidian rocks do not belong to the vicinity of the Nora site, because there are no outcrops bearing these petro-volcanological characteristics. However, their wide use in the theatre mortars may suggest either a local availability or a not very distant origin. The geochemical

Table 8 Correlation matrix for some rare earths of volcanic glasses from the theatre mortars

Variable	LA139	CE140	ND146	SM149	EU151	GD157	TB159	YB173	LU175
^{139}La	1	0.6649	0.7133	0.4746	0.2950	0.3404	0.4364	0.4580	0.3527
^{140}Ce	0.6649	1	0.4862	0.2514	0.3817	0.1514	0.1603	0.3011	0.1525
^{146}Nd	0.7133	0.4862	1	0.441	0.2148	0.4084	0.4284	0.4943	0.3718
^{149}Sm	0.4746	0.2514	0.4410	1	0.1470	0.1611	0.4301	0.2755	0.3164
^{151}Eu	0.2950	0.3817	0.2148	0.1470	1	− 0.0092	0.1018	0.1328	0.0409
^{157}Gd	0.3404	0.1514	0.4084	0.1611	− 0.0092	1	0.3511	0.3104	0.2397
^{159}Tb	0.4364	0.1603	0.4284	0.4301	0.1018	0.3511	1	0.1904	0.2632
^{173}Yb	0.4580	0.3011	0.4943	0.2755	0.1328	0.3104	0.1904	1	0.2955
^{175}Lu	0.3527	0.1525	0.3718	0.3164	0.0409	0.2397	0.2632	0.2955	1

Table 9 Subdivision of 232 chemical analyses in the groups identified in advance to make the discriminant analysis on the basis of the major elements

Rock	#	De La Roche et al. (1980) classification
Volcanic glasses from mortars	50	Rhyolites
Volcanics from Mount Arci	7	Rhyolites
	111	Alkali-rhyolites
	37	Alkali-rhyolites
Volcanics from Saint Antioco	6	Rhyolites
	22	Alkali-rhyolites

comparison of data suggests that the mortar glasses have a source from the volcanic complex of Mt. Arci (central-western Sardinia; Fig. 1) where there are volcanic rocks with similar characteristics. As showed by statistical step-wise linear discriminant analysis, the samples from the locality of *Perdas Urias* (east of Mt. Arci volcanic complex) show a geochemical similarity (especially on the basis of trace elements) with the volcanic glasses from the mortars, suggesting a provenance from *Perdas Urias* of the obsidian glasses used in the mortars of Nora theatre. The Mt. Arci obsidian deposits are well-known both in the archaeological and geological literature, (Barca et al. 2007; De Francesco et al. 2008, 2011; Freund 2014; Freund and Batist 2014; Le Bourdonnec et al. 2006, 2010, 2015; Léa 2012; Lilliu 1988; Lugliè 2003, 2009a, 2010; Lugliè 2013; Lugliè et al. 2006, 2007, 2008, 2011; Macciotta et al. 2004; Mackey and Warren 1983; Marchi et al. 2005; Tykot 1996, 1997, 2002; Tykot et al. 2008). The obsidian rocks (emphatically called the “black gold” of the prehistoric period) is an important lithic raw material that has been used since the Early Neolithic with a high diffusion in many Neolithic to Chalcolithic sites in Sardinia and in a part of the Western Mediterranean area. This type of volcanic material was commonly reduced to produce chipped tools (e.g., cutting tools such as axes and arrowheads).

From an archaeological point of view, two possible hypotheses on their procurement in the Roman period can be made: (a) the obsidian was already present in the vicinity of the site of Nora (e.g., as a waste or residue of previous processing of the material) and (b) it was extracted from an ancient quarry of Mt. Arci outcrops, which was well-known for the high presence of obsidians.

Considering the widespread Sardinian road network in the Roman time (Fig. 1; Mastino 2005) and their intensive use in the theatre of Nora, it is conceivable to imagine a procurement of these obsidians from the Mt. Arci area. In fact, in agreement with the archaeological literature, the road connecting the Roman villages of *Karales* (today Cagliari city, south Sardinia; Fig. 1) and *Turris Lybisonis* (today Porto Torres, NW Sardinia; Fig. 1) passed near the eastward side of Monte Arci volcanic complex. Moreover, in the middle of this ancient road stood the archaeological site of *Forum Traiani* (today Fordongianus village; Fig. 1) and the Roman village of Mulargia (Fig. 1), both well-known for its thermal baths and for its ancient quarries of ignimbrite rocks, respectively. Mulargia is a very important

Table 10 (**a**) Classificative functions for the discriminant analysis on the basis of the major elements. (**b**) Summary of the classification of sample groups

(a)				
Variable		TN	MA	SA
CaO		16.546	− 10.842	− 2.697
FeO_T		63.419	63.97	85.609
P_2O_5		− 191.734	− 246.048	− 282.898
Al_2O_3		37.784	39.945	45.11
Constant		− 295.945	− 289.794	− 401.319
(b)				
Group	Correct percent	# TN	# MA	# SA
Theatre	100	50	0	0
Mt. Arci	100	0	155	0
S. Antioco	92.86	1	1	26
Total	99.14	51	156	26

TN, Nora Theater; MA, Mt. Arci; SA, St. Antioco; #, number of samples

Table 11 (**a**) Coefficients of canonical functions (root 1 and root 2) for the discriminant analysis on the basis of the major elements. (**b**) Equations (as y = ax + b) of dividing straight lines (1, 2, 3)

(a)		
Variable	Root 1	Root 2
CaO	4.5298	1.755
FeO_T	− 0.7997	3.9348
P_2O_5	10.7059	− 6.1706
Al_2O_3	− 0.5462	0.9192
Constant	3.9207	− 18.0525
(b)		
y = ax + b	a	b
Straight line 1	− 5.606425	10.015314
Straight line 2	1.347037	0.469467
Straight line 3	0.056704	2.24111

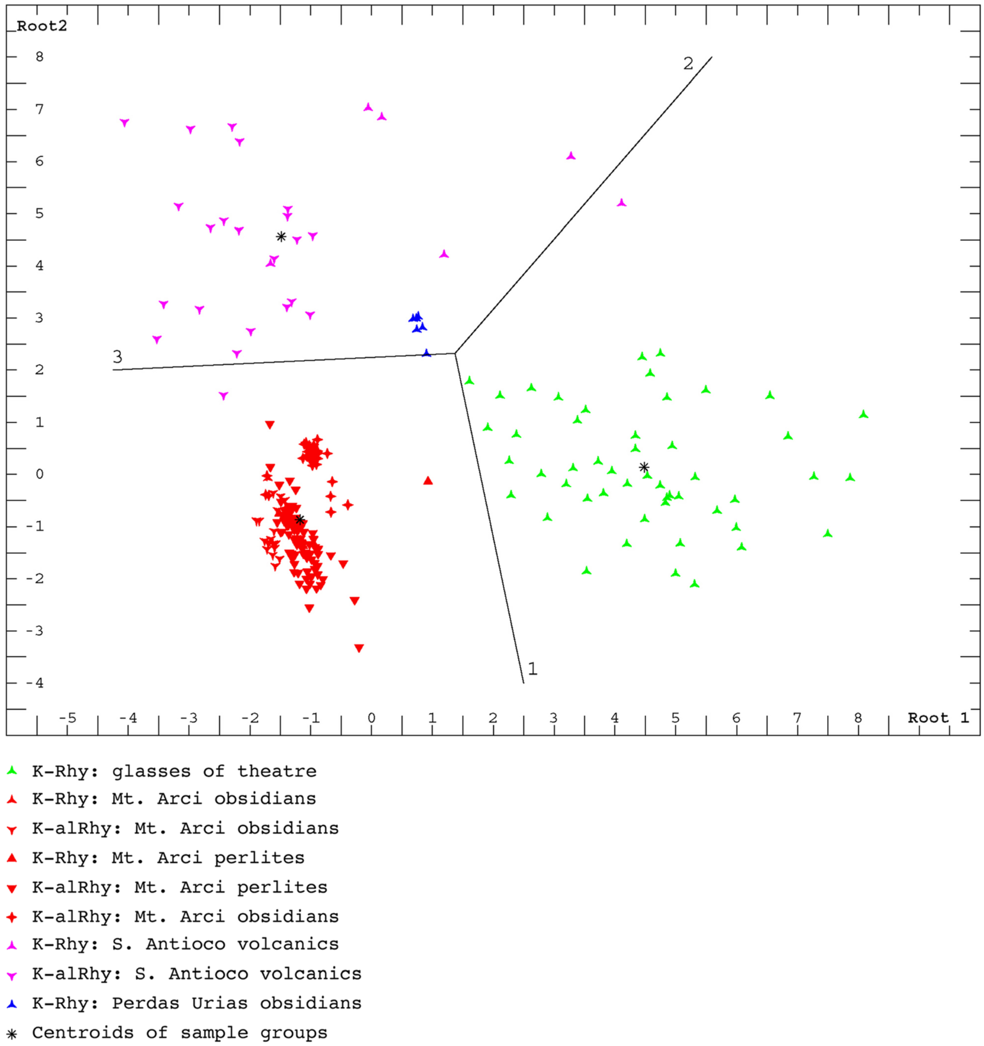

Fig. 15 Discriminant diagram (root 1 vs. root 2) on the basis of the major elements of volcanic glasses from the mortars and volcanic samples from Mt. Arci and St. Antioco areas. Abbreviations as the legend in Fig. 8

Table 12 (**a**) Classificative functions for the discriminant analysis on the basis of the trace elements

(a)				
Variable		TN	MA	SA
Sr		2.041	0.904	0.685
Ce		1.071	0.275	0.766
V		0.593	0.846	− 0.196
Ba		− 0.092	− 0.069	0.01
Rb		0.752	0.687	0.444
Y		− 1.865	− 1.032	− 0.712
(b)				
Group	Percent correct	# TN	# MA	# SA
Theatre	100	112	0	0
Mt. Arci	100	0	37	0
S. Antioco	100	0	0	14
Total	100	112	37	14

Abbreviations as caption in Fig. 9

Table 13 (**a**) Coefficients of canonical functions (root 1 and root 2) for the discriminant analysis on the basis of the trace elements. (**b**) Equations (as y = ax + b) of dividing straight lines (1, 2, 3)

(a)		
Variable	Root 1	Root 2
Sr	0.0963	0.085
Ce	0.059	− 0.0275
V	− 0.0072	0.1284
Ba	− 0.0029	− 0.0118
Rb	0.0085	0.036
Y	− 0.0726	− 0.0838
Constant	− 12.6758	− 4.7147
(b)		
y = ax + b	a	b
Straight line 1	10.327408	30.872576
Straight line 2	− 1.24852	− 3.943814
Straight line 3	0.591842	1.588636

Fig. 16 Discriminant diagram (root 1 vs. root 2) on the basis of the trace elements of volcanic glasses from the mortars and volcanic samples from Mt. Arci

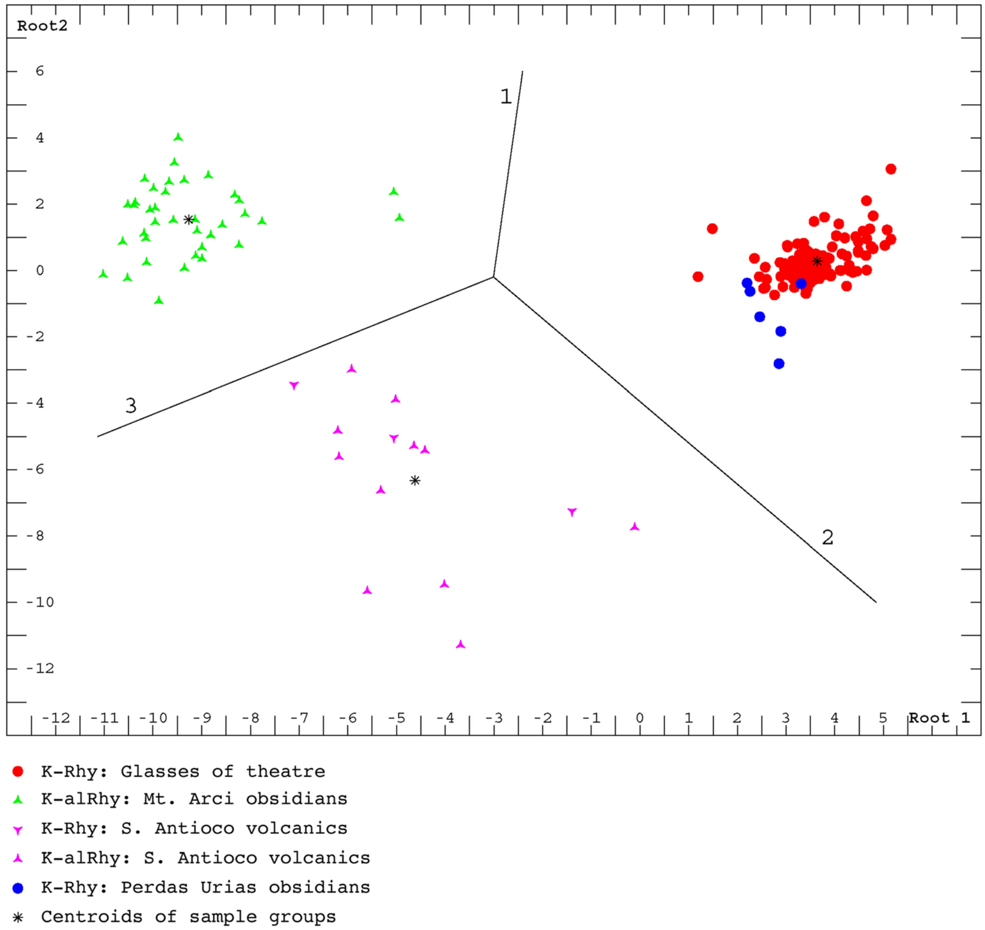

Roman site for the production of Roman millstones, exported in various parts of the Mediterranean (e.g., North Africa, Antonelli et al. 2014a) and for the existence of ancient commercial routes of different kinds of stone. Moreover, many Roman public buildings, *villae* and rural settlements are known in close proximity to the many obsidian sources scattered along the western, southern and north-western flanks of the Monte Arci volcanic massif. For these reasons, it is not unlikely to assume a gathering and transportation activity, even if occasional, of obsidians along the Roman road network.

However, in the frame of a long-term archaeological project on Monte Arci obsidians carried out since 2002 (Lugliè 2003, 2013), including systematic and careful surveys along the north-eastern flanks of the mounting around the so-named Perdas Urias outcrop, no evidence was found thus far to support the local exploitation of this raw material during later historic times. In spite of this intense archaeological exploration of the direct supply area, the possibility of an intended gathering activity of obsidian by Romans still remains in the state of an *argumentum ex silentio*.

Therefore, the first hypothesis on the obsidian origin seems to be by far more likely, because of the unicity of this case and due to the presence of some prehistoric settlement in the Nora area or its surroundings as in the *S'Abuleu* region (Migaleddu 1996) and, possibly, in the same site of Nora (Lugliè 2009b). In fact, during the last prehistory in these two settlements, the obsidian reduction of shaped cores transported from the Monte Arci workshops was a daily activity to produce a plentiful of artefacts and specialized tools. Moreover, obsidian is commonly found in the form of finished tools in Nora territory even in later Nuragic times; in fact, indeed, all around the Roman Nora town, many Nuragic sites are scattered in the plain and on the hills, among which stands out the complex tower and village of *Antigori* (near to the Sarroch city). This is a large site occupied from the 14th to 8th centuries B.C. (Russell 2010; Balmuth 1992) with castle-like structures, heavy multi-towered walls and associated villages, which Webster (1996) labeled as one of 14 known Class III settlements in Sardinia. Like in this last case, reoccupation of Bronze age Nuraghi in Roman times for civil and ritual purposes is a common behaviour that for sure could have put in contact Roman people with abundant obsidian elements.

Conclusions

The research allowed us to define the geochemical characteristics and the probable provenance of obsidian glasses used in the ancient mortars of the Roman Nora theatre.

This kind of volcanic glass, together with a quartz-feldspar sandy and subordinately local Oligo-Miocenic calc-alkaline volcanics and Palaeozoic rocks, was used as mortar aggregate for the different sectors of the theatre (i.e., *tribunalia* vaults, *cavea* foundation, vaults and inner walls of the external niches, brick and stone walls). Considering its low bulk density, it is probable that it was used also to lighten some structures (e.g., concrete of *tribunalia* vaults), together with subdecimetric fragments of other local stones (i.e., volcanic rocks and sandstones), which has also low bulk density due to their high porosity. Given its chemical–physical features, characterised by an amorphous state reacting with the binder, it was also used as pozzolana, conferring hydraulic properties and high mechanical strengths to the mortars and concretes of the monument, especially in the structural parts where it has been intensively used.

Given the good hydraulic features and their massive use in the theatre, it is probable that the Romans intentionally used the volcanic glasses in place of *cocciopesto*, to make the mortars much resistant to weathering. Moreover, the unusual presence of volcanic fine aggregate in the plasters of the open-air *cavea* sector of the theatre confirms the intention of Roman constructors to improve the hydraulic characteristics of the mortars and their resistance to decay processes. It is not accident that the theatre, an open construction designed without roofing, is also one of the best preserved buildings in the Nora site.

The use of these obsidian glasses as pozzolana today represents a novelty in the production of Roman mortars in the archaeological site of Nora, especially considering that in the area surrounding Nora, the obsidian is not available as a raw material.

The results of discriminant analysis highlights that the volcanic glasses show a geochemical similarity with the volcanics of *Perdas Urias* outcrops, indicating a provenance from Mt. Arci volcanic complex, a well-known source as early as the Neolithic period (Lilliu 1988; Lugliè 2009a). Since an archaeological evidence for the obsidian procurement directly from the source in Roman times is still lacking, this hypothesis on the origin of glasses opens new scenarios from a historical and cultural point of view, raising up new and interesting issues.

From a technical-constructive point of view, it opens up further interesting research topics to understand if the use of obsidian rocks as aggregate in the mortars of a theatre (a) was a local experiment to make the hydraulic mortars of theatre or (b) extends to other buildings of the Nora site and/or in other Sardinian Roman settlements. Considering that currently there is no archaeological evidence about both the use of these obsidian glasses in other Sardinian Roman sites and about the presence of any Roman raw material procurement in the source area, at the moment it is unlikely to suppose that the Romans supplied obsidians directly from Mt. Arci. Assuming the first case, Romans probably used shattered and discarded artefacts from a local pre-existing “source” of obsidian, consisting in an earlier production activity during Neolithic times in the Nora area. In fact, the obsidian processing wastes are usually abundant in these prehistoric sites and well known in the archaeological literature, so it is easy to suppose a later exploitation of crushed earlier obsidian artefacts as temper for the mortars to be used in a single building like the theatre.

In any case, the detection of these glasses inside the mortars of the theatre raises a strong interest in the development of new archaeological investigation and further geochemical and petrographic studies either to check the possible use of Mt. Arci obsidians in other Roman Sardinian sites or, more likely, to find further evidence of their prehistoric storage and processing in the Nora area.

Acknowledgments Special thanks to the University of Cagliari for funding this research; the Superintendence for Archaeological Heritage for the Provinces of Cagliari and Oristano for authorization to sample the materials from the monument; and the staff and tourist guides of the archaeological site of Nora for their willingness regarding the study activities of the Roman theatre.

References

AA.VV (2000) In: Tronchetti C (ed) Ricerche su Nora—I (anni 1990–1998). Sainas Ed, Cagliari

Adam JP (2006) L’arte di costruire presso i Romani, materiali e tecniche vol 10. Longanesi

Adriano P, Santos Silva A, Veiga R, Mirão J, Candeias AE (2009) Microscopic characterization of old mortars from Santa Maria Church in Évora. Mater Charact 60(7):610–620

Advokaat EL, Van Hinsbergen DJJ, Maffione M, Langereis CG, Vissers RLM, Cherchi A, Schroeder R, Madani H, Columbu S (2014) Eocene rotation of Sardinia, and the paleogeography of the western Mediterranean region. Earth Planet Sci Lett 401:183–195

Alvarez JI, Navarro I, Martin A, Garcia Casado PJ (2000) A study of the ancient mortars in the north tower of Pamplona’s San Cernin Church. Cem Concr Res 30:1413–1419

Anders E, Grevesse N (1989) Abundances of the elements: meteoric and solar. Geochim Cosmochim Acta 53:197–214

Antonelli F, Columbu S, De Vos Raaijmakers M, Andreoli M (2014a) An archaeometric contribution to the study of ancient millstones from the Mulargia area (Sardinia, Italy) through new analytical data on volcanic raw material and archaeological items from Hellenistic and Roman North Africa. J Archaeol Sci 50:243–261

Antonelli F, Columbu S, Lezzerini M, Miriello D (2014b) Petrographic characterization and provenance determination of the white marbles used in the Roman sculptures of Forum Sempronii (Fossombrone, Marche, Italy). Appl Physics A 115:1033–1040

Balmuth MS (1992) Archaeology in Sardinia. American Journal of Archaeology 96(4):663–697.

Barca D, De Francesco AM, Crisci GM (2007) Application of laser ablation ICP-MS for characterization of obsidian fragments from peri-Tyrrhenian area. J Cult Herit 8(2):141–150

Beccaluva L, Macciotta G, Manetti P, Peccerillo A, Poli G (1984) Pliocene–Quaternary alkaline to subalkaline volcanism in Sardinia: magma genesis and evolution. Dip. Sc. Terra, Firenze, p 50

Beccaluva L, Civetta L, Macciotta G, Ricci CA (1985) Geochronology in Sardinia: results and problems. Rend Soc It Min Petr 40:57–72

Beccaluva L, Brotzu P, Macciotta G, Morbidelli L, Serri G, Traversa G (1989) Cainozoic tectono-magmatic evolution and inferred mantle sources in the Sardo-Tyrrenian area. In: Boriani A, Bonafede M, Piccardo GB, Vai GB (Eds.) The lithosphere in Italy. Advances in earth science research. Atti Conv. Acc. Naz. Lincei, vol 80, pp 229–248

Beccaluva L, Coltorti M, Galassi B, Macciotta G, Siena F (1994) The Cainozoic calcalkaline magmatism of the western mediterranean and its geodynamic significance. Boll. di Geofisica Teorica e Applicata 36(141–144):293–308

Beccaluva L, Bianchini G, Coltorti M, Siena F, Verde M (2005a) Cenozoic tectono-magmatic evolution of the central-western Mediterranean: migration of an arc–interarc basin system and variations in the mode of subduction. In: Finetti I (Ed.) Elsevier special volume, “crop project—deep seismic exploration of the Central Mediterranean and Italy”, pp 623–640

Beccaluva L, Bianchini G, Bonadiman C, Coltorti M, Macciotta G, Siena F, Vaccaro C (2005b) Within-plate Cenozoic volcanism and lithospheric mantle evolution in the western-central Mediterranean area. In: Finetti I. (Ed.) Elsevier special volume, “crop project—deep seismic exploration of the Central Mediterranean and Italy”, pp 641–664

Beccaluva L, Bianchini G, Natali C, Siena F (2011) Geodynamic control on orogenic and anorogenic magmatic phases in Sardinia and Southern Spain: inferences for the Cenozoic evolution of the western Mediterranean. Lithos 123:218–224

Bejor G (1999) L’area del teatro. In: Tronchetti C (ed) AA. VV. Ricerche su Nora-I (anni 1990–1998). Sainas Ed, Cagliari

Bertorino G, Franceschelli M, Marchi M, Luglié C, Columbu S (eds) (2002) Petrographic characterisation of polished stone axes from Neolithic Sardinia, archaeological implications. Per. Mineral., Special Issue: Archaeometry and Cultural Heritage 71:87–100

Bianchini G, Marrocchino E, Vaccaro C (2004) Chemical and mineralogical characterisation of historic mortars in Ferrara (NE, Italy). Cem Concr Res 34(8):1471–1475

Bultrini G, Fragala I, Ingo GM, Lanza G (2006) Minero-petrographic, thermal and microchemical investigation of historical mortars used in Catania (Sicily) during the XVII century A.D. Appl Physics A 83(4):529–536

Cagnana A (2000) Archeologia dei materiali da costruzione. SAP Società Archeologica S.r.l., Mantova

Cherchi A, Mancin N, Montadert L, Murru M, Putzu MT, Schiavinotto F, Verrubbi V (2008) The stratigraphic response to the Oligo-Miocene extension in the western Mediterranean from observations on the Sardinia graben system (Italy). Bull Soc Geol Fr 179:267–287

Cioni R, Macciotta G, Marchi M, Padalino G, Simeone R, Palomba M (2001) Water–rock interaction in genesis of perlite at Monte Arci volcanic complex (West Sardinia, Italy). In: Cidu (ed) Water–rock interaction 2001. Swets & Zeitlinger, Lisse, pp 693–696

Colby JW (1971) Magic IV: a computer program for quantitative electron microprobe analysis. Bell Telephone Laboratories Inc., Allentown

Columbu S (2017) Provenance and alteration of pyroclastic rocks from the Romanesque Churches of Logudoro (north Sardinia, Italy) using a petrographic and geochemical statistical approach. Appl Phys A Mater Sci Process 123 (3)(165):1–28. https://doi.org/10.1007/s00339-017-0790-z

Columbu S (2018) Petrographic and geochemical investigations on the volcanic rocks used in the Punic-Roman archaeological site of Nora (Sardinia, Italy). Earth Environmental Sciences, in press

Columbu S, Garau AM (2017) Mineralogical, petrographic and chemical analysis of geomaterials used in the mortars of Roman Nora theatre (south Sardinia, Italy). Ital J Geosci 136(2):238–262

Columbu S, Verdiani G (2014) Digital survey and material analysis strategies for documenting, monitoring and study the Romanesque churches in Sardinia, Italy. In: Lecture notes in computer science, vol 8740. Springer, pp 446–453

Columbu S, Garau AM, Macciotta G, Marchi M, Marini C, Carboni D, Ginesu S, Corazza G (2011) Manuale sui materiali lapidei vulcanici della Sardegna centrale e dei loro principali impieghi nel costruito. Iskra Edizioni, Ghilarza, p 302

Columbu S, Antonelli F, Lezzerini M, Miriello D, Adembri B, Blanco A (2014a) Provenance of marbles used in the *Heliocaminus* Baths of Hadrian's Villa (Tivoli, Italy). J Archaeol Sci 49:332–342

Columbu S, Gioncada A, Lezzerini M, Marchi M (2014b) Hydric dilatation of ignimbritic stones used in the church of Santa Maria di Otti (Oschiri, northern Sardinia, Italy). Ital J Geosci 133:149–160

Columbu S, Cruciani G, Fancello D, Franceschelli M, Musumeci (2015a) Petrophysical properties of a granite-protomylonite-ultramylonite sequence: insight from the Monte Grighini shear zone, central Sardinia, Italy. Eur J Mineral 27(4):471–486

Columbu S, Sitzia F, Verdiani G (2015b) Contribution of petrophysical analysis and 3D digital survey in the archaeometric investigations of the Emperor Hadrian’s Baths (Tivoli, Italy). Rendiconti Lincei 26(4):455–474

Columbu S, Lisci C, Sitzia F, Buccellato G (2017a) Physical-mechanical consolidation and protection of Miocenic limestone used on Mediterranean historical monuments: the case study of Pietra Cantone (southern Sardinia, Italy). Environ Earth Sci 76(4):148. https://doi.org/10.1007/s12665-017-6455-6

Columbu S, Sitzia F, Ennas G (2017b) The ancient pozzolanic mortars and concretes of Heliocaminus baths in Hadrian’s Villa (Tivoli, Italy). Archaeol Anthropol Sci 9:523–553

Columbu S, Antonelli F, Sitzia F (2018a) Origin of Roman worked stones from St. Saturno Christian Basilica (south Sardinia, Italy). Mediterranean Archaeology and Archaeometry, in press

Columbu S, Piras G, Sitzia F, Pagnotta S, Raneri S, Legnaioli S, Palleschi V, Lezzerini M, Giamello M (2018b) Petrographic and mineralogical characterization of volcanic rocks and surface-depositions on Romanesque monuments. Mediterranean Archaeology and Archaeometry, in press

Columbu S, Palomba M, Sitzia F, Murgia MR (2018c) Geochemical, mineral-petrographic and physical-mechanical characterization of stones and mortars from the Romanesque Saccargia Basilica (Sardinia, Italy) to define their origin and alteration. Ital J Geosci 137(3):1-27. DOI: https://doi.org/10.3301/IJG.2018.04

Cox KG, Bell JD, Pankhurst RJ (1979) The interpretation of igneous rocks. George Allen & Unwin, London, p 450

Criss JW (1977) NRLXRF: a fortran program for X-ray fluorescence analysis. Cosmic, Athens

Cross W, Iddings JP, Pirsson LV, Washington HS (1903) Quantitative classification of igneous rocks. University of Chicago Press

De Francesco AM, Crisci GM, Bocci M (2008) Non-destructive analytic method using XRF for determination of provenance of archaeological obsidians from the mediterranean area: a comparison with traditional XRF methods. Archaeometry 50(2):337–350

De Francesco AM, Bocci M, Crisci GM (2011) Non-destructive applications of wavelength XRF in obsidian studies. X-ray fluorescence spectrometry (XRF) in geoarchaeology:81–107

De La Roche H, Leterrier J, Grandclaude P, Marchal M (1980) A classification of volcanic and plutonic rocks using R1–R2 diagram and major-element analyses—its relationships with current nomenclature. Chem Geol 29:183–210

De Luca R, Cau Ontiveros MA, Miriello D, Pecci A, Le Pera E, Bloise A, Crisci GM (2013) Archaeometric study of mortars and plasters from the Roman City of Pollentia (Mallorca-Balearic Islands). Per Mineral 82:353–379

De Luca R, Miriello D, Pecci A, Domìnguez-Bella S, Bernal-Casasola D, Cottica D, Bloise A, Crisci GM (2015) Archaeometric study of mortars from the Garum Shop at Pompeii, Campania, Italy. Geoarchaeology 30:330–351

Folk RL (1954) The distinction between grain size and mineral composition in sedimentary rock nomenclature. J Geol 62(4):344–359

Folk RL (1968) Petrology of sedimentary rocks. Hemphill's Austin, Texas

Franzini M, Leoni L, Saitta M (1975) Revisione di una metologia analitica per fluorescenza-X, basata sulla correzione completa degli effetti di matrice. Soc. It. Min. Petrol.—Rendiconti 31(2):365–378

Franzini M, Leoni L, Lezzerini M, Sartori F (2000) The mortar of the "Leaning Tower" of Pisa: the product of a medieval technique for preparing high-strength mortars. Eur J Mineral 12:1151–1163

Freund KP (2014) Obsidian consumption in Chalcolithic Sardinia: a view from Bingia 'e Monti. J Archaeol Sci 41:242–250

Freund KP, Batist Z (2014) Sardinian obsidian circulation and early maritime navigation in the Neolithic as shown through social network analysis. Journal of Island and Coastal Archaeology 9(3):364–380

Ghiotto AR (2004) L'architettura romana nelle città della Sardegna. Edizioni Quasar, Roma, p 268

Giuliani Cairoli F (2006) L'edilizia nell'antichità. Carocci, Roma

Gutiérrez GMA, Plumed HR, Soutelo SG, Savin MC, Lapuente P, Chapoulie R (2016) The marble of O Incio (Galicia, Spain): quarries and first archaeometric characterisation of a material used since roman times. ArcheoSciences (40, 1):103–117

Irvine TN, Baragar WRA (1971) A guide to the chemical classification of the common volcanic rocks. Can J Earth Sci 8:523–548

Kuno H (1968) Differentiation of basalt magma. In: Hess H, Poldervaart A (eds) The Poldervaart treatise on rocks of basaltic composition, vol II. Wiley & Sons, New York, pp 623–688

Lapuente P (2014a) Archaeometry on stones. Multi-method approach to investigate stone provenance. studied cases from Roman Hispanic marmora. Archeometriai Műhely (1786-271X) 11(3):149–158

Lapuente P (2014b) White marble sculptures from the National Museum of Roman Art (Mérida, Spain): sources of local and imported marbles. Eur J Mineral 26(2):333–354

Lapuente P, León P, Nogales T, Royo H, Preite-Martinez M, Blanc Ph (2012) White sculptural materials from Villa Adriana: study of provenance. In: Gutiérrez Garcia A, Lapuente P, Rodà I (Eds.) Interdisciplinary studies on ancient stone. Proceedings of the IX ASMOSIA Conference, Tarragona, pp 364–375

Le Bourdonnec FX, Poupeau G, Lugliè C (2006) SEM-EDS analysis of western Mediterranean obsidians: a new tool for Neolithic provenance studies. Compt Rendus Geosci 338(16):1150–1157

Le Bourdonnec FX, Bontempi JM, Marini N, Mazet S, Neuville PF, Poupeau G, Sicurani J (2010) SEM-EDS characterization of western Mediterranean obsidians and the Neolithic site of A Fuata (Corsica). J Archaeol Sci 37(1):92–106

Le Bourdonnec FX, D'Anna A, Poupeau G, Lugliè C, Bellot-Gurlet L, Tramoni P, Marchesi H (2015) Obsidians artefacts from Renaghju (Corsica Island) and the Early Neolithic circulation of obsidian in the Western Mediterranean. Archaeol Anthropol Sci 7(4):441–462

Le Maitre RW, Streckeisen A, Zanettin B, Le Bas MJ, Bonin B, Bateman P, Bellieni G, Dudek A, Efremova S, Keller J, Lamere J, Sabine PA, Schmid R, Sorensen H, Woolley AR (2002) Igneous rocks: a classification and glossary of terms. In: Recommendations of the International Union of Geological Sciences, Subcommission of the Systematics of Igneous Rocks. Cambridge University Press, Cambridge

Léa V (2012) The diffusion of Obsidian in the Northwestern Mediterranean: toward a new model of the Chassey culture? J Mediterr Archaeol 25(2):147–173

Lezzerini M, Antonelli F, Columbu S, Gadducci R, Marradi A, Miriello D, Parodi L, Secchiari L, Lazzeri A (2016) The documentation and conservation of the cultural heritage: 3D laser scanning and Gis techniques for thematic mapping of the stonework of the façade of St. Nicholas Church (Pisa, Italy). International Journal of Architectural Heritage: Conservation, Analysis, and Restoration 10(1):9–19

Lezzerini M, Pagnotta S, Columbu S, Gallello G (2018a) Archaeometric study of mortars from the Pisa's Cathedral Square (Italy). Measurement 126:322-331

Lezzerini M, Pagnotta S, Raneri S, Legnaioli S, Palleschi V, Columbu S, Neri NF, Mazzoleni P (2018b) Examining the reactivity of volcanic ash in ancient mortars by using a micro-chemical approach. Mediterranean Archaeology and Archaeometry, in press

Lilliu G (1988) La civiltà dei sardi: dal paleolitico all'età dei nuraghi. Nuova ERI, Torino

Lofgren G (1971) Experimentally produced devitrification textures in natural rhyolitic glass. Geol Soc Am Bull 82:111–124

Lugliè C (2003) First report on the study of obsidian prehistoric workshops in the eastern side of Monte Arci (Sardinia). Les Matières Premières Lithique en Préhistoire, Actes de la Tab.-Ronde d'Aurillac (Préhistoire du Sud-ouest, Supplément 5), pp. 207–209

Lugliè C (2009a) L'obsidienne néolithique en Méditerranée occidentale. In: Moncel MH, Frohlich F (eds) L'Homme et le Précieux Matières Minérales Précieuses, BAR International Series 1934. BAR, Oxford, pp 199–211

Lugliè C (2009b) I manufatti litici preistorici. In: Bonetto J, Falezza G, Ghiotoo AR (eds) Nora. Il foro romano. Storia di un'area urbana dall'età fenicia alla tarda antichità 1997–2006. II.1 I materiali preromani. Università di Padova, Padova, pp 1–2

Lugliè C (2010) L'ossidiana del Monte Arci nel Mediterraneo: nuovi apporti sulla diffusione, sui sistemi di produzione e sulla loro cronologia: Proceedings of V° International Congress (Pau, Italia, 27–29 giugno 2008). Nur, Ales

Lugliè C (2013) From the perspective of the source. Neolithic production and exchange of Monte Arci obsidians (Central-western Sardinia). In: Networks in the Neolithic. Raw materials, products and ideas circulation in the Western Mediterranean basin (VII-III aC) (Proceedings of the International Conference). Revista Rubricatum, 5: 173–180

Lugliè C, Le Bourdonnec FX, Poupeau G, Bohn M, Meloni S, Oddone M, Tanda G (2006) A map of the Monte Arci (Sardinia Island, Western Mediterranean) obsidian primary to secondary sources. Implications for Neolithic provenance studies. Comptes Rendus Palevol 5(8):995–1003

Luglié C, Le Bourdonnec FX, Poupeau G, Atzeni E, Dubernet S, Moretto P, Serani L (2007) Early neolithic obsidians in Sardinia (western Mediterranean): the Su carroppu case. J Archaeol Sci 34(3):428–439

Lugliè C, Le Bourdonnec FX, Poupeau G, Congia C, Moretto P, Calligaro T, Sanna I, Dubernet S (2008) Obsidians in the Rio Saboccu (Sardinia, Italy) campsite: provenance, reduction and relations with the wider Early Neolithic Tyrrhenian area. Comptes Rendus Palevol 7(4):249–258

Lugliè C, Le Bourdonnec FX, Poupeau G (2011) Neolithic obsidian economy around the Monte Arci source (Sardinia, Italy): the importance of integrated provenance/technology analyses. In: Turbanti-Memmi, I., (Ed.), Berlin: Springer, Proceedings of the 37th International Symposium on Archaeometry, 12th–16th May 2008, Siena, Italy, pp 255–260

Lustrino M, Morra V, Melluso L, Brotzu P, d'Amelio F, Fedele L, Franciosi L, Lonis R, Petteruti Liebercknecht AM (2004) The Cenozoic igneous activity of Sardinia. Per Min 73:105–134

Lustrino M, Morra V, Fedele L, Franciosi L (2009) Beginning of the Apennine subduction system in central western Mediterranean: constraints from Cenozoic “orogenic”magmatic activity of Sardinia, Italy. Tectonics 28:TC5016

Lustrino M, Duggen S, Rosenberg CL (2011) The Central-Western Mediterranean: anomalous igneous activity in an anomalous collisional tectonic setting. Earth Sci Rev 104:1–40

Lustrino M, Fedele L, Melluso L, Morra V, Ronga F, Geldmacher J, Duggen S, Agostini S, Cucciniello C, Franciosi L, Meisel T (2013) Origin and evolution of Cenozoic magmatism of Sardinia (Italy). A combined isotopic (Sr–Nd–Pb–O–Hf–Os) and petrological view. Lithos 180–181:138–158

Macciotta G, Columbu S, Garau AM, Marchi M (2004) Obsidian in the geochemical–petrographical evolution of Plio-Quaternary volcanics from Monte Arci. In: Castelli, P. (Ed.), Proceedings of 1st International Conference “L'ossidiana del Monte Arci nel Mediterraneo: recupero dei valori di un territorio”. Oristano-Pau (Italy), 29 November–1 December 2002, pp 35–46

Mackey M, Warren SE (1983) The identification of obsidian sources in the Monte Arci region of Sardinia. In: Aspinall A, Warren SE (eds) Proceedings of the 22nd Symposium on Archaeometry. University of Bradford, Bradford, pp 420–431

Maravelaki-Kalaitzaki P, Bakolas A, Moropoulou A (2003) Physico-chemical study of Cretan ancient mortars. Cem Concr Res 33:65–61

Marchi M, Garau AM, Columbu S, Macciotta G (2005) Definizione, nel Monte Arci, di possibili siti di provenienza di manufatti ossidianacei, mediterranei, per mezzo della loro caratterizzazione petrografica e geochimica. In: Proceedings of 3rd International Conference “L'ossidiana del Monte Arci nel Mediterraneo: le vie dell’ossidiana nel Mediterraneo ed in Europa”. Oristano-Pau (Italy), 25–26 September 2004, PTM Editor

Mastino A (2005) Storia della Sardegna antica. Ed. Il Maestrale, Sassari

Melis S, Columbu S (2000) Matériaux de construction en époque romaine et aves les anciennes carrières: l’exemple du théâtre de Nora (Sardaigne SO, Ietalie). In: Lorenz, J., Tardy, D., Coulon, G. (Eds.), La pierre dans la ville antique et médiévale. Analyse méthodologie et apports, Argentoun sur Creuse. St.-Marcel: Musée d'Argentomagus (Ed.), pp 103–117

Middlemost EAK (1975) The basalt clan. Earth Sci Rev 11:337–364

Migaleddu M (1996) Nora IV. Ricognizione. L'insediamento preistorico di S.Abuleu. Quaderni Soprint Arch Prov Ca Or 13:189–209

Miriello D, Barca D, Bloise A, Ciarallo A, Crisci GM, De Rose T, Gattuso C, Gazineo F, La Russa F (2010) Characterisation of archaeological mortars from Pompeii (Campania, Italy) and identification of construction phases by compositional data analysis. J Archaeol Sci 37:2207–2223

Miriello D, Antonelli F, Apollaro C, Bloise A, Bruno N, Catalano E, Columbu S, Crisci GM, De Luca R, Lezzerini M, Mancuso S, La Marca A (2015) New data about the ancient mortars from the archaeological site of Kyme (Turkey): compositional characterization. Per Min 84:497–517

Moropoulou A, Bakolas A, Bisbikou K (2000) Investigation of the technology of historic mortars. J Cult Herit 1:45–58

Moropoulou A, Bakolas A, Aggelakopoulou E (2004) Evaluation of pozzolanic activity of natural and artificial pozzolans by thermal analysis. Thermochim Acta 420:135–140

Morra V, Secchi FA, Assorgia A (1994) Petrogenetic significance of peralkaline rocks from Cenozoic calk-alkaline volcanism from SW Sardinia, Italy. Chem Geol 118:109–142

Peccerillo A, Taylor SR (1976) Geochemistry of Eocene calc-alkaline volcanic rocks from the Kastamonu area, northern Turkey. Contrib Mineral Petrol 58:63–81

Pollione MV (1521 15 BC) De Architecture. Vol. II. In: Cesariano C, De Architectura Libri Dece, 1521, Como

Previato C (2016) Nora. Le cave di pietra della città antica, Edizioni Quasar, Roma, p 144

Ramacciotti M, Rubio S, Gallello G, Lezzerini M, Columbu S, Hernandez E, Morales-Rubio A, Pastor A, De La Guardia M (2018) Chronological classification of ancient mortars employing spectroscopy and spectrometry techniques: Sagunto (Valencia, Spain) Case. Journal of Spectroscopy 2018:1-10. DOI: 10.1155/2018/9736547

Riccardi MP, Duminuco P, Tomasi C, Ferloni P (1998) Thermal, microscopic and X-ray diffraction studies on some ancient mortars. Thermochim Acta 321:207–214

Russell A (2010) Foreign materials, islander mobility and elite identity in Late Bronze Age Sardinia. In P. van Dommelen and A.B. Knapp (eds), Material Connections in the Ancient Mediterranean: Mobility, Materiality and Identity: 106–26. London, Routledge

Shand SJ (1951) Eruptive rocks; their genesis, composition, classification, and their relation to ore-deposits, with a chapter on meteorites, 4th edn. Wiley, New York

Smith P, Smith RM (2009) Bricks and mortar: a method for identifying construction phases in multistage structures. Hist Archaeol 43:40–60

Stanislao C, Rispoli C, Vola G, Cappelletti P, Morra V, De Gennaro M (2011) Contribution to the knowledge of ancient Roman seawater concretes: Phlegrean pozzolan adopted in the construction of the harbour at Soli-Pompeiopolis (Mersin, Turkey). Per Min 80(3): 471–488

Thornton CP, Tuttle OF (1960) Chemistry of igneous rocks, I. Differentiation index. Am J Sci 258:664–684

Türkmenoglu AG, Tankut A (2002) Use of tuffs from central Turkey as admixture in pozzolanic cements. Assessment of their petrographical properties. Cem Concr Res 32:629–637

Tykot RH (1996) Obsidian procurement and distribution in the central and western Mediterranean. J Mediterr Archaeol 9(1):39–82

Tykot RH (1997) Characterization of the Monte Arci (Sardinia) obsidian sources. J Archaeol Sci 24(5):467–479

Tykot RH (2002) Chemical fingerprinting and source tracing of obsidian: the central Mediterranean trade in black gold. Acc Chem Res 35(8): 618–627

Tykot RH, Glascock MD, Speakman RJ, Atzeni E (2008) Obsidian subsources utilized at sites in Southern Sardinia (Italy). Materials Research Society Symposium Proceedings, Materials Issues in Art and Archaeology VIII, Boston, MA (United States), 1047:175–183

Van Achterbergh E, Ryan CG, Griffin WL (1999) Glitter: on-line interactive data reduction for the laser ablation ICP-MS microbrobe. Proc. 9th V.M. Goldschmidt Conf. (Boston)

Verdiani G, Columbu S (2010) E. Stone, an archive for the Sardinia monumental witnesses. Third International Conference, EuroMed 2010, Lemessos, Cyprus, November 8–13, 2010. Book Chapter. ‘Lecture Notes in Computer Science’ (LNCS), Springer. Berlin-Heidelberg Vol. 6436:356–372

Verdiani G, Columbu S (2012) E. Stone, an archive for the Sardinia monumental witnesses. Int J Heritage Digital Era 1(1):75–102

Vola G, Gotti E, Brandon C, Oleson JP, Hohlfelder RL (2011) Chemical, mineralogical and petrographic characterization of roman ancient hydraulic concretes cores from Santa Liberata, Italy, and Caesarea Palestinae, Israel. Per Min 80(2):317–338

Webster GS (1996) A prehistory of Sardinia 2300-500 BC. Monographs in Mediterranean Archaeology 5. Sheffield Academic Press

Wentworth CK (1922) A scale of grade and class terms for clastic sediments. J Geol 30:377–392

Wilson RJA (1980) Sardinia and Sicily during the Roman empire: aspect of the archeological evidence. Kokalos 26/27:219–242

Wood DA (1979) A variably veined suboceanic upper mantle—genetic significance for mid-ocean ridge basalts from geochemical evidence. Geology 7:499–503